An Experimental Investigation of Modeling and Optimal Control of Modified Space Structures

Thesis by

Albert N. Moser

In Partial Fulfillment of the Requirements

for the Degree of

Doctor of Philosophy

California Institute of Technology

Pasadena, California

1992

(Defended March 13, 1992)

Acknowledgements

I would like to express my deepest gratitude to Dr. Thomas K. Caughey for the many discussions regarding the directions of this work and for allowing me to explore these topics at my own pace. I am also grateful to him for the evaluation and review of this thesis.

I am also greatly indebted to Dr. John C. Doyle for allowing me to work with his computational and experimental equipment. Without access to this equipment, my work would not have occurred. Financial help from Dr. Doyle was also crucial. I am grateful to Dr. Jim K. Knowles, Dr. Joel W. Burdick, and Dr. James L. Beck for their encouragement and for their comments on this thesis.

Financial support from the California Institute of Technology in the forms of a Graduate Fellowship and several teaching assistanceships have proven invaluable. Funding from NASA through a Graduate Student Research Fellowship (Program grant #50528-1) has also made this work possible. I thank Dr. Jim Fanson and Mr. John Garba at the Jet Propulsion Laboratory for their assistance in obtaining the NASA Fellowship.

To the research group in controls, I am also greatly indebted. Thanks to Roy, Bobby, Matt, Pete, Carolyn, Hector, and Jorge for helping me learn the control theory mathematics. To Gary, who suggested this topic, I am especially grateful. Additionally, I appreciate the useful discussions with Bob, Kevin, Andrew, and the rest of the SOPS group. On the non-technical side, I particularly thank the Masters swim team members who have proven to be great friends throughout.

Finally, it is difficult to express in words how much I am grateful to my family for their moral and financial support. To my parents and grandparents, I am thankful for the encouragement, without which none of this would have happened; to my brother Mike, thanks for the discussions and guidance; and to my brother Chuck, thanks for the suggestions and for offering the big picture.

Abstract

Future space missions will rely on structures with many closely spaced and lightly damped modes. To meet the alignment performance requirements of the missions, these structures will need to incorporate active control. Control which does not destabilize the system requires very accurate models of all modes present in a certain bandwidth of the structure's response. Development of the accurate models through system identification is significantly complicated by modes with almost equal frequencies and dampings which appear as single peaks in the structure's frequency response function. Similarly, difficulty in control will be increased by changes in the system due to docking of other systems.

A structure was built at Caltech for identification and control experiments which exhibits many of the features of large space structures. Identification, modification, and control experiments have been conducted on this system to develop optimal controllers which are robust to system changes. This thesis presents the theory and experimental results behind the modeling of modifications on the structure. It also details use of H_∞/μ-synthesis methods for this problem. Robust controllers have been implemented so as to remove responses of the lowest nine modes of the structure. These controllers perform very well even when the structure is modified by the addition of dynamics.

Table of Contents

Title Page i

Acknowledgements ii

Abstract iii

Table of Contents iv

List of Figures x

List of Tables xiii

1. Introduction 1

1.1. Organization of this Thesis 4

1.2. References for Chapter 1 7

2. Literature Surveys 10

2.1. Literature Review of Structural Identification 10

2.1.1. Introduction 10

2.1.2. Time Domain Methods 11

2.1.3. Frequency Domain Methods 13

2.1.4. Parametric Model Identification 13

2.1.5. System Excitation Methods 14

2.1.6. Closely Spaced Structural Modes 15

2.1.7. Experimental Examples 15

2.2. Literature Review of Structural Modification 15

2.2.1. Introduction 15

2.2.2. Component Mode Synthesis 16

2.2.3. Localized Modification Methods 17

2.2.4. Power Series Expansion Methods 17

2.2.5. Receptance/Compensator Methods 18

2.3. Literature Review of Structural Control 19

2.3.1. Introduction 19

2.3.2. Difficulties with Structural Control 20

2.3.3. Classical/SISO Control Methods 22

2.3.4. State Space Methods 23

2.3.5. Nonlinear Control 25

2.3.6. Robustness Measures 26

2.3.7. Demonstrations/Applications 27

2.4. References for Chapter 2 29

3. Identification of The Caltech Flexible Structure 43

3.1. Introduction 43

3.2. Curve Fit Algorithm 44

3.2.1. Choice of Norm for Minimization 45

3.2.2. Newton Method 46

3.2.3. Steepest Descent 47

3.2.4. Initial Estimates 48

3.3. Benchmark Tests of the Algorithm 49

3.3.1. Single Input Single Output (SISO) Tests 49

3.3.2. MIMO Multiple Mode Test 50

3.4. Description of the Caltech Flexible Structure 52

3.4.1. Actuators 54

3.4.2. Modeling of the Proof Mass Actuators 55

3.4.3. Sensors 56

3.4.4. Data Acquisition and Control System 56

3.5. Modal Properties of the Structure 56

3.5.1. Excitation 56

3.5.2. Curve Fit 58

3.5.3. Finite Element Estimates 60

3.5.4. Closely Spaced Modes 61

3.6. Conclusions 62

3.7. References for Chapter 3 63

4. Response Mode Synthesis using Linear Fractional Transformations and Identified Models 66

4.1. Introduction 66

4.2. Linear Fractional Transformations - Basic Definition 68

4.3. Spring-Damper-Mass System 69

4.4. A More General System 73

4.4.1. A Plate Attached to a Beam 73

4.4.2. Addition of a Mass to a System 76

4.4.3. Connection of Systems with Dynamics 77

4.4.4. Restrictions of the Connection Method 81

4.5. Conclusion 81

4.6. References for Chapter 4 82

5. Numerical and Experimental Applications of the Assembly Methodology 85

5.1. Introduction 85

5.2. Necessary Information from Identification 85

5.3. Systems with Noncolocated Sensor/Actuator Geometries 86

5.3.1. Uniqueness of Identified Modal Models 87

5.3.2. Systems with Actuator Dynamics 87

5.3.3. Modal Assumption 87

5.4. Numerical Example 89

5.5. Experimental Connection of Two Lightly Damped Structures 92

5.5.1. Secondary Structure to be Attached 93

5.5.2. Identification of Secondary System 94

5.5.3. Identification of Modal Masses 97

5.5.4. Results of Connection of the Structures 98

5.6. Discussion of Experimental Results 99

5.6.1. Case 1 100

5.6.2. Case 2 104

5.6.3. *A Posteriori* Improvement of Case 2 107

5.7. Observations and Suggestions for Experimental Improvements . . . 107

5.8. Conclusions 109

5.9. References for Chapter 5 110

6. Structural Control Using H_∞/μ-Synthesis 111

6.1. Introduction 111

6.2. Difficulties with Structural Control 111

6.3. H_∞/μ-Synthesis: Theory 113

6.3.1. H_∞-Optimal Control 114

6.3.2. μ-analysis 115

6.3.3. D-scaling 117

6.3.4. μ-synthesis 117

6.4. Implementational Issues of H_∞/μ-Synthesis 118

6.4.1. Nominal Model 118

6.4.2. Specification of Desired Performance 119

6.4.3. Controller Shaping 122

6.4.4. Uncertainty Descriptions 125

6.5. Other Issues in the Synthesis Setup 130

6.5.1. Computational Delays 130

6.5.2. Sensor and Actuator Dynamics 130

6.5.3. Optimality of the H_∞ Controller 131

6.5.4. Computation of μ 133

6.5.5. Using D-scales to Study Interactions in the Synthesis Setup . 133

6.5.6. Assembly of the Models 135

6.6. Conclusions 138

6.7. References for Chapter 6 138

7. Experimental Control of the Caltech Flexible Structure - Without and With Str2 Attached 141

7.1. Introduction 141

7.2. Results of Control of the Caltech Flexible Structure 141

7.2.1. Measuring Performance 141

7.2.2. Control Experiments 143

7.2.3. Performance Results - Voice Coil Control Actuation 143

7.2.4. Performance Results - Proof Mass Control Actuators 146

7.3. Robust Control of Modified Structures 148

7.3.1. Setup for Structural Modification Uncertainty 149

7.3.2. Results of Modification Experiments 153

7.4. Conclusions 157

7.5. References for Chapter 7 158

8. Conclusions and Directions for Future Work 160

8.1. Main Results 160

8.1.1. Identification 160

8.1.2. Modification Modeling 161

8.1.3. Active Control 161

8.1.4. Active Control of a Modified Structure 162

8.2. Directions for Further Work 162

8.3. References for Chapter 8 163

i. A Variational Incomplete Proof to the H_∞-optimal Controller Problem 164

i.1. Introduction 164

i.2. Full Information 165

i.3. The Output Estimation Problem 167

i.4. Complete OE Solution 170

i.5. References for Appendix i 170

List of Figures

3.1. Fit of Uncorrupted System 50

3.2. Fit of Corrupted System 51

3.3. MIMO Transfer Function Channel 1 52

3.4. MIMO Transfer Function Channel 2 53

3.5. MIMO Transfer Function Channel 3 53

3.6. MIMO Transfer Function Channel 4 54

3.7. Caltech Prototype Space Structure 54

3.8. Fourier Transform of Sine Sweep: .2 to 20. hz 57

3.9. RMS Responses of Structure, Model, and Error 59

3.10. Caltech Structure and Model Response for Actuator 1 to Accelerometer 1 60

3.11. Transfer Functions 2 and 3: Modes at 5.60 and 6.23 rad/sec 63

3.12. Transfer Functions 2 and 3: Modes at 5.56 and 5.60 rad/sec 64

4.1. Basic LFT Structure 69

4.2. State Space for Spring-Damper-Mass System 70

4.3. Two Spring-Damper-Mass Systems in Series 70

4.4. Two SDM Systems Attached via an LFT 71

4.5. General Series Spring-Damper-Mass Block 72

4.6. LFT for Addition of Mass 72

4.7. Addition of a Mass to Identified System 73

4.8. Geometry of Plate and Accelerometer i 74

4.9. State Space Description of Plate System 76

4.10. Adding a Mass to a Plate 77

4.11. Combined System Transfer Functions 80

4.12. Combined System Simplified Transfer Functions 80

4.13. State Space Representation of Combined Systems 81

5.1. Modified Transfer Function 88

5.2. Unmodified SDM Systems: Full Identification 91

5.3. Mass Modified Spring-Damper-Mass Systems 92

5.4. Coupled Spring-Damper-Mass Systems 93

5.5. Caltech LSS and Secondary Structure 95

5.6. Str2, Case 1, Accel. 2, Directions 1&2 97

5.7. Str2, Case 2, Accel. 2, Directions 1&2 97

5.8. Modified and Original Caltech LSS, RMS Responses 99

5.9. RMS Magnitude, Modified Str2: Case 1, Case 2 98

5.10. RMS Sums of Combined Behavior: Case 1 102

5.11. RMS Sums of Combined Behavior: Case 2 103

5.12. Transfer Functions from VC #1 to Accelerometer #2 on Str2: Case 1. 104

5.13. Transfer Functions from VC #1 to Accelerometer #2 on Str2: Case 2. 106

5.14. Experimental and Predicted RMS Behaviors for Connected Structures. Model Improved by Altering Parameters 108

5.15. Transfer Function from VC #1 to Accelerometer #2 on Str2: Improved 107

6.1. Linear Fractional Transformations Leading to M and μ 116

6.2. Comparison of Sensing Types to Show Inherent Rolloff 120

6.3. Noise and Disturbance Rejection for Performance Specification 121

6.4. Performance Specification for the CFS 123

6.5. Typical Schematic Form of Additive Uncertainty 126

6.6. Additive Uncertainty for Caltech Flexible Structure 128

6.7. Graphical Representation of Multiplicative Uncertainty 128

6.8. Common Interactions of D-scales in Synthesis Setup 134

6.9. Standard Synthesis Setup 136

6.10. Caltech Flexible Structure Synthesis Setup 137

7.1. Best Voice Coil Controller 145

7.2. Best Voice Coil Controller: PF 1 to Accel. 6 146

7.3. Best Voice Coil Controller, Response at all Accelerometers 147

7.4. Voice Coil Controller with Less Performance Specified, Response at all Accelerometers 148

7.5. Proof Mass Controller Response 149

7.6. Model and Experimental Response for Colocated Proof Mass/Accelerometer Pair 150

7.7. Transformation from LFT in $\hat{\Delta}$ to one in Δ 152

7.8. Transfer Matrix for Structure Connection Uncertainty 152

7.9. State Space Representation of Combined Structure Model for Structural Uncertainty Descriptions 153

7.10. Controller with Mass-Modified CFS 154

7.11. Best Voice Coil Controller for Nominal System 156

7.12. Voice Coil Controller Robust to Structural Modification 156

7.13. Controller with Larger Uncertainty Acting on Both Plants 157

i.1. System of Differential Equations which Leads to an Algebraic Riccati Equation for X_∞ 167

i.2. Initial System of Differential Equations for Y_{tmp} 169

i.3. Hamiltonian for OE Riccati Equation 170

List of Tables

3.1. Application of Algorithm to Theoretical System 49

3.2. MIMO Example 52

3.3. Identified and Finite Element Frequencies and Dampings 61

5.1. Numerical Examples: 2SDM Systems: Basic Properties 90

5.2. Numerical Examples: 2SDM Systems: Properties when Modified 90

5.3. Numerical Examples: 2SDM Systems: Identified Modal Weights 92

5.4. Numerical Examples: 2 Coupled SDM Systems: Predicted and Exact . . 94

5.5. Original and Mass-Modified Systems: Caltech LSS, Case 1, and Case 2 100

5.6. Joined System Predicted Modes: Case 1, and Case 2 101

Chapter 1. Introduction

The need for active control of structural systems presently is driven by proposed projects such as NASA's twenty meter large deployable reflector. This type of system has evolved from smaller space systems which obtained significant scientific data. Interest has shifted to data at different wavelengths, thus larger systems are necessary. Costs for placing devices in orbit are still rising, so in order to implement larger systems, it is necessary to make them very light. Unfortunately with structures, lower system mass generally results in greater flexibility. If the structural system is too flexible it will not be able to perform its necessary task. For example, deformations of surface shapes due to vibrations greatly degrade the focus quality of parabolic dishes.

Initial work to reduce vibratory responses is directed at adding damping to the structural components of the scientific data gathering satellites. The main examples of damping elements are viscous fluid shock absorbers and viscoelastic solid inserts. These devices, however, either lose their fluid or lose their elasticity with time. Additionally, and more importantly, they allow motions which may be too large for the system to meet performance requirements. For example, for interferometry it will be necessary to keep relative motions in the micron range for components that are tens of meters apart from each other.

Active control methods can be used to help meet these objectives quite effectively without great increases in total system mass. The goals for feedback systems are to minimize vibratory responses to disturbances and to improve point to point alignment of particular sensors. Disturbances such as vibrations and static loads will come from station keeping and from thermal and gravity gradients. Because of the large sizes of the structures and low internal damping, the disturbances will

easily cause responses of the primary system modes which are expected to be at frequencies below five hertz.

For effective and stable active control, very high quality models of the structure to be controlled are needed. It is very difficult, however, to obtain the necessary model quality before the systems are deployed for several reasons. Most consequentially, properties of individual components and joints between them are not known very well. This causes inaccuracies in predictions based on tools such as finite element analysis (FEA) programs. Since FEA codes, which are the only currently available tools for economically predicting behavior of complex structures, will not give very accurate results, experimental identification of the deployed structure will be required.

The flexibility of the structures further complicates the modeling procedure. In environments with gravity, the structures will not be strong enough to support their own weight. That is, when constructed on the ground the systems will buckle because of their flexibility. Similarly, any support mechanisms will change the structural behavior, thus invalidating the model. Closely spaced modes are an additional difficulty since it may be nearly impossible to uniquely identify modes at almost identical frequencies.

Once deployed, the first two of these two problems (structural weight and support conditions) are no longer issues since the system will be in the configuration for which it is designed. Close spacing of modes, however, will still be a problem. The first approach to separating close modes is to use data acquisition systems with very high resolutions, thereby obtaining transfer function responses with separate peaks (in the frequency domain) for each mode. If high enough resolution data acquisition is not available, closely spaced modes can still be discerned through use of multiple excitation and multiple sensing locations, as shown in this thesis. The differences in mode shapes are used. Finally, the predictions from numerical analyses such as FEA codes can be used to give initial estimates for curve fit identification procedures.

Excitation of the structures to develop models for control synthesis is done using the control actuators. Several types of motors have been suggested. The first type includes inertial devices such as proof mass actuators and torque wheels. These impart force to the structure by changing their position in inertial space.

Thus they can cause position and attitude changes of the whole system when controlling flexible modes. Therefore, for internal/modal motion control the second type of actuation is more appropriate: A technique known as active member control uses devices such as voice coils and piezoelectric elements to impart force through structural load paths directly. Only flexible motions are changed by this technique.

Sensing may be done with relative or absolute sensors similarly. Relative sensors include strain gauges and laser range finders that work on point-to-point motions within the system. These only detect internal motions. Inertial sensors such as accelerometers measure both internal and rigid body motions. It is sometimes possible to decompose these signals so that they may be used to effectively sense for vibration reduction.

Once the base model of the system is developed, the proper control algorithm synthesis method must be chosen. There are basically three types of algorithms which work for structural systems: Single input single output (SISO) - which use Nyquist or equivalent plots to determine performance and stability; Multiple input multiple output (MIMO) loop-at-a-time - which also use SISO methods, but do not have the same stability guarantees; and full MIMO multivariable - some of which have complete stability and performance guarantees. The SISO techniques are the simplest to use and implement, but do not generally have the performance levels of the MIMO methods. Examples are gain stabilization, direct velocity feedback, and loopshaping.

The loop-at-a-time MIMO techniques extend the SISO methods by building up SISO controllers for sensor/actuator pairs one pair (loop) at a time. That is, the compensators are composed of several SISO controllers working simultaneously on various input/output transfer channels. Unfortunately, destabilizing interactions between the multiple compensators are often difficult to predict, so stability guarantees are not very strong.

Finally, multivariable MIMO algorithms such as Linear Quadratic Gaussian (LQG) [KwS] and H_∞-optimal control [DGK] result in compensators which use all actuator-sensor transfer channels simultaneously. (Letters in the square brackets correspond to references at the end of each chapter.) While more complex than the other techniques, these controllers can take advantage of the multiple control paths to obtain greater performance than the SISO methods which are constrained

to single path dynamics. (Further descriptions of all these methods are given in Chapter 2.) Robustness and performance guarantees exist for some of these MIMO multivariable methods.

Robustness of a feedback compensator describes how much the base system can change without instability of the controlled system occurring. That is, the controllers essentially add energy to the system. If added correctly, motions can be cancelled out; however, if the energy is placed at the wrong frequency (or with the wrong phase), the motions may be augmented to the point of destabilization of the whole system.

Some of the newest synthesis methods have procedures which increase the compensator robustness. To be robust to changes in the system or to errors in models, the models for controller synthesis must incorporate uncertainty/modification models in addition to the base system model. Currently, these are developed using *ad hoc* methods such as estimating a certain percentage error in the model. Good quality descriptions are needed because larger uncertainty descriptions cause reduced controller performance. Thus, with very accurate uncertainty models, the best performance of the controlled system can be obtained.

One type of system uncertainty or change that needs to be developed is the alteration of structure behavior due to physical changes such as addition of dynamics (docking) and movement of components (robot arm configuration changes). While these can easily be modeled with analytical techniques such as FEA, as previously discussed, these methods are not very accurate. Ideally, the most correct model development method is to combine identified models of each subsystem in the appropriate configuration. This is a process called *response mode synthesis* or *component mode synthesis.* With a good model of the change to the structure, a robust, high performance controller can then be designed for both the original and the modified structure. That is, the modification can be precisely modeled and treated as an uncertainty (as opposed to the *ad hoc* methods currently used).

1.1 Organization of this Thesis

The most important step in designing a control algorithm for active structural control is modeling or identification of the system of interest. The first part of this thesis presents a frequency domain identification method and experiments

carried out on a structure at Caltech [Ba2]. Through use of several single input multiple output experiments assembled as a multiple input multiple output (MIMO) data set, lightly damped modes with nearly equal frequencies and dampings were characterized distinctly. Results of identification experiments and estimates from finite element models are presented. A significant difference exists between the finite element estimates and the identified model.

The second part of this thesis presents a generalization of response mode synthesis[Bla], [CKR], [Ewi], [Hur], [SpT] to systems where only experimental data is available. The most difficult step in response/component mode synthesis procedures has been normalization of the experimentally determined models of the individual components so that they are compatible with models of other systems. This has been especially difficult when only experimental input/output information is available. Similarly, the procedure has been limited by factors including reliance on colocated sensor/actuator geometries and on references of the transducers to physical quantities.

A technique is presented which uses linear fractional transformations (LFTs), as used in feedback frameworks, to assemble substructures. LFTs are very appropriate for modal synthesis since they incorporate effects of each subsystem on the others via feedback. The procedure demonstrated herein bypasses many of the limitations of previously used response mode synthesis procedures. For example the method is amenable to noncolocated transducer geometries, only needs input/output experimentally measured information (no physical units on force or length are needed), and can use acceleration sensing and locally controlled actuators. A simple theoretical example and a complex experimental structure case are presented to demonstrate the methodology.

The key to the technique is that two experiments must be done on each subsystem in the assembly: The first is a straightforward modal identification; the second involves adding a known mass to each substructure and identifying modal parameters based on the original systems' models and on the modified structures' responses. The effects of the mass modification is easily modeled through an LFT. With the modal parameters, the input/output models of the systems can be connected to predict the behavior of the combined structures.

In the numerical example, two spring-damper-mass systems are identified separately and are connected using the suggested procedure. Then, they are theoretically connected using the exact expressions. The resulting models and responses come out almost identical demonstrating that the method is theoretically correct. Experimental results are for a very lightly damped single mode beam-like structure which is attached to lightly damped multi-degree-of-freedom structure with closely spaced modes. The responses predicted by the theoretical method come close to the actual response of the combined system. A discussion is given on the sources of the errors which include poor experimental fixturing and lack of rotational sensors. Overall, however, the procedure seems quite successful.

The third portion of this work deals with active control of the structures. While the control objective in this work is vibration suppression, the methods discussed extend to model matching. Several different configuration schemes and control algorithms are being tested (by other researchers) to determine the effectiveness of active control on structures [WFC]. The most straightforward ones are classical methods such as gain and phase stabilization using colocated sensor/actuator geometries. While these have nice robustness and high performance features, it is not always possible to colocate the sensors and the actuators. Also these methods can fail because finite sensor and actuator dynamics can destabilize the system. Colocation also means that only the regions where actuation devices are placed are controlled.

The difficulty of colocating sensing and actuation devices has led to significant interest in methods which allow noncolocation such as linear quadratic Gaussian (LQG) and H_∞-optimal synthesis techniques. Robust optimal control methods such as H_∞/μ-synthesis are used in this work. Control of flexible structures using this method requires good models of the base structure, knowledge of the uncertainties in these models, adequate specification of desired performance, and ideas on the properties of the controller to be designed. H_∞/μ-synthesis is a technique which can incorporate all this information in a mathematical formulation to compute optimal controllers. The resulting compensators overcome the many difficulties of structural control including spillover and nonminimum phase transmission zeroes.

Experimental results of implementation of optimal controllers on the Caltech Flexible structure are presented along with discussions of theoretical and implementational issues of H_∞/μ-synthesis. It is shown that modal responses can be almost

completely removed by active control, especially if the control actuators are in the structural load paths. The controllers are robust to modeling errors and small physical changes of the system.

Further, a method is presented to use the H_∞/μ-synthesis control synthesis technique to design controllers which will remain stable for structures modified by docking of other structures. Results of experimental implementation of this design tool are presented showing the necessity of incorporation of uncertainties into the controller synthesis setup. Proper controller design results in excellent performance of the controlled structure in its original and in its modified state. Without the uncertainties, the controlled system becomes unstable, as demonstrated. The examples presented for the modification work represent active control of two structures which dock to each other. Modeling of uncertainties is a current topic of research in the control implementation fields. Here, the docking structure is treated as uncertainty in a well understood framework.

The above topics are divided into the following chapters: Chapter 2 gives a literature survey for structural identification, structural modification modeling, and control theory. In Chapter 3, an identification method and experimental results on the Caltech Flexible Structure are presented. This chapter is an extended version of [Mos]. The use of LFTs for response mode synthesis is outlined in Chapter 4, followed by the generalizations previously mentioned and by experimental results of combination of structures in Chapter 5. Chapters 6 contains a description of the procedures for H_∞/μ-controller synthesis for the Caltech structure. Experimental results of control of the Caltech Flexible Structure are given in Chapter 7. This chapter also contains the combination of LFT structural modeling and robust control for design and implementation of controllers which are robust to docking of structures. Chapter 8 gives some conclusions based on this work.

1.2 References for Chapter 1

Bmu: Balas, G., *et al.*, (1991),**μ-Analysis and Synthesis Toolbox,** MUSYN, Inc., and The Math Works, Inc., Natick, Massachusetts.

Ba2: Balas, G., (1990), **Robust Control of Flexible Structures: Theory and Experiments,** Ph.D. Thesis, Department of Aeronautical Engineering, California Institute of Technology, Pasadena, California.

Bla: Blackwood, G.H., (1988), "Experimental Component Mode Synthesis of Structures with Joint Freeplay," Report SSL#16-88, Space Systems Laboratory, Massachusetts Institute of Technology, Cambridge, Massachusetts.

CKR: Crowley, J.R., Klosterman, A.L., Rocklin, G.T., and Vold, H., (1984), "Direct Structural Modification Using Frequency Response Functions," *Proceedings of the 2^{nd} International Modal Analysis Conference,* Union College, Schenectady, NY, pp. 930-936.

DGK: Doyle, J., Glover, K., Khargonekar, P., and Francis, B., (1989), "State Space Solutions to standard H_2 and H_∞ Control Problems," *IEEE Transactions on Automatic Control* Vol. AC 34, pp. 831-847.

Ewi: Ewins, D.J., (1985), "Modal Test Requirements for Coupled Structure Analysis Using Experimentally Derived Component Models," **Combined Experimental/Analytical Modeling of Dynamic Structural Systems,** ASCE/ASME Mechanics Conference, AMD, Vol. 67, pp. 1-30.

Hur: Hurty, W.C., (1965), "Dynamic Analysis of Structural Systems using Component Modes," *AIAA Journal,* Vol 3, No. 4, pp. 678-685.

KwS: Kwakernaak, H., and Sivan, R., (1972), **Linear Optimal Control Systems**, Wiley-Interscience, New York.

Mos: Moser, A.N., and Caughey, T.K., (1991) "Some Experience with Identification of the Caltech Experimental Space Structure." *Proceedings of the 1991 American Controls Conference,* Boston, Massachusetts.

NeS: Newlin, M.P., and Smith, R.S., (1991), "Model Validation and a Generalization of μ," *Proceedings of the 30^{th} Conference on Decision and Control,* Brighton, England.

Pac: Packard, A., (1988), "What's New with μ," Ph.D. Thesis, Mechanical Engineering Department, University of California at Berkeley, Berkeley, California.

SpT: Spanos, J.T., and Tsuha, W.S., (1989), " Multibody Dynamics: Modeling Component Flexibility with Fixed, Free, Loaded, Constraint, and Residual Modes," *Proceedings of the 3^{rd} Annual Conference on Aerospace Computational Control,* JPL Publication 89-45, Pasadena, CA, pp. 761-777.

StF: Strang, G., and Fix, G.J., (1973), **An Analysis of the Finite Element Method** Prentice-Hall Inc., Englewood Cliffs, New Jersey.

WFC: Wada, B.K., Fanson, J.L., and Crawley, E.F., (1990), "Adaptive Structures," *Mechanical Engineering,* Vol. 112, No. 11, pp. 41-46.

Chapter 2. Literature Surveys

2.1 Literature Review of Structural Identification

2.1.1. Introduction

Significant work has been done in the field of structural identification, where the main goal is development of mathematical models of structures. These models should be as representative of the actual system as possible. Several excellent reviews of the field have been made over the years. For example, [Hsi] reviews the philosophies and motives for both linear and nonlinear identification. Among the needs cited for identified models are structural control, behavior modeling, and as pointed out in [Sch], prediction of changes in response due to physical changes of the system.

The types of models resulting from the identification procedures are outlined in [Ibr], [Lju], [Nat], [Sag], and [Str], just to list a few. These papers also review cases where different types of excitations are advantageous for use on structures. [Sag] and [McB] include much of the above information, but also discuss many of the statistical aspects of the resulting models. Different types of transmission zeroes that result in systems and from the models are outlined in [Toh]. Finally, [Ibr] and [Vol] discuss the effects of closely spaced modes on the identification procedure, and review the types of models and identification methods necessary for identification in these situations.

Identification of structures can basically be categorized as black box (non-parametric), modal model based parametric, and structural parametric. The black box nonparametric models, as reviewed in [Lju], can also be applied to systems other than structures. These are generally limited to being either single-input

multiple-output (SIMO) or multiple-input single-output (MISO). It is often difficult to model lightly damped modal systems or systems with closely spaced modes with these methods, because in these cases, allowing for higher order models usually results in models that fit noise in the data rather than structural effects [BrR]. Some examples of models developed with these techniques are, in the time domain, the autoregressive-moving average (ARMAX), box-Jenkins, and output estimation; and in the frequency domain, Chebyshev polynomial [Dai]. To obtain multiple-input multiple-output models, often the goal of the identification, the SIMO or MISO models may be assembled into MIMO form, and their orders may be reduced by one of the various methods outlined in [Spa] and [Bmu].

When *a priori* information is to be incorporated into the resulting model, modal model based parametric identification can be used. Here, a model based on structural properties and basic physical principles is chosen. Then, the parameters for the model form are identified. The identification procedure generally consists of a least squares or nonlinear optimization (as outlined in many of the references). The error to be minimized can be developed in either the time or the frequency domain.

2.1.2. Time Domain Methods

Brief explanations of the time domain methods are given in [Bec], [Bro], [Cra], [CrB], [Ful], [Ibr], [McB], [Nat], [Sag], and [Vol]. The basic methods are known as the Ibrahim time domain (ITD) [Ibr], the Polyreference [Vol], the Prony method [Ibr], and modal sweep [Bec].

The most common time domain methods (ITD, Polyreference, and Prony's method) use free decay data to set up a least squares minimization problem similar to the ones used in the black-box methods. One of the advantages of these methods is that initial estimates of parameters are not needed. The results of the least squares minimization are in a form not related to modal properties of structures. Imposition of modal qualities is what differentiates the methods. Numerical difficulties often arise in the procedure to extract the modal quantities such as eigenvalues and eigenvectors. For extracting the natural frequencies of the system, the ITD method uses properties of the complex exponential, the Polyreference technique uses finite rank arguments, and Prony's method approximates the eigenvectors by polynomials

whose roots are then found. These methods are quite effective as demonstrated in [Vol], even with closely spaced modes.

Unfortunately, there are many situations where free decay response is not very effective. These are caused by rapid rises in noise to signal ratios. To reduce the effects of noise, larger initial displacements may be applied. This, however, may excite the structure in a nonlinear range, or worse, it may damage it by causing large deformation.

Füllekrug [Ful] extended the principles of the above methods to accept a persistent excitation. The main assumption is that the excitation is constant over the sampling period. This should be a reasonable assumption if there is a fast enough sampling rate. A more general methodology (from which the above methods may be derived) is the Kalman filter [Bro][Sag]. This algorithm is implementable for real-time state estimation. The matrices computed from here may also be processed to obtain modal model data. The main drawback of the above time domain methods, as reported in the various cited references, is the need to sense (or synthesize) two of the three quantities of displacement, velocity, and acceleration. Similarly, physical knowledge of the system is not incorporated until after the least squares minimization is done. To choose the order of the model, either the data set size must be reduced, or a model reduction scheme must be applied.

Beck [Bec][McB] used a modal model based approach to develop a square error in the time domain. Responses of a model are synthesized via the inverse fast Fourier transform (FFT), and a modal sweep is done. That is, the response of a single mode is simulated in time, an error quantity is calculated in the time domain, a least squares nonlinear optimization is carried out on the modal parameters, and the resulting modal behavior is subtracted from the time domain response of the structure. With the resulting time response data, the next mode is treated. The process is repeated until the desired accuracy of the model is obtained. Unfortunately, this method requires initial estimates of parameters. The main advantage of this method is that transfer function models may be derived for any sensing method. Also, knowledge of the physical system may be incorporated into the model.

Another form of time domain identification is resonance testing, where an attempt is made to excite pure modes of the system using multiple exciters [Cau][Nat]. By tuning the frequency of excitation and the relative phases and magnitudes of

the exciters, excellent models of modal behavior may be obtained. These methods, however, are extremely time consuming. Also, they may cause damage to structures by exciting them in resonance for significant periods of time [Ibb].

2.1.3. Frequency Domain Methods

Most frequency domain methods use the FFT to convert wide frequency band data from the time domain to the frequency domain. Data from stepped-sine testing may also be used. The standard concept is to minimize some measure of the error between the FFT of the data and the synthesized frequency response of the model by varying the model's parameters. In [Bow], the basic parameter variation techniques are discussed, and their computational aspects are reviewed. [McV], [Mos], [Ebe], and [Pot] have examples of application of a standard modal model to theoretical and experimental systems. In this type of method, the nonlinear minimization is done by a Newton, Newton-Raphson, Levenberg-Marquartd, or other numerical scheme. The main user decisions for effective use of these methods are good initial estimates of parameters, selection of number of modes in the model, and choice of the right excitation for the structure (to avoid aliasing and leakage from the FFT). The advantages of the method are that user input regarding prior knowledge of the system may be incorporated to develop input/output models and that any (linear in amplitude) excitation and sensing method may be used. Variations of parameters due to changes over time may be traced more easily since the form of the model does not change. And finally, noise may be averaged in a modal sense by choosing models with fewer modes. These methods often result in the smallest size descriptions of the systems. The main drawback is that the user might have to interact with the computational method to help improve convergence. Frequency domain versions of the least squares time domain methods such as ITD also exist [Cra].

Another use of modal analysis is refinement of finite element models. In these cases, the goal is to identify or alter the mass, stiffness, and damping matrices of the system model. As stated in [Ber], [Cau], and [Kie], in order to uniquely determine these parameters, there is a minimum requirement on the number of sensors and actuators in the system. Thus, it might be too costly to do this procedure. Also since the behavior of a system is completely described in a given frequency range by a modal model, it may be unnecessary to identify the individual physical parameters.

2.1.4. Parametric Model Identification

Analogues of both the time domain methods and the frequency domain methods have been developed to do physical parameter identification. Among them are [CrB] which extends the simultaneous frequency domain method by Coppolino, and [Oja] which uses a least squares algorithm. Methodologies from control theory, such as eigenstructure assignment have also been developed [Min]. Significant amounts of both theoretical and experimental work has been done in this field, but will not be discussed here.

2.1.5. System Excitation Methods

The choice of which excitation signal to use is strongly dependent on the structure being tested and the excitation quantity used. For most of the time domain methods, the only allowable excitation is an impulse [Str]. If methods for creating large repeatable excitations are available, this often gives the cleanest responses. However, if there are limits on system motion amplitude or if there is a large noise to signal ratio, other methods should be employed.

In resonance methods, a harmonic excitation at a single frequency is applied, and the structure is allowed to achieve steady state. This method can give arbitrarily fine frequency resolution (sine-step testing), however it is very time consuming and expensive. Multiple shakers may be used simultaneously in an attempt to excite pure modes. The structure, unfortunately, may be damaged by being kept in resonance.

Random and pseudo-random signals may also be used with single exciters or multiple exciters[Sag]. These excitations give data with wider frequency band content (more frequencies are represented). For systems where ambient excitation is the only choice [Hsi][McB], by assuming that the input is Gaussian white noise, models for the systems' power spectra may be developed. These models, however, will not have information on the phase shifts from inputs to outputs due to the structure. If the excitation is controllable, pseudo-random band limited data may be used quite effectively. The main drawback of random data is that the frequency response functions of the excitations are not very smooth: Transfer functions might result with discontinuities for which the structure is not responsible[Lju]. Allemang [Sag] used multiple random excitations to obtain system models.

When signals with smooth time and frequency domain characteristics are desired, a chirp is a good choice [Mos]. As with random data, it may be windowed in the time domain to to give zero starting and ending conditions thereby avoiding leakage and aliasing with the FFT. The advantage of these methods is that all the energy of the input signal may be concentrated in a frequency range of choice.

2.1.6. Closely Spaced Structural Modes

One of the major difficulties with transfer function identification is the presence of closely spaced modes. With single input data, unless the resolution of the FFT is greater than a certain value related to the spacing of the modes [Ibr], it is not possible to separate the modes. Unique identification may be done through use of multiple exciters as shown in [Vol] and [Mos]. Here, geometric properties of the modes (linearly independent eigenvectors) are exploited.

2.1.7. Experimental Examples

Most of the references cited herein have examples of usage of the methods on numerical or experimental systems. Of particular note are the following: In [Vol], the Polyreference time domain method is applied to a symmetric plate with multiple closely spaced modes using multiple free decay experiments. Excellent identification results were obtained on this difficult problem. Similarly, [Mos] presents a frequency domain experimental model developed from a structure with closely spaced modes using multiple chirp inputs.

[Sir] presents experimental analysis of a beam sensed by laser Doppler velocimetry and excited with impulses. The data is then used for modeling. In [Che], a structure is excited by both active members and a shaker. It is shown that the active members give as good, if not better excitations than the shaker. Active members are load carrying active devices. A commercial package was used for identification of the frequencies and dampings, so the algorithm is unknown.

2.2 Literature Review of Structural Modification

2.2.1. Introduction

Structural modification, or reanalysis, aims to calculate the behavior of a modified structure based on previously computed models of the original system. The key to an effective reanalysis technique is that it gives accurate estimates for the new system and that it takes significantly less computational effort than would be needed for a complete analysis of the new system. The savings in computational effort comes about by using information from the analysis of the unmodified system.

In [Aro], [BaH], and [Brac], excellent reviews of structural reanalysis methods are given. The main methods are Component Mode Synthesis [Hur], Weissenburger's localized modification [Wei], the power series expansion [Zas], and the Receptance [CKR][SBC] /Compensator [HEN] method (also known as response mode synthesis[Bla].) Component mode synthesis and the receptance method are general substructure assembly methods which may be used to add dynamics to the base structure. The others are only able to predict modifications due to mass, stiffness, or damping changes to individual members of the system.

The basic concept these methods utilize is recombination of the natural frequencies and shapes of the original systems to model the behavior of a new system. When the recombinations are done symbolically in component mode synthesis or in the receptance method[TsY], the resulting matrix generates the exact equations of motion for the system. This symbolic matrix is what would result from the Holzer-Mykelstad method [ClP] for structural analysis. As stated by Hale and Meirovitch [HaM], convergence of the methods improves if more modes (natural frequencies and vibration shapes) are retained for further analysis. This, however, increases computational costs.

The choice of what shape shape functions (mode shapes) to use also affects the rate of convergence of the method [HaM]. In cases where it is difficult to obtain the exact mode shape for each substructure, polynomial or other smooth trial functions may be used in combination with the Rayleigh-Ritz method. This, however, makes it difficult to specify the eigenproblem uniquely. Likewise, if the trial functions do not completely satisfy conditions at the interfaces of the substructures, accuracy decreases.

2.2.2. Component Mode Synthesis

Component mode synthesis was introduced by Hurty [Hur]. This method uses one or more trial polynomials for each structure, and assembles modal data derived from the functions using energy methods. Hamilton's principle is applied to obtain approximate satisfaction of the interface conditions for each substructure. Thus, proper coefficients for the polynomials are calculated at the substructure level. For reanalysis, a new substructure is attached to the original structure using this method. Several choices exist as to what interface conditions to assume when calculating the model for each subsystem. In [SpT], a review of the basic choices is given: Craig and Brampton [CBr] used fixed interfaces and added constraint shapes; MacNeal and Rubin used free interface conditions with effects of residual modes added in; and Benfield and Hruda used interfaces loaded by masses and stiffnesses. The last choice gives the most accurate results, but is the most expensive computationally. In [GLM], an experimental demonstration of mass loaded elements is given with component mode synthesis. It gave more accurate results than unloaded members.

2.2.3. Localized Modification Methods

Weissenburger [Wei] introduced a reanalysis method based on localized modifications by point masses, scalar stiffnesses, or scalar dampers. Here, the original eigenvalues and eigenvectors of the structure are used to develop a characteristic equation for the new system. The characteristic equation is then solved numerically using a root finder such as the Newton-Raphson method. This can be done successively for each modification, resulting in a series of rank 1 modifications. The method was extended by Pomazal and Snyder [PoS] and Hallquist and Snyder [HaS] to systems with damping, both proportional and non-proportional. Other extensions and examples of this idea are given in [Jon], [Hal], [WSR], and [PoS]. Although exact for any size modification, this technique is computationally expensive because of the need to find the roots of the new characteristic equations.

2.2.4. Power Series Expansion Methods

In [Zas], [RHR], and several other works, a power series expansion reanalysis method is described. The concept is to expand the eigenvalue and eigenvector problems for the modified system in a power series of a modification parameter and of the original eigenvalues and eigenvectors. Terms with equal powers in the modification parameter are equated to obtain corrections to the original values. This

method is only good for small parameter modifications, but is relatively inexpensive computationally. To determine accuracy of the corrections, sensitivity of the eigenvalues and eigenvectors to the parameter changes may be computed using the expressions in [FoK] and [Jez]. Noor and Whitworth [NoW] suggest a perturbation method based on a single parameter variation to reanalyze large space structures. The perturbation idea may also be used to select optimal locations and sizes of modifications to obtain desired system behavior [ZWA].

2.2.5. Receptance/Compensator Methods

The receptance modification strategy [Brac] [CKR] is the most general reanalysis method. It is also quite accurate. Here, either modal models [Brac] or frequency response functions (FRF) [CKR] of substructures are connected using the physical quantities they represent (such as generalized forces or displacements). These methods are equivalent to Kron's tearing method [SBC] and to compensator based methods [HEN]. If the models of the systems are in state space, this method can easily handle non-proportional damping [AOM][Bra]. Brandon [Brab] points out the main limitation of this method: If the change is too large, in some cases the method may fail because of inversion of a singular matrix. The main advantages of the method are that it is relatively accurate (keeping more modes gives greater accuracy, but larger computation time), it can be used directly with experimentally obtained FRF's (if good models are not available), and that it is easy to implement computationally using the Redheffer star product [Kai]. Nice experimental demonstrations of the method are given in [CKR] where the space shuttle was modified theoretically and experimentally, and in [HEN] where an electrical network was used to simulate a mechanical system to alter another mechanical system. [Fla], [Ozg], and [Lar] give numerical examples of beams which are being connected via the receptance method.

The major errors with the receptance method are due to joint effects [WaL], lack of enough retained modes [Fla], noise [CKR], and closely spaced modes [SeD]. In [WaL] a measurement of joint effects was made. These results could then be applied to assembly of substructures. By keeping more modes in each substructure, Flashner [Fla] showed improvement in the accuracy of two Bernoulli-Euler beams that were connected. Because of the difficulty in obtaining models for closely spaced modes, frequency functions may be used directly to obtain the FRF of the new structure [SeD][CKR]. However, as pointed out in [CKR], noise may cause extraneous peaks

in the new FRF's. The inconsistencies may show up upon modal identification. If good enough models are available, it is preferable to use models for the assembly. [Bla] presents experimental connection of two beams and shows extraneous peaks due to noise.

The feature common to all the above reanalysis methods is use of some combination of modal frequencies and shapes of an original system, or set of subsystems, to obtain the behavior of a modified, or assembled system. The methods vary in their accuracy and computational cost, but the above techniques are all more efficient than a total analysis of the new system. Several other methods, which will not be discussed here, have been proposed, but they have about the same efficiency as (if not worse than) total analysis. For example, [LuM] and [StH] identify parameters from experiments to obtain a base model. A new model based on altered parameters is then computed. This involves a new analysis of the system.

2.3 Literature Review of Structural Control

2.3.1. Introduction

Active structural control's main purpose is reduction or alteration of modal responses in structural systems due to external excitations. The main applications currently envisioned are large space structures (LSS) and earthquake excited civil structures. LSS will be very light, and thus flexible, assemblies to support experimental payloads in gravity and atmosphere free environments. Since no external damping (due to an atmosphere) will be available, these systems will be very lightly damped [Bal][Fan][FaG]. For effectiveness of experiments mounted on these systems, end to end misalignment and vibrations will have to be kept at miniscule levels. LSS will have many closely spaced, lightly damped modes which may be difficult to model. Because of their flexibility it will not be possible to ground test large structures such as the large optical interferometer being designed by the Jet Propulsion Laboratory (JPL) in Pasadena, California[FaG]. The main sources of excitations expected on these systems are movement of payloads on the systems (robotic arms), attitude control maneuvers, gravity and thermal gradients, and docking with other structures[Fan][MOT].

The goal of active control on civil structures such as bridges and buildings will be to minimize motion, and thus damage due to earthquake excitations

[MBC][YLW]. Earthquakes can have large enough motions that the building being excited deforms into its plastic, or permanent deformation region. At that point the motion of the building becomes nonlinear, thus more difficult to control.

The most common methods of reducing vibrations in structures are addition of passive dampers (viscous fluid shock absorbers)[WiD], and strengthening of the structural elements. Both of these methods significantly increase the weight of the system. For LSS, since the equipment must be put in orbit, the increase in weight dramatically increases the cost of placing the system in space. Maintaining end-to-end alignment required on LSS is almost impossible with passive dampers because of their softness. Also, the passive devices tend to loose their viscous fluids over time, thus becoming useless. For civil structures, the excitations are often too rapid for passive dampers to be as effective as desired. Active methods avoid many of these complications by being able to add energy to the system in such a manner that motion is minimized.

Several types of algorithms for active control have been developed. They may be categorized as classical methods[FPE], state space methods [DGK][KwS], and adaptive/nonlinear methods [IBA][Isi]. The classical methods depend highly on the skill and experience of the designer for good performance. Their stability and robustness properties are easy to verify since they are single input single output (SISO) techniques. State space methods are more general, but require that the control designer specify the problem mathematically. These techniques can be used to design multiple input multiple output (MIMO) controllers. In these cases, stability and robustness properties are somewhat more difficult to quantify. Nonlinear methods have varying degrees of complexity: from simple on-off ("bang-bang") type algorithms to fully nonlinear algorithms. Robustness and stability of these methods also varies significantly.

The many difficulties with control of structures will be discussed below. Following that, a more detailed description of the various control methodologies shall be given. Some robustness measures will be presented, and finally, a few of the numerical and experimental demonstrations of structural control will be listed.

2.3.2. Difficulties with Structural Control

As discussed in [BCF] and [ZLA], there are several problems that need to be solved for good control of structures. These issues include poor mathematical models of the systems, destabilization of the controlled system due to spillover, actuator and sensor dynamics, modeling of exogenous inputs and system noise, and modeling of physical changes in the structure.

Poor models of systems mainly result from inexact knowledge of physical properties of the system such as material constants and inter-element joint behavior[Bal][BCF][Fan]. Other causes include poor modeling assumptions, discretized models of continuous systems, and lack of knowledge of the damping in and around the system. In [SaF], a brief demonstration is given of the errors caused by choice of beam models for truss structures. [CMV] discusses the errors caused by assuming classical behavior in a nonclassically damped structure. Possible *a priori* choices of damping in the structure are given in [FaG] and [KMC]. These choices are usually inaccurate with respect to the actual damping in the systems.

Instability in the controlled system is most often caused by spillover [BCF] [FaC] [ZLA], where the controller inadvertently excites poorly described, unmodeled, or higher frequency modes. Since LSS will often have large numbers of closely spaced modes[KMC], it will be difficult to decide which modes should be kept for control synthesis. It will also be difficult to improve models of these modes with experimental data. Generally, keeping more modes increases the size and computational costs of the controller[DGK][SaF].

Higher frequency modes are often left out of models developed by methods such as finite element analysis (FEA) because of the errors inherent in applying a discrete modeling technique such as FEA to theoretically continuous structures. Spillover instability may also be caused by finite actuator dynamics on a continuous system [FaC][IBA][SiP][ZiI]. [FaC] and [IBA] describe ways to analyze the interactions of finite dynamic actuators and sensors with continuous structures.

The type of actuators and sensors that are used is another area of concern. Attitude control systems incorporate actuators such as momentum exchange devices or reaction jets. In performing rigid body motions, however, these also excite flexible modes. Thus, for vibrations control, an actuator that does not cause coupling between rigid and flexible motions is desired. Active members [AMF] have been developed for this purpose. The dual problem with sensors is that accelerometers

and rate sensors measure the combination of rigid and flexible motions. It is difficult to separate these for proper control. Strain based and differential sensing may solve this problem [Fan].

Locating the sensors and actuators on the structure to obtain optimal control is also important. According to [BaD], noncolocation limits the effectiveness of the control system as the actuators must use structural load paths to induce the desired effect. Colocation, however, is often impossible because of mission requirements. [NoS] gives an outline for an integer programming problem to choose the optimal locations. [FBC] presents a method for location selection based on energy arguments.

Often sensors and actuators are noisy or inaccurate. If this is not accounted for, instability may also occur. The choice of what type of noise may be expected will affect optimality of the controller. Allowing for more noise, or more uncertainties in the system [BCD][BaD][Smi] will result in a more robust controller; however, as robustness is increased, achievable performance is decreased.

Robustness to physical changes in the structure may also be incorporated in the controller. Some common system alterations are expenditure of fuel by reaction jets, docking with other structures, sensor or actuator failure, and component failure [GoC][OMT]. [HJP] showed by simulation that decreases in structural masses on the system (fuel usage, for example) destabilize the controlled system much more rapidly than increases in mass.

Uncertainty about the system may be reduced by increased identification of the assembled system. This, however, may be difficult and expensive. The tradeoff between identification and control is described mathematically in [UdF], where a two point boundary value problem results.

2.3.3. Classical/SISO Control Methods

Classical methods have been developed and used since the 1930's. For systems where the sensors and actuators are colocated, these methods can be designed to have nice robustness and stability properties. Also, because of relatively simple form, they are easy to implement. Design of these controllers is usually done using

a trial and error approach which utilizes Bode and Nyquist plots of the controlled system to achieve desired properties[FPE].

For general systems, the standard classical methods are gain stabilization and phase stabilization[Rut]. For gain stabilization, the gain of the controller is reduced at selected frequencies. This method is robust to phase uncertainty, but its performance is not always very good. The system being controlled must have a band in the frequency domain without any modes so that the controller's gain may be rolled off (reduced) without danger of destabilizing the plant.

For phase stabilization, the gain crossover is chosen at a frequency where the amplitude of the plant's response begins to roll off (bending frequency). This results in a controller with a larger bandwidth and with higher performance than a gain stabilizing one. Unfortunately these controllers are difficult to design, and they are not very robust to uncertainty.

Structural systems are of a form where under ideal conditions direct velocity feedback (DVF) can be used to increase the system's damping [CaG] [GCa]. According to [CaG], spillover due to unmodeled modes is beneficial for DVF, but spillover due to finite sensor and actuator dynamics may cause instability [CaG][ZiI]. Noncolocated DVF is more difficult since wave travel speeds must be accounted for. When multiple inputs and outputs are available for use, decentralized controllers may be designed such that a controller is designed for each sensor/actuator pair.

Another method for structures was developed by Caughey and Goh [CaG] [Fan]. This technique, known as positive position feedback (PPF) is also stable to spillover. Proofs on stability and performance of this tuning filter method exist and are stronger than those for DVF. Another nice feature is that the method has an inherent two pole rolloff, thus it will not destabilize higher frequency modes.

When the system is modal, as lightly damped structures are assumed to be, independent modal control may be used[ZLA]. Here, the equations of motion are transformed to modal coordinates, and a desired eigenstructure is imposed by using a feedback gain matrix. Unfortunately, this method requires a large number of sensors and actuators.

2.3.4. State Space Methods

Linear Quadratic Gaussian Control

The most often used state space control synthesis method is presently linear quadratic Gaussian control (LQG)[KwS]. In this method, cost functions based on the expected value of a disturbance of chosen frequency spectrum are minimized, thereby giving the optimal controller[DGK][HJP]. The cost of actuator usage can also be included in the cost function, thereby setting up a tradeoff between actuator cost and achievable performance.

The standard LQG problem has no guarantees as to robustness to parametric/structured uncertainty in the model of the plant. It is able to handle this type of uncertainty only if it is treated as an additive noise (unstructured uncertainty)[WiG]. This however, leads to a much more conservative controller with lower performance than if the uncertainty were treated as structured.

Several modifications have been made to the LQG problem formulation to allow for different kinds of noise and uncertainties. [BlM] modifies the method by adding structured uncertainty to the cost function. The technique does not have guaranteed stability properties, but a tradeoff is set up where the controller may be made insensitive to parameter variations. In [PaS], set theoretic disturbances are applied to allow for unknown, but bounded disturbances. This allows for imposition of time-domain constraints to a problem formulated in the frequency domain. Structured and unstructured uncertainties are collapsed into the cost function in [CaB] to reduce sensitivity of the LQG controller to structured uncertainty. [PhC] contains several examples of LQG with maximum entropy/optimal projection, which incorporates a tradeoff between sensor accuracy, controller order, and robustness, against performance.

H_∞ Optimal Control

Because of the lack of guarantees of robustness of LQG controllers, in the 1980's H_∞-optimal state space methods were developed. While LQG control is designed for signals of bounded energy with known spectra, H_∞ control has guaranteed robustness to the worst case signals of bounded magnitude [BHN][DGK][DGF][HJP]. When this method is combined with μ-analysis [Bal][BCD][Pac], structured uncertainties can be incorporated into the description

of disturbances to the system. Then the controller will have guaranteed stability to these structured uncertainties. Also, because of allowance for disturbances of bounded amplitude, persistent excitations may also be considered for control. More complete descriptions of μ-synthesis are given in [BCD] [CMV][Pac].

[DGK] gives a synthesis procedure which results in controllers of the same order (size in state space) as the plant to be controlled. Thus, smaller descriptions of the structure result in smaller order controllers. This makes computation simpler. (LQG has the same feature).

2.3.5. Nonlinear Control

There is a large number of techniques that are classifiable as nonlinear control, but only a few of these shall be discussed here. The simplest control system is an on-off, or bang-bang type controller[FPE][BVJ] [MBC]. For slewing maneuvers, these methods turn an actuator on fully until the system reaches a neighborhood of the desired position, at which time the actuator output is reversed. The actuator effort is switched until the motion of the system stays within a particular region of the desired configuration.

Application of this type of control to civil structures is discussed in [MBC] where external excitation is caused by earthquakes. The author points out that the method can be used for both linear and nonlinear structures, but continuous monitoring of the system's states is required. The switching of the actuator is designed to apply forces at optimum times to keep the motion of the structure minimized. The switching often introduces time lags which must be accounted for.

Another commonly used nonlinear strategy for structures is adaptive control [IBA][SiN]. Here a gain on a linear control algorithm such as LQG or H_∞ is updated often to give the optimum signal for control. [SiN] presents four adaptive control algorithms for scheduling the gains on a proportional-integral-derivative scheme. That is, displacement, velocity, and the integral of displacement are measured and fed back to the actuators. Several nonlinear equations need to be solved at each time step based on desired eigenvalues and steady state errors. [IBA] discusses use of model-reference-adaptive control, where the main concerns are unmodeled dynamics, input saturation, and time delay saturations. The method is described as inherently robust to unmodeled dynamics.

A quadratic cost for flexible structures with stochastic excitations is presented in [YLW]. This scheme requires solution of the LQG equations at every time step. This instantaneous optimal control is not robust to uncertainties. Unfortunately, it also suffers from being quite expensive computationally. As with [IBA], the observer for this system ends up being a Kalman filter. In [IBA] the filter is used for rate estimation, while in [YLW] it is used for state estimation.

[Isi] presents theory for entirely nonlinear controllers. Robustness of these methods is minimal, as they require inversion of the plant model, followed by application of linear controllers.

2.3.6. Robustness Measures

One of the most important features of feedback control systems is robustness to noise and parameter uncertainties. If proper provision is not made for these effects, the controller's performance will be dramatically reduced. The reduction may be enough for the controller to cause instability of the closed loop system.

Determination of robustness of classic controllers is done using Nyquist and Bode plots. The standard measures are gain margin and phase margin. For SISO systems, these are generally quite good measures. For MIMO systems, however, interaction between control inputs and outputs is not accounted for, so these quantities are not informative robustness indices.

Situations can arise in SISO and MIMO systems where variation of a single parameter would give large stability margins, but simultaneous variations of multiple parameters gives unacceptably small margins [Doya]. Thus, a measure based on the maximum singular value of a perturbation matrix has been introduced for robustness analysis[Pac] [Doya].

This measure, known as μ [BCD], uses information about relationships between uncertain parameters (structured uncertainty) to find the worst case perturbation that would destabilize a controlled system. Based on scalings used to find these worst case signals, filters can be placed on the disturbance models specified for the H_∞-synthesis to make the controller robust to parametric type uncertainties. This gives rise to the μ-synthesis procedure [Bal][Pac].

The concepts of μ-synthesis have been applied to LQG control in [BlM] and [WiG], however, in these cases, guarantees on stability of the system do not hold. In H_∞ theory, the guarantees hold because the method is designed for the worst case disturbance. In LQG, the method designs for a known spectrum of disturbance, which is usually not the worst case.

Another robustness measure procedure is to test the closed loop system with the various parameters set to the upper and lower bounds [BlM][BWG]. Based on Kharitonov's theorem [Sid], if all combinations of upper and lower bounds are tested, bounds on stability of all possible combinations of parameters are developed. Thus one only needs to test the outer limits of variation. For problems with many parameters, this becomes very expensive computationally.

2.3.7. Demonstrations/Applications

Implementation of the above vibration reduction methods to structural systems often illustrates advantages and errors of the particular techniques. [WiD] demonstrates passive damping on numerical simulations of the Hubble telescope and a on truss system. Settling time was improved significantly.

In [Rut], a numerical comparison is made of classical gain and phase stabilization methods with H_∞-optimal control on a flexible missile. Ruth [Rut] showed that the best classical controllers achieve about the same performance levels as the H_∞ designed compensator, but the state space method is more robust.

Direct velocity feedback was used in tendon control of a beam in [MOT]. This experimental demonstration obtained some performance for low frequency modes, but higher frequency modes were unstable due to tendon flexibility.

Control work on truss structures at the Jet Propulsion Laboratory is discussed in [BCD], [BCF], [FaG], [FaC], and [FBC]. Work began with positive position feedback on a cantilevered beam[Fan] [FaC], where 20% critical damping was obtained by Fanson. Here, strain-based sensing and active-member actuation were used. A truss structure was then constructed[FBC] for further experiments. Among the control methods used, decentralized positive position feedback, decentralized colocated velocity feedback, LQG, and H_∞ control have been applied with varying degrees of success.

In [PSW], Padula *et al,* discuss combined structure and controller optimization using LQG methods. The goal is to minimize mass and power consumption of the control system while constraining strength, vibration characteristics, and damping of the structure. A numerical example is presented as a demonstration of the procedure. [WiG] gives a numerical simulation of LQG control of a truss structure. Persistent excitations, such as those caused by parameter uncertainties are incorporated into the problem specification.

A set of four excellent experimental demonstrations which use an LQG algorithm with increased robustness through use of maximum entropy/optimal projection method is given in [PhC]. These demonstrations were on a multi-link pendulum, a thin plate, a multi-hex optical reflector, and a truss structure. One of the conclusions the authors present is that more work needs to be done on control of sampled data systems.

Numerical simulations of H_∞-optimal control are given in [Rut], as already discussed, and in [BWG] and [HBY]. In [BWG] effects of inertia changes due to motion of a robotic arm are discussed. In [HBY] good theoretical increases in damping were shown on a reduced size model of a truss. When the controller was applied to a more complete model of the system, the controller still obtained decent performance, although it was not as good as that on the reduced order representation.

Experimental demonstrations of H_∞/μ-synthesis have been made at Caltech and at JPL [Bal][BCD][BaD]. Balas demonstrated good vibration attenuation on a lightly damped structure with very closely spaced modes using both colocated and noncolocated sensor/actuator pairs. The parameter variations and disturbances used to synthesize these robust controllers were developed from *ad hoc* judgement methods. Much work remains on development of uncertainty models. H_∞/μ-synthesis was also demonstrated on the JPL/AFAL hoop ring antenna structure [BCD]. Here, several SISO and MIMO controllers were designed based on theoretical models of the system. Large amounts of uncertainty were incorporated into the synthesis models because of poor models of the system. More performance could have been obtained with better models.

Numerical simulations of nonlinear on-off type control are given in [MBC] and [YLW] for civil structures and in [BVJ] for a prototype flexible structure. In [IBA],

adaptive control is experimentally demonstrated on the JPL/AFAL structure. Good perturbation reduction was achieved. Some of the implementation difficulties are discussed.

In [MFK], docking and separation of a truss with variable geometry is shown experimentally. Here, the variable geometry of the system is used to compensate for changes in inertia properties of the base system.

2.4 References for Chapter 2

References for Structural Identification

Bmu: Balas, G., *et al.*, (1991),**μ-Analysis and Synthesis Toolbox,** MUSYN, Inc., and The Math Works, Inc., Natick, Massachusetts.

Bec: Beck, J.L., (1990), "User's Guide for Mode-ID," Version 5.0, Pasadena, California.

BkB: Beck, R.T., and Beck, J.L., (1985), "Comparison Between Transfer Function and Modal Minimization Methods for System Identification," EERL Report # 85-06, California Institute of Technology, Pasadena, California.

Ber: Berman, A., (1984), "System Identification of Structural Dynamics Models - Theoretical and Practical Bounds," AIAA Paper # 84-0929.

Bow: Bowles, R.L., and Straeter, T.A., (1972), "System Identification Computational Considerations," from *System Identification of Vibrating Structures, Mathematical Modes from Test Data,* Pilkey, W.D., and Cohen, R., eds., ASME Winter Annual Meeting.

Bra: Brandon, J.A., (1988), "On the Robustness of Algorithms for the Computation of the Pseudo-Inverse for Modal Analysis," *Proceedings of the 6^{th} International Modal Analysis Conference,* Kissimmee, Florida, pp. 397-400.

BrR: Braun, S., and Ram, Y., (1988), "On the Fitting of Structural Models to Data," *Proceedings of the 6^{th} International Modal Analysis Conference,* Kissimmee, Florida, pp. 789-793.

Bro: Brogan, W.L., (1985), **Modern Control Theory,** 2^{nd} Ed., Prentice-Hall, Englewood Cliffs, NJ.

Cau: Caughey, T.K., (1982), "Structural Dynamics Analysis, Testing, and Correlation," JPL Publication 81-72, Pasadena, CA.

Che: Chen, J.C., and Fanson, J.L., (1989), "System Identification Test Using Active Members," AIAA Paper # 89-1290.

Cra: Craig Jr., R.R., Kurdila, A.J., and Kim, H.M., (1990), "State-Space Formulation of Multi-Shaker Modal Analysis," *International Journal of Analytical and Experimental Modal Analysis,* 5(3), pp. 169-183, July.

CrB: Craig Jr., R.R., and Blair, M.A., (1985), " A Generalized Multiple-Input, Multiple-Output Modal Parameter Estimation Algorithm," *AIAA Journal* 23(6), pp. 931-937, June.

Dai: Dailey, R.L., and Lukich, M.S., (1987), "MIMO Transfer Function Curve Fitting Using Chebyshev Polynomials," *Proceedings of SIAM 35th Anniversary Meeting,* Denver, CO.

Ebe: Ebersbach, P., and Irretier, H., (1989), "On the Application of Modal Parameter Estimation using Frequency Domain Algorithms," *International Journal of Analytical and Experimental Modal Analysis,* (4) 4, pp. 109-116, Oct.

Ful: Füllekrug, U., (1989) "Structural Dynamics Identification in the Time Domain: Estimation of Modal Parameters Based on Forced Vibrations," *International Journal of Analytical and Experimental Modal Analysis,* pp. 59-67, April, and (1988), *Proceedings of the 6th International Modal Analysis Conference,* Kissimmee, FL, pp. 1053-1062.

Hsi: Hsieh, B.J., Kot, C.A., and Srinivasan, M.G., (1983), "Evaluation of System Identification Methodology and Application," U.S. Nuclear Regulatory Committee Report NUREG/CR-3888.

Ibr: Ibrahim, S., (1985), "Modal Identification Techniques: Assessment and Comparison," *Proceedings of the 3rd International Modal Analysis Conference,* Orlando, FL, January.

Ibb: Ibrahim, S., (1988), "Modal Identification from Control versus Structural Dynamics Views," *Proceedings of the 6th International Modal Analysis Conference,* pp. 1-7, Kissimmee, FL.

Kie: Kientzy, D., Richardson, M., and Blakely, K., (1983), "Using Finite Element Data to set up Modal Tests," *Sound and Vibration,* pp. 16-23, June.

Lie: Lieven, N.A.J., and Ewins, D.J., (1988), "Spatial Correlation of Mode Shapes, The Coordinate Modal Assurance Criterion (COMAC)," *Proceedings of the 6th International Modal Analysis Conference,* Kissimmee, Florida, pp. 690-695.

Lju: Ljung, L., (1987), **System Identification: Theory for the User,** Prentice-Hall, Inc., Englewood Cliffs, NJ.

McV: McVerry, G.H., (1979), "Frequency Domain Identification of Structural Modes from Earthquake Records," EERL Report # 79-02, California Institute of Technology, Pasadena, CA, October.

McB: McVerry, G.H., and Beck, J.L., (1983), "Structural Identification of JPL Building 180 Using Optimally Synchronized Earthquake Records," EERL Report # 83-01, California Institute of Technology, Pasadena, CA, August.

Min: Minas, C., and Inman, D.J., (1988), "Correcting Finite Element Models via Measured Modal Results using Eigenstructure Assignment Methods," *Proceedings of the 6th International Modal Analysis Conference,* Kissimmee, Florida, pp. 583-587.

Mos: Moser, A.N., and Caughey, T.K., (1991), "Some Experiences with Identification of the Caltech Space Structure," *Proceedings of the 1991 American Controls Conference,* Boston, MA, June.

Nat: Natke, H.G., (1978), "Survey on Identification of Mechanical Systems," *Road Vehicle Systems and Related Mathematics Workshop,* Turin, Italy, June.

Oja: Ojalvo, I.U., Ting, T., and Pizon, D., (1989), "PAREDYM- A Parameter Refinement Computer Code for Structural Dynamics Models," *International Journal of Analytical and Experimental Modal Analysis,* 5(1), pp. 43-49, January.

Pot: Potter, R., and Olsen, N., (1988), "Modal Analysis for the Connossieur," *Sound and Vibration,* pp. 18-25, January.

Sag: Sage, A.P., (1972), "System Identification History, Methodology, Future Prospects," *System Identification of Vibrating Structures-Mathematical Models from Test Data,* ASME Winter Annual Meeting, pp. 1-21.

Sch: Schmidtberg, R., and Pal, T., (1986), "Solving Vibration Problems Using Modal Analysis," *Sound and Vibration,* pp. 16-21, March.

Sir: Siriam, P., Craig, J.I., and Hanagard, S., (1990), "A Scanning Laser Doppler Velocimeter for Modal Testing," *International Journal of Analytical and Experimental Modal Analysis,* 5(3), pp. 155-167, July.

Spa: Spanos, J.T., (1990), "Order Reduction and Synthesis of Transfer Function Models," JPL Publication D-8065, Pasadena, CA, December.

Str: Stroud, R.C., (1987), "Excitation, Measurement, and Analysis Methods for Modal Testing," *Sound and Vibration,* pp. 12-27, August.

Toh: Tohyama, M., (1989), "Zeroes of a Transfer Function in a Multi-Degree-of-Freedom Vibrating System," *Journal of the Acoustical Society of America,* 86(5), November.

Vol: Vold, H., Kundrat, J., Rocklin, G.T., and Russel, R., (1982), "A Multi-Input Modal Estimation Algorithm for Mini-Computers," SAE Paper #820194.

References for Structural Modifications

AOM: Avitable, P., O'Callahan, J., and Milani, J., (1988), "Comparison of Complex and Proportional Mode Structural Dynamic Modification Techniques," *Proceedings of the 6^{th} International Modal Analysis Conference,* Kissimmee, FL, pp. 555-564.

Aro: Arora, J.S., (1976), "Survey of Structural Reanalysis Techniques," *ASCE Journal of the Structural Division,* pp. 783-802, April.

BaH: Baldwin, J.F., and Hutton, S.G., (1985), "Natural Modes of Modified Structures," *AIAA Journal,* 23(11), pp. 1737-1743, November.

Ben: Bernard, D.E., (1989), "Component Mode Reduction Via the Projection and Assembly Method," *Proceedings of the 3^{rd} Annual Conference on Aerospace Computational Control,* JPL Publication 89-45, Vol. 2., Pasadena, CA.

Bla: Blackwood, G.H., (1988), "Experimental Component Mode Synthesis of Structures with Joint Freeplay," Report SSL#16-88, Space Systems Laboratory, Massachusetts Institute of Technology, Cambridge, Massachusetts.

Bra: Brandon, J.A., (1988), "On the Robustness of Algorithms for the Computation of the Pseudo-Inverse for Modal Analysis," *Proceedings of the 6^{th} International Modal Analysis Conference,* Kissimmee, Florida, pp. 397-400.

Brab: Brandon, J.A., (1984), "Limitations for the Use of an Exact Formula for Receptance Reanalysis," *International Journal for Numerical Methods in Engineering,* 20, pp. 1575-1580.

Brac: Brandon, J.A., (1990), **Strategies of Structural Dynamics Modifications,** Engineering Dynamics Series, Vol. 6., John Wiley & Sons.

Bro: Brogan, W.L., (1985), **Modern Control Theory,** 2^{nd} Ed., Prentice-Hall, Englewood Cliffs, NJ.

ChS: Chiatti, G., and Sestieri, A., (1979), " Analysis of Static and Dynamic Structural Problems by a Combined Finite Element-Transfer Matrix Method," *Journal of Sound and Vibration* 67(1), pp. 35-42.

ClP: Clough, R.W., and Penzien, J., (1975), **Dynamics of Structures** M°Graw-Hill Book Co., pp. 232-235.

CBr: Craig Jr., R.R., and Brampton, M.C.C., (1968), "Coupling of Substructures for Dynamic Analysis," *AIAA Journal,* 6(7), pp. 1313-1319, July.

CrB: Craig Jr., R.R., and Blair, M.A., (1985), " A Generalized Multiple-Input, Multiple-Output Modal Parameter Estimation Algorithm," *AIAA Journal* 23(6), pp. 931-937, June.

CKR: Crowley, J.R., Klosterman, A.L., Rocklin, G.T., and Vold, H., (1984), "Direct Structural Modification Using Frequency Response Functions," *Proceedings of the* 2^{nd} *International Modal Analysis Conference,* Union College, Schenectady, NY, pp. 930-936.

Dok: Dokainish, M.A., (1972), "A New Approach for Plate Vibrations: Combination of Transfer Matrix and Finite Element Techniques," *ASME Journal of Engineering in Industry,* May, pp. 526-530.

Fla: Flashner, H., (1986), "An Orthogonal Decomposition Approach to Modal Synthesis", *International Journal for Numerical Methods in Engineering* 23, p. 471-493.

FoK: Fox, R.L., and Kapoor, M.P., (1968), "Rates of Change of Eigenvalues and Eigenvectors," *AIAA Journal,* 6(12), pp. 2416-2419, December.

GLM: Gwinn, K.W., Lauffer, and J.P., Millar, A.K., (1988), "Component Mode Synthesis using Experimental Modes Enhanced by Mass Loading", *Proceedings of the 6^{th} International Modal Analysis Conference,* Kissimmee, FL, pp. 1088-1093.

HaM: Hale, A.L., and Meirovitch, L., (1980), "A General Substructure Method for the Dynamic Simulation of Complex Structures," *Journal of Sound and Vibration,* 69(2), pp. 309-326.

Hal: Hallquist, J.O., (1976) "An Efficient Method for Determining the Effects of Mass Modifications in Damped Systems," *Journal of Sound and Vibration,* 44(3), pp. 449-459.

HaS: Hallquist, J.O., and Snyder, V.W., (1973), "Linear Damped Vibratory Systems with Arbitrary Support Conditions," Brief Note in *ASME Journal of Applied Mechanics,* pp. 312-313, March.

HEN: Hedges, T., Elliot, S.J., and Nelson, P.A., (1988), "The Active Simulation of Structural Frequency Response Functions," *Proceedings of the 6^{th} International Modal Analysis Conference,* Kissimmee, FL, pp. 67-72

Hur: Hurty, W.C., (1965), "Dynamic Analysis of Structural Systems using Component Modes," *AIAA Journal,* Vol 3, No. 4, pp. 678-685, April.

Jez: Jezequel, L., (1990), "Procedure to Reduce the Effects of Modal Truncation in Eigensolution Reanalysis," *AIAA Journal,* 28(5), May.

Jon: Jones, R.P.N., (1960), "The Effect of Small Changes in Mass and Stiffness on the Natural Frequencies and Modes of Vibrating Systems," *International Journal of Mechanical Sciences,* 1, pp. 350-355.

Kai: Kailath, T., (1980), **Linear Systems**, Prentice-Hall, Englewood Cliffs, New Jersey.

Ker: Kerstens, J.G.M, (1981), "Vibration of Complex Structures: The Modal Constraint Method," *Journal of Sound and Vibration,* 76(4), pp. 467-480.

Kerb: Kerstens, J.G.M, (1982), "Vibration of Modified Discrete Systems: The Modal Constraint Method," *Journal of Sound and Vibration,* 83(1), pp. 81-92.

Lar: Larsson, P.O., (1989), "Dynamic Analysis of Assembled Structures using Frequency Response Functions: Improved Formulation of Constraints," *International Journal of Analytical and Modal Analysis,* 5(1): pp. 1-12, January.

LuM: Luk, Y.W., and Mitchell, L.D., (1982), "System Modeling and Modification via Modal Analysis," *Proceedings of the 1st International Modal Analysis Conference,* Orlando, FL, pp. 423-429.

Mah: Mahalingam, S., (1975), "The Synthesis of Vibrating Systems by use of Internal Harmonic Receptances," *Journal of Sound and Vibration,* 40(3), pp. 337-350.

Min: Minas, C., and Inman, D.J., (1988), "Correcting Finite Element Models via Measured Modal Results using Eigenstructure Assignment Methods," *Proceedings of the 6th International Modal Analysis Conference,* Kissimmee, Florida, pp. 583-587.

NoW: Noor, A.K., and Whitworth, S.L., (1988), "Reanalysis Procedure for Large Structural Systems," *International Journal for Numerical Methods in Engineering,* 26, pp. 1729-1748.

OcC: O'Callahan, J.C., and Chou, C.M., (1988), "Localization of Model Changes for Optimized System Matrices Using Modal Test Data," *Proceedings of the 6th International Modal Analysis Conference,* Kissimmee, FL, pp. 49-55.

Ojb: Ojalvo, I.U., (1988), "Origins and Advantages of Lanczos Vectors for Large Dynamic Systems," *Proceedings of the 6th International Modal Analysis Conference,* Kissimmee, FL, pp. 489-494.

Ozg: Ozguven, H.N., (1990), "Structural Modification using Frequency Response Functions," *Mechanical Systems and Signal Processing,* 4(10), pp. 53-63.

Paz: Paz, Mario, (1984), "Dynamic Condensation," Technical Note: *AIAA Journal,* 22(5), May.

PoS: Pomazal, R.J., and Snyder, V.W., (1971), "Local Modifications of Damped Linear Systems," *AIAA Journal,* 9(11), pp. 2216-2221, Nov.

RHR: Romstad, K.M., Hutchinson, J.R., and Runge, K.H., (1973), "Design Parameter Variation and Structural Response," *International Journal for Numerical Methods in Engineering,* 5, pp. 337-349.

SBC: Sadeghipour, K., Brandon, J.A., and Cowley, A., (1985), "The Receptance Modification Strategy of a Complex Vibrating System," *International Journal of Mechanical Sciences*, 27 (11/12), pp. 841-846.

SeD: Sestieri, A., D'Ambrogio, W., (1988), "Why be Modal: i.e., How to Avoid the use of Modes in the Modification of Vibrating Systems," *Proceedings of the 6^{th} International Modal Analysis Conference,* Kissimmee, FL, pp. 1100-1106.

Spa: Spanos, J.T., (1990), "Order Reduction and Synthesis of Transfer Function Models," JPL Publication D-8065, Pasadena, CA, December.

SpT: Spanos, J.T., and Tsuha, W.S., (1989), "Multibody Dynamics: Modeling Component Flexibility with Fixed, Free, Loaded, Constraint, and Residual Modes," *Proceedings of the 3^{rd} Annual Conference on Aerospace Computational Control,* JPL Publication 89-45, Pasadena, CA, pp. 761-777, December.

StH: Stetson, K.A., and Harrison, I.R., (1981), "Redesign of Structural Vibration Modes by Finite Element Inverse Perturbation," *ASME Journal of Engineering for Power,* 103, pp. 319-325, April.

SuS: Suarez, L.E., and Singh, M.P., (1987), "A Modal Coupling Procedure for Structural Dynamics," *Proceedings of ASCE Dynamics of Structures, Structures Congress,* Orlando, FL, pp. 1-14.

TsY: Tsuei, Y.G., and Yee, E.K.L., (1988), "An Investigation to the Solution of Component Modal Synthesis," *Proceedings of the 6^{th} International Modal Analysis Conference,* Kissimmee, FL pp. 383-396.

WSR: Wallace, P., Skoog, P., and Richardson, M., (1988), "Simultaneous Structural Dynamics Modification (S^2DM)," *Proceedings of the 6^{th} International Modal Analysis Conference,* Kissimmee, FL, pp. 1033-1038.

WaL: Wang, J.H., and Liou, C.M., (1989), "Experimental Substructure Synthesis with Special Consideration of Joint Effects," *International Journal of Analytical and Experimental Modal Analysis,* 5(1): pp. 13-24.

Wei: Weissenburger, J.T., (1968), "Effect of Local Modifications on the Vibratory Characteristics of Linear Systems," *ASME Journal of Applied Mechanics,* pp. 327-332, June.

Zas: Zastrau, B.W., (1988), "Energy-Based Modal Coupling of Multi Degree of Freedom Substructures-A Finite Element Approach," *Proceedings of the 6^{th} International Modal Analysis Conference,* Kissimmee, FL, pp. 291-298

ZWA: Zhang, Q., Wang, W., Allemang, R.J., and Brown, D.L., (1989), "Prediction of Mass Modification for Desired Natural Frequencies," *International Journal of Analytical and Experimental Modal Analysis,* pp. 39-45, April.

References for Control Theory and Applications

AlJ: Alt, T.R., and Jabari, P., (1990), "Bounds on Parameter Uncertainties for Preserving a Minimum Damping of a Vibration Suppression System," AIAA #90-3357.

AMF: Anderson, E.H., Moore, D.M., Fanson, J.L., and Early, M.A., (1990), "Development of an Active Member using Piezoelectric and Electrostrictive Actuation for Control of Precision Structures," AIAA #90-1685, *Proceedings of the AIAA/ASME/ASCE 31^{st} Structures, Structural Dynamics, and Materials Conference,* Long Beach, CA April.

Bal: Balas, G.J., (1990), "Robust Control of Flexible Structures: Theory and Experiments," Ph.D. Thesis, Aeronautical Engineering Department, California Institute of Technology, Pasadena, CA.

BCD: Balas, G.J., Chu, C.C., and Doyle, J.C., (1989), "Vibration Damping and Robust Control of the JPL/AFAL Experiment Using μ-synthesis," *Proceedings of the 28^{th} Conference on Decision and Control,* Tampa, FL, December.

BaD: Balas, G.J., and Doyle, J.C., (1990), "Collocated versus Non-collocated Multivariable Control for Flexible Structures," *Proceedings of the American Controls Conference,* San Diego, CA.

BDo: Balas, G.J., and Doyle, J.C., (1988), "On the Caltech Experimental Large Space Structure," *Proceedings of the American Controls Conference,* Atlanta, Georgia.

BHN: Bernstein, D.S., Haddad, W.M., and Nett, C.N., (1989), "Minimal Complexity Control Law Synthesis, Part 2: Problem Solution via H_2/H_∞ Optimal State Feedback,' *Proceedings of the American Controls Conference,* Pittsburgh, PA.

BCF: Blackwood, G.H., Chu, C.C., Fanson, J.L., and Sirlin, S.W., (1989), "Uncertainty Modeling for the Control of an Active Structure," *ASME #AD Vol. 15, 1989 Winter Annual Meeting,* San Francisco, CA, December.

BlM: Bleloch, P.A., and Mingori, D.L., (1990), "Robust Linear Quadratic Gaussian Control for Flexible Structures," *AIAA Journal of Guidance and Control,* 13(1), pp. 66-72.

Bro: Brogan, W.L., (1985), **Modern Control Theory,** 2^{nd} Ed., Prentice-Hall, Englewood Cliffs, NJ.

BVJ: Byers, R.M., Vadali, S.R., and Junkins, J.L., (1990), "Near Minimum Time, Closed Loop Slewing of Flexible Spacecraft," *AIAA Journal of Guidance and Control,* 13(1), pp. 57-65.

BWG: Byun, K.W., Wie, B., Geller, D., and Sunkel, J., (1990), "Robust H_∞ Control Design for the Space Station with Structured Parameter Uncertainty," AIAA #90-3319, *Proceedings of the AIAA Guidance, Navigation, and Control Conference,* Portland, OR, August.

CaB: Calise, A.J., and Byrns, Jr., E.V., (1989), "Robust Fixed Order Dynamic Compensation," AIAA #89-3458, *Proceedings of the AIAA Guidance, Navigation, and Control Conference,* Boston, MA, August.

CaG: Caughey, T.K., and Goh, C.J., (1983), "Vibration Suppression in Large Space Structures," *Proceedings of the Workshop on Application of Distributed System Theory to the Control of Large Space Structures,* JPL Publication 83-45, pp. 119-142.

CMV: Caughey, T.K., Moser, A.N., and Vakakis, A.F. (1989), "On Modeling and Control of Uncertain Systems Representative of Large Space Structures." *Dynamics Laboratory Research Report, DYNL # 89-02,* California Institute of Technology, Pasadena, California.

Doya: Doyle, J., (1988), "Analysis of Control Systems", Lecture Notes, California Institute of Technology.

Doyb: Doyle, J., (1988), "Synthesis of Control Systems", Lecture Notes, California Institute of Technology.

DGK: Doyle, J., Glover, K., Khargonekar, P., and Francis, B., (1989), "State Space Solutions to standard H_2 and H_∞ Control Problems," *IEEE Transactions on Automatic Control* Vol. AC 34, pp. 831-847. Aug.

DGF: Doyle, J., Glover, K., Khargonekar, P., and Francis, B., (1988), "State Space Solutions to standard H_2 and H_∞ Control Problems," *Proceedings of the American Controls Conference,* Atlanta, GA.

DoG: Doyle, J. and Glover, K., (1988), "State Space Formulae for all Stabilizing Controllers that Satisfy an H_∞-norm Bound and Relations to Risk Sensitivity," Submitted for Publication, April.

Fan: Fanson, J.L., (1987), "An Experimental Investigation of Vibration Suppression in Large Space Structures using Positive Position Feedback", Ph.D. Thesis, Applied Mechanics Department, California Institute of Technology, Pasadena, CA.

FaG: Fanson, J.L., and Garba, J.A., (1988), "Experimental Studies of Active Members in Control of Large Space Structures," *AIAA #88-2207.*

FaC: Fanson, J.L., and Caughey, T.K., (1987), "Positive Position Feedback Control for Large Space Structures," *AIAA #87-0902.*

FBC: Fanson, J.L., Blackwood, G.H., and Chu, C.C., (1989), "Active Member Control of Precision Structures," *AIAA #89-1329.*

Fra: Francis, B.A., (1987), **A Course in H_∞ Control Theory,** Springer-Verlag, Berlin.

FPE: Franklin, G.F., Powell, J.D., and Emami-Naemi, A., (1985), **Feedback Control of Dynamic Systems,** Addison-Wesley, Reading, MA.

GoC: Goh, C.J., and Caughey, T.K., (1985), "A Quasi-linear Vibration Suppression Technique for Large Space Structures via Stiffness Modification," *International Journal of Control,* 41(3), pp. 803-811.

GCa: Goh, C.J., and Caughey, T.K., (1985), "On the Stability Problem Caused by Finite Actuator Dynamics in the Collocated Control of Large Space Structures," *International Journal of Control,* 41(3), pp. 787-802.

HBY: Heise, S., Banda, S., and Yeh, H., (1990), "Robust Control of a Flexible Space Structure in the Presence of Parameter Variations and Unmodeled Dynamics," *Proceedings of the 28th Aerospace Sciences Meeting,* Reno, Nevada, AIAA#90-0752, pp. 1-9.

HJP: Hwang, C.N., Jayasuriya, S., Parlos, A., and Sunkel, J.W., (1990),"Active Rejection of Persistent Disturbances in Flexible Structure," *Proceedings of the AIAA Guidance, Navigation, and Control Conference,* Portland, OR, August.

IBA: Ih, C.H.C., Bayard, D., Ahmed, A., and Wang, S.J., (1990), "Experimental Study of Robustness in Adaptive Control for Large Flexible Structures," AIAA #90-3498, *Proceedings of the AIAA Guidance, Navigation, and Control Conference,* Portland, OR, August.

Isi: Isidori, A., (1989), **Nonlinear Control Systems,** 2^{nd} Ed., Springer-Verlag, Heidelberg.

Kai: Kailath, T., (1980), **Linear Systems,** Prentice Hall, Englewood Cliffs, NJ.

KMC: Kaszubowski, M.J., Martinovic, Z.N., and Cooper, P.A., (1990), "Structural Dynamic Characterization of a Space Station Freedom First Assembly Flight Concept," *Proceedings of the 28^{th} Aerospace Sciences Meeting,* Reno, Nevada, AIAA#90-0748.

KwS: Kwakernaak, H., and Sivan, R., (1972), **Linear Optimal Control Systems,** John Wiley and Sons, New York.

MBC: Masri, S.F., Bekey, G.A., and Caughey, T.K., (1981), "Optimum Pulse Control of Flexible Structures," *ASME Journal of Applied Mechanics,* Vol. 48.

MFK: Matsuzaki, Y., Furuya, H., Kuwao, F., and Takahara, K., (1990) "Docking/ Separation Test of a Two-Dimensional Truss Structure with Variable Geometries," AIAA #90-0845, *Proceedings of the AIAA/ASME/ASCE 31^{st} Structures, Structural Dynamics, and Materials Conference,* Long Beach, CA, April.

MSR: M^{c}Greevy, S., Soong, T.T., and Reinhorn, A.M., (1988) "An Experimental Study of Time Delay Compensation in Active Structure Control," *Proceedings of the 6^{th} International Modal Analysis Conference,* Kissimmee, Florida, pp. 733-739.

MoZ: Morari, M., and Zafiriou, E., (1989), **Robust Process Control,** Prentice Hall, Englewood Cliffs, NJ.

MOT: Murotsu, Y., Okubo, H., Terui, F., Senda, K., and Shinoda, K., (1988), "Dynamics and Control of Experimental Tendon Control for Flexible Space Structures," *Proceedings of the AIAA Guidance, Navigation, and Control Conference,* Minneapolis, MN.

NoS: Norris, G.A., and Skelton, R.E., (1989), "Selection of Dynamic Sensors and Actuators in the Control of Linear Systems," *ASME Journal of Dynamic Systems, Measurement, and Control,* Vol. 111, pp. 389-397, September.

OMT: Okubo, H., Murotsu, Y., and Terui, F., (1987), "Failure Detection and Identification in the Control of Large Space Structures," *Proceedings of the 10^{th} IFAC World Congress on Automatic Control,* Munich, July.

Pac: Packard, A., (1988), "What's New with μ," Ph. D. Thesis, Mechanical Engineering Department, University of California at Berkeley.

PSW: Padula, S.L., Sandridge, C.A., Walsh, J.L., and Haftka, R.T., (1990), "Integrated Controls-Structures Optimization of a Large Space Structure," AIAA #90-1058, *Proceedings of the AIAA/ASME/ASCE 31^{st} Structures, Structural Dynamics, and Materials Conference,* Long Beach, CA, April.

PaS: Parlos, A.G., and Sunkel, J.W., (1990), "A Nonlinear Optimization Approach in Disturbance Rejection in Flexible Space Structures," AIAA #90-3361, *Proceedings of the AIAA Guidance, Navigation, and Control Conference,* Portland, OR, August.

PhC: Phillips, D., and Collins, Jr., E.G., (1990), "Four Experimental Demonstrations of Active Vibration Control for Flexible Structures," AIAA #90-3483, *Proceedings of the AIAA Guidance, Navigation, and Control Conference,* Portland, OR, August.

Rut: Ruth, M.J., (1989), "A Classical Perspective on Application of H_∞ Control Theory to a Flexible Missile Airframe," *AIAA #89-3851-CP.*

SaF: Safonov, M.G., and Flashner, H., (1989), "Modeling and Robustness Issues in Control Design for Flexible Structures," *Proceedings of the American Controls Conference,* Pittsburgh, PA.

Sid: Sideris, A., (1989), "Synthesis of Control Systems", Lecture Notes, California Institute of Technology.

SiN: Silverberg, L., and Norris, M.A., (1990), "Self Tuning Algorithms for Uniform Damping Control of Spacecraft," AIAA #90-1174, *Proceedings of the AIAA/ASME/ASCE 31st Structures, Structural Dynamics, and Materials Conference,* Long Beach, CA, April.

SiP: Silverberg, L.M., and Park, S., (1990), "Interaction Between Rigid-Body and Flexible-Body Motions in Maneuvering Spacecraft," *International Journal of Guidance and Control,* 13(1), pp. 73-81.

SmD: Smith, R.S., and Doyle, J.C., (1988), "The Two Tank Experiment: A Benchmark Control Problem," *Proceedings of the American Controls Conference,* Atlanta, GA.

Smi: Smith, R.S., (1990), "Model Validation for Uncertain Systems," Ph.D. Thesis, Electrical Engineering Department, California Institute of Technology, Pasadena, California.

UdF: Udwadia, F.E., and Flashner, H., (1988), "Trade-offs Between Identification and Control in Dynamic Systems," *ASME Journal of Applied Mechanics,* pp. 939-945, Vol. 55, December.

WiG: Wie, B., and Gonzales, M., (1990), "Active Control Synthesis for Flexible Space Structures Excited by Persistent Disturbances," AIAA #90-3427, *Proceedings of the AIAA Guidance, Navigation, and Control Conference,* Portland, OR, August.

WiD: Wilson, J.F., and Davis, P.L., (1988), "Very High Damping in Large Space Structures," *Proceedings of the ASME Vibrations Conference,* Boston, MA.

YLW: Yang, J.N., Long, F.X., and Wong, D., (1988), "Optimal Control of Nonlinear Structures," *ASME Journal of Applied Mechanics,* Vol. 55, pp. 931-938, December.

ZLA: Zhang, Q., Liu, J.Y.H., Allemang, R.J., and Tsuei, Y.G., (1988), "Active Vibration Control of Flexible Structures by Eigenstructure Assignment Technique," *Proceedings of the 6th International Modal Analysis Conference,* Kissimmee, Florida, pp. 1015-1019.

ZiI: Zimmerman, D.C., and Inman, D.J., (1990), "On the Nature of the Interaction Between Structures and Proof Mass Actuators," *AIAA Journal of Guidance, Control, and Dynamics,* 13(1), pp. 82-84.

Chapter 3. Identification of The Caltech Flexible Structure

3.1 Introduction

As work proceeds in development of optimal control synthesis methods, the need for good modeling and identification techniques becomes more critical. Large space structures magnify the need for good models since they have multiple closely spaced modes with very light damping. Omission of a mode from the control model could easily result in system destabilization when active control is applied.

Significant work has been done on structural identification with varying degrees of success. Reviews are found in [Ibr], [Nat], [Sag], and [Str]. An experimental demonstration of a system with closely spaced modes was presented by [VKR], where excellent models are determined using the Polyreference technique with impulse responses.

Here, a demonstration is made of a frequency domain identification method, and the persistent excitation used to generate system motion is discussed. The error minimization algorithm is also discussed since it was found to have robust convergence properties. The frequency response function (FRF) for each input location was obtained by single point excitation and multiple point sensing (single input multiple output, or SIMO). If each SIMO FRF had been curve fit independently, the model developed would have more states than those necessary to adequately describe it. This would have complicated computation and implementation of the control system. Thus, the ideal identification of a linear system is multiple input multiple output (MIMO).

The choice was made to use only single point excitations, although Allemang has developed conditions for an effective multiple input excitation method [Str]. The main limitation of the multi-point excitations that were tried here is that transmission zeroes are obscured. At a particular frequency, there may be a sensor location which does not respond to excitation from a certain input location. This results in a transmission zero since the sensor signal is zero. However, if there is excitation from another location, the sensor's output may be nonzero. Since the computed transfer function is the quotient of the ouput and input signals (in the frequency domain), the system's response (to the first input) which should be zero will appear to be nonzero. For the experiments done here, the MIMO curve fit algorithm was applied to several SIMO experiment results assembled as a single MIMO data set. Each actuator was used to excite the structure, and the SIMO FRF's were assembled appropriately. If the structure is linear, this assembly should be equivalent to a MIMO experiment.

The main purpose of this chapter is to relate the problems and solutions experienced using a frequency domain curve fit algorithm on a structure with closely spaced modes. The input signals are discussed to provide a possible method for excitations of structures assembled in space. The numerical aspects of the curve fit method are explained since the minimization algorithms were found to be very robust to poor initial parameter estimates.

This chapter is organized as follows. In Section 2 a description is given of the algorithm used to perform the MIMO curve fit. As a basis for comparison, results of the application of this method to simple numerically generated examples are presented in Section 3. Section 4 describes the experimental system at Caltech which supplied the data. Then, the final section presents results of finite element models of the system, results of the curve fit, and a brief discussion of some of the difficulties experienced because of the closely spaced modes.

3.2 Curve Fit Algorithm

For curve fit, a frequency domain modal model was chosen. This is very similar in nature to ones used by [Mcv] and [EbI]. The idea is to model the FRF as a sum of FRF's of individual modes. Assume the system may be modeled by M modes, J inputs, and I outputs. The inertance transfer function from the j^{th} input to the i^{th} output at the k^{th} frequency sampling point ω_k is modeled as

$$T_{ij}(\omega_k) = \sum_{m=1}^{M} \frac{c_i^{(m)} b_j^{(m)} (-\omega_k^2)}{(f_m^2 - \omega_k^2) + 2\sqrt{-1} f_m \zeta_m \omega_k} + b_j^r c_i^r. \tag{3.1}$$

Here, $b_j^{(m)}$ is the j^{th} input weight, $c_i^{(m)}$ is the i^{th} output weight, f_m is the angular frequency (in rad/sec), and ζ_m is the per unit critical damping for the m^{th} mode. Effects of modes above the frequency band of interest are modeled as quasi-static input and output contributions through b_j^r and c_i^r. The structure is assumed to have classical normal modes, so the parameters are taken as real. The quantity $T_{ij}(\omega_k)$ is complex and corresponds to the Fourier transform of a system with force inputs and acceleration sensing (inertance) [Ewi].

The fit of the curve described by $T_{ij}(\omega_k)$ is to be iteratively improved, thus an error is defined. Data taken in the time domain may be transformed to the frequency (Fourier) domain using a fast Fourier transform giving the FRF

$$\gamma_{ij}(\omega_k) = \alpha_{ij}(\omega_k) + \sqrt{-1}\beta_{ij}(\omega_k), \tag{3.2}$$

where $\alpha_{ij}(\omega_k)$ and $\beta_{ij}(\omega_k)$ are real quantities. The discrepancy at each frequency point for the j^{th} input and i^{th} output channel is

$$E_{ij}(\omega_k) = T_{ij}(\omega_k) - \gamma_{ij}(\omega_k). \tag{3.3}$$

Therefore the error is defined as the differences between the complex FRFs of the responses of the experiment and of the model. This avoids problems with computation of amplitudes and phases of the responses. The model parameters with respect to which we want to reduce the error may be organized as a vector

$$\begin{aligned} \underline{x} = [&b_1^{(1)}, \ldots, b_J^{(M)}, c_1^{(1)}, \ldots, c_I^{(M)}, \\ &f_1, \ldots, f_M, \zeta_1, \ldots, \zeta_M, b_1^r, \ldots, b_J^r, c_1^r, \ldots, c_I^r]^T. \end{aligned} \tag{3.4}$$

Ideally, correct parameter values will obtain $E_{ij}(\omega_k) = 0$ for each ω_k; however, due to noise and nonlinear behavior of the system, this is not possible (in real situations). Here the choice is made to minimize the square of the absolute value of the integral of each channels' error.

$$f_{ij} = \sum_{k=1}^{K} \overline{E}_{ij}(\omega_k) E_{ij}(\omega_k) \approx \int_{\omega_{low}}^{\omega_{high}} |E_{ij}(\omega)|^2 d\omega \tag{3.5}$$

where the overbar denotes complex conjugation.

3.2.1. Choice of Norm for Minimization

At this point, a standard norm may be chosen to be minimized through a traditional algorithm (conjugate gradient, steepest descent, Newton, etc.) [RRR][PaW]. Philosophically, whenever a norm is taken of a matrix, detailed information about individual components is lost. That is, all the information contained in members of a vector or matrix is collapsed into a scalar quantity. This is the motivation for the present algorithm. Using an iterative scheme, the goal is to find the minima of all the elements f_{ij} simultaneously with respect to $\underline{x}$.

The channel errors f_{ij} are positive definite, so progress towards their zeroes will be in the same direction as the minima. The minimization schemes used are a vector version of a first order Newton zero finding algorithm and a vector version of the steepest descent idea. The values f_{ij} are assembled as a vector $\underline{F}$ so that iterations may be carried out to find the zeros/minima of the elements of $\underline{F}$.

3.2.2. Newton Method

The vectorized Newton method used here is derived straightforwardly from the Taylor series expansion.

$$\underline{F}(\underline{x}_o + \Delta\underline{x}) = \underline{F}(\underline{x}_o) + \nabla\underline{F}(\underline{x}_o)\Delta\underline{x} + \frac{1}{2}\Delta\underline{x}^T\nabla^2\underline{F}(\underline{x}_o)\Delta\underline{x} + \text{ higher order terms.} \qquad (3.6)$$

Note that $\underline{F}(\underline{x})$ is a real vector of length IJ; $\nabla\underline{F}(\underline{x})$ is the Jacobian of $\underline{F}(\underline{x})$ which is a real rectangular matrix of size $IJ \times N$, where N is the number of parameters in $\underline{x}$ and $\Delta\underline{x}$; and $\nabla^2\underline{F}(\underline{x})$, the Laplacian of $\underline{F}(\underline{x})$ is a rank 3 tensor of size $(IJ) \times N \times N$. Here only information about the vector function $\underline{F}(\underline{x})$ and the Jacobian $\nabla\underline{F}(\underline{x})$ are used.

The goal is to make the next iterate of the vector to be as close to zero as possible, so it is set as such to get the scheme:

$$\underline{F}(\underline{x}_o + \Delta\underline{x}) = \underline{0} = \underline{F}(\underline{x}_o) + \nabla\underline{F}(\underline{x}_o)\Delta\underline{x} + \text{ higher order terms.} \qquad (3.7)$$

Note that as defined here, all elements of $\underline{F}$ are positive semi-definite. For the moment, the higher order terms are disregarded to obtain

$$\underline{\nabla F}(\underline{x}_o)\Delta\underline{x} = -\underline{F}(\underline{x}_o.) \tag{3.8}$$

Since the Jacobian is rectangular in general, the Moore-Penrose pseudoinverse [GoV], [Bra] can be used. The Jacobian is rank deficient because of its shape and because the parametrization chosen is not unique. (Uniqueness of the parametrization is discussed in Chapter 4.) Denoting the pseudoinverse with the superscript † , and the iterate number with ν, the iteration procedure is

$$\underline{x}_{\nu+1} = \underline{x}_\nu - [\underline{\nabla F}(\underline{x}_\nu)]^\dagger \underline{F}(\underline{x}_\nu). \tag{3.9}$$

The pseudoinverse then gives the smallest two norm step $\Delta\underline{x} = \underline{x}_{\nu+1} - \underline{x}_\nu$. The pseudoinverse is computed using singular value decomposition routines from LINPACK[DBM].

To look at the sensitivity of the scheme, substitute back into the Taylor expansion for $\underline{F}(\underline{x}_o + \Delta\underline{x})$.

$$\begin{aligned}\underline{F}(\underline{x}_o + \Delta\underline{x}) =& \underline{F}(\underline{x}_o) - \underline{\nabla F}(\underline{x}_o)[\underline{\nabla F}(\underline{x}_o)]^\dagger \underline{F}(\underline{x}_o) \\ &+ \text{ higher order terms.}\end{aligned} \tag{3.10}$$

If $\underline{\nabla F}(\underline{x})$ were of full rank, the pseudoinverse would equal the exact inverse, and the expression would simply leave the higher order terms. As previously stated, the Jacobian is not full rank, so something extra needs to be done to assure convergence of the algorithm and to reduce the effects of the higher order terms. For this, a line minimization along the direction specified by $\Delta\underline{x}$ can be implemented. To do this minimization a scalar function is needed. Here, the 1-norm of $\underline{F}(\underline{x})$ is chosen: $\|\underline{F}(\underline{x})\|_1 = \sum_{i=1}^{I}\sum_{j=1}^{J}|f_{ij}(\underline{x})|$. So, a bisection routine is used to find the α which minimizes $\|\underline{F}(\underline{x}_\nu + \alpha\Delta\underline{x})\|_1$ along the direction $\Delta\underline{x}$.

Noting the Taylor expansion of $\underline{F}(\underline{x}_o + \Delta\underline{x})$,

$$\begin{aligned}\underline{F}(\underline{x}_o + \alpha\Delta\underline{x}) =& \underline{F}(\underline{x}_o) + \alpha\underline{\nabla F}(\underline{x}_o)\Delta\underline{x} \\ &+ \alpha^2\frac{1}{2}\Delta\underline{x}^T\underline{\nabla}^2\underline{F}(\underline{x}_o)\Delta\underline{x} + \text{ higher order terms.}\end{aligned} \tag{3.11}$$

As the iteration approaches the minimum for $\|\underline{F}(\underline{x})\|_1$, the size of α generally decreases, so the size of the higher order terms also decreases. This helps convergence of the routine.

3.2.3. Steepest Descent

The steepest descent method used here is also a vector version of the standard method. It is combined with line minimization as above to find a scaling which gives the minimum $\|\underline{F}(\underline{x})\|_1$. The iteration direction is

$$\Delta\underline{x} = -\alpha[\underline{\nabla F}(\underline{x})]^T \underline{F}(\underline{x}). \tag{3.12}$$

The two above iterative schemes are alternated to complement each other. Experience with these problems has indicated that the best alteration scheme is two Newton steps and one Steepest Descent step. When the procedure is started (when the error is large), the Steepest descent method converges very slowly. Here, the Newton method seems to work quite well. As the error becomes small, however, the Newton method's effectiveness is decreased: The Newton zero finder works on a function which is positive definite because of noise. Therefore, it will jump between parameter sets near the minimum. Here, the steepest descent method becomes useful.

3.2.4. Initial Estimates

There are several ways that initial estimates may be obtained for $\underline{x}$. The most complete set of starting values comes from results of finite element analyses of the structure in question. These give the input and output location geometric weights, the number of modes to be fit, and estimates of the natural frequencies of the structure. The participation weights can be scaled if there are any amplifiers in the physical system and the amplifier gains are known accurately. Estimates for modal damping values may be made from the FRF's and from experience.

If finite element results are not available, estimates for all parameters may be made from single mode SISO fits or starting values such as 1.0 for the input and output weights may be used. In many cases, the algorithm is able to converge from poor starting values.

To prevent divergence and lack of physical basis of the results, limits are placed on the modal frequency and damping estimates. The user chooses allowable variations of these values based on experience. For example, a negative damping value would not be physically possible for a passive structure. In this implementation, when a particular frequency value is computed to be outside the prescribed

bounds, it is reset to the originally estimated value. Damping values are reset to a particular limit if the algorithm pushes them beyond it. This is where user insight is most important.

The iterations are stopped when either the scalar error diverges for a large number of steps, or the parameters stop changing. In most MIMO cases, the method diverged for a few steps, and then started converging again. Thus, divergence alone was not a sufficient reason for stopping the iterations.

3.3 Benchmark Tests of the Algorithm

3.3.1. Single Input Single Output (SISO) Tests

To verify the accuracy of the algorithm, it was applied to a single input, single output, single mode system that was numerically generated. The system for comparison was chosen to have a mode at 3.0 hz (18.8496 rad/sec) with per unit critical damping of 1.66667%. For simplicity, the input-output gain was set at 1.0. To check robustness of the algorithm, a data set was also set up with the above system disturbed by noise in the Fourier transforms of both the real and imaginary parts. The noise was generated as a random normal distribution with zero mean and variance equal to 5% of the peak amplitude of response over frequency.

Variable	exact nominal	initial estimate	Final Estimate uncorrupted	corrupted
Freq (rad/sec)	18.850	18.00	18.850	18.868
Damping	1.6667%	14.0%	1.714%	1.810%
Gain	1.000	0.30	1.028	1.166
Initial Error			916.4	1231.1
Final Error			.367	237.69
Minimum possible			0.0	228.7
Computation real time (sec)			60	60
iterations			150	150

Table 3.1 - Application of Algorithm to Theoretical System.

The results shown in Table 3.1 did not incorporate user assistance with estimate choices other than the initial ones. In general, when the user alters the estimates according to their experience, the error reduces more rapidly. Further iterations also reduce the errors. Plots of these cases are shown in Figures 3.1 and 3.2. In state space, this data was collected as a 2 state SISO model.

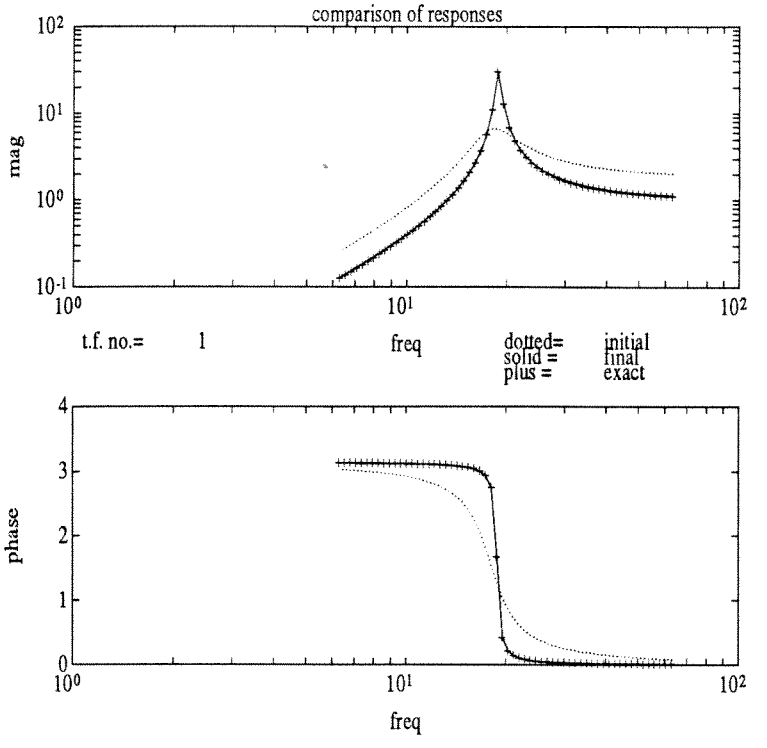

Figure 3.1 - Fit of Uncorrupted System.
The final estimate (solid) overlaps the exact (plusses) completely. The initial estimate (dotted) could be much better.

In both cases, good agreement was obtained between the model data and the numerical experiment. The noise changed the final estimates of the corrupted data somewhat, but the algorithm still produced a model very close to the uncorrupted original one. The algorithm converged in both cases even though the initial estimates were not very good.

3.3.2. MIMO Multiple Mode Test

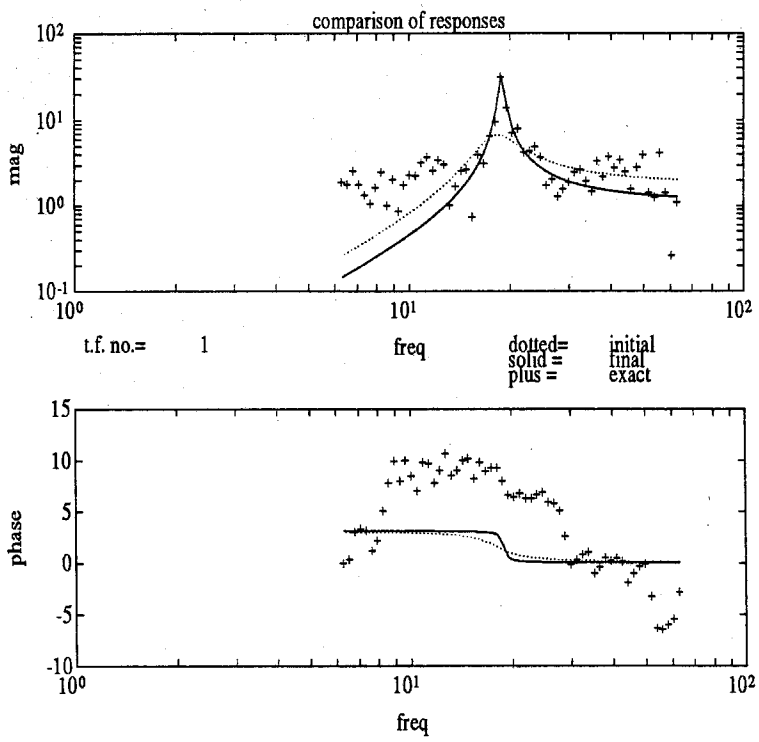

Figure 3.2 - Fit of Corrupted System.
Here, the exact data is corrupted by noise. The phase of the values with small amplitudes varies greatly because of the corruption. The final fit still manages to capture the modal peak quite nicely. Discrepancies which are multiples of 2π in the plots of phase versus frequency are due to the MATLAB routine which computes the phase. When plots of real and imaginary part of the response versus phase are done, these errors disappear.

The true power of this routine is its ability to handle multiple input multiple output multiple mode systems. Thus, a test was devised with 2 inputs, 2 outputs, and 2 modes with the parameters shown in Table 3.2. Initial and final estimates are also shown. (The frequencies here are in radians/second.)

The plots in Figures 3.3- 3.7 show the exact solution, the initial estimates, and the final estimates for the various channels. Note that the initial estimates for the input and output weights are of the opposite sign from the exact solution in some cases. These results took 150 iterations which took approximately 150 seconds real time to run on a SUN Microsystems SPARCstation 1. Further iterations significantly reduced the error.

Variable	exact values		initial estimate		final estimate	
	mode 1	mode 2	mode 1	mode 2	mode 1	mode 2
sensor 1	0.80	0.10	1.e-4	1.e-4	0.853	0.099
sensor 2	-0.20	-1.00	1.e-4	1.e-4	-0.206	-0.998
actuator 1	1.00	1.00	1.0	1.0	1.00	1.00
actuator 2	0.50	-15.00	1.0	1.0	0.484	-15.02
Frequency	18.85	37.70	18.00	37.00	18.85	37.70
Damping (%)	0.010	0.010	0.100	0.100	0.011	0.010

Table 3.2 - MIMO Example.
Frequency is in rad/sec. This data is not corrupted by noise.

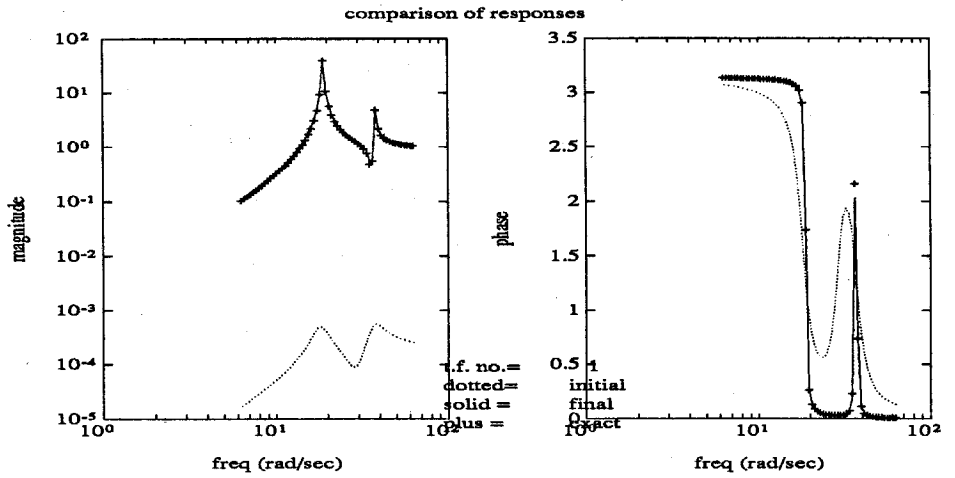

Figure 3.3 - MIMO Transfer Function Channel 1.
Initial estimates in all these cases have amplitudes which are too small and dampings which are too large.

Here, as with the SISO case, the algorithm was able to obtain good estimates of the system parameters, even though the initial estimates were quite poor. A user with more experience could have come up with much better starting estimates if they had desired to. The state space model for these fits has 4 states, 2 inputs, and 2 outputs.

3.4 Description of the Caltech Flexible Structure

The prototype large space structure at Caltech, which was used for the experiments described in this thesis, is a 3 bay triangular cross-section hanging truss. The top bay (referred to as the first bay) is attached to a large aluminum plate

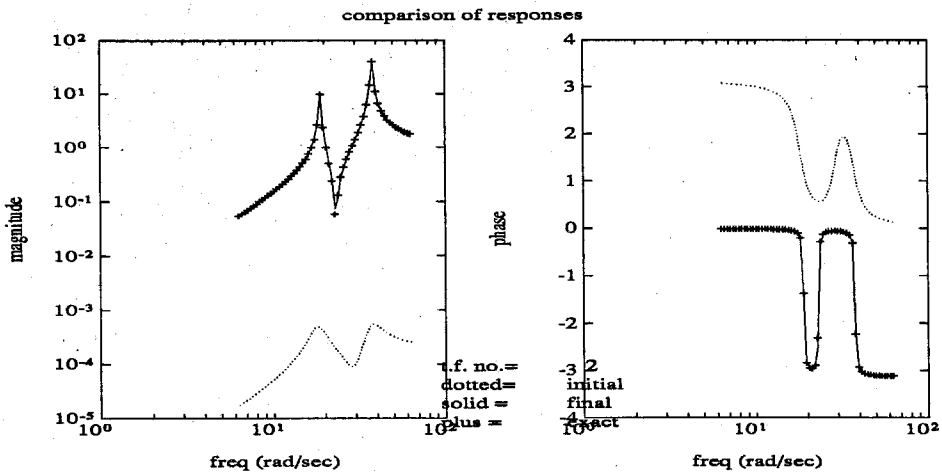

Figure 3.4 - MIMO Transfer Function Channel 2.
Note that for this channel the phase of the initial estimates is off by π radians.

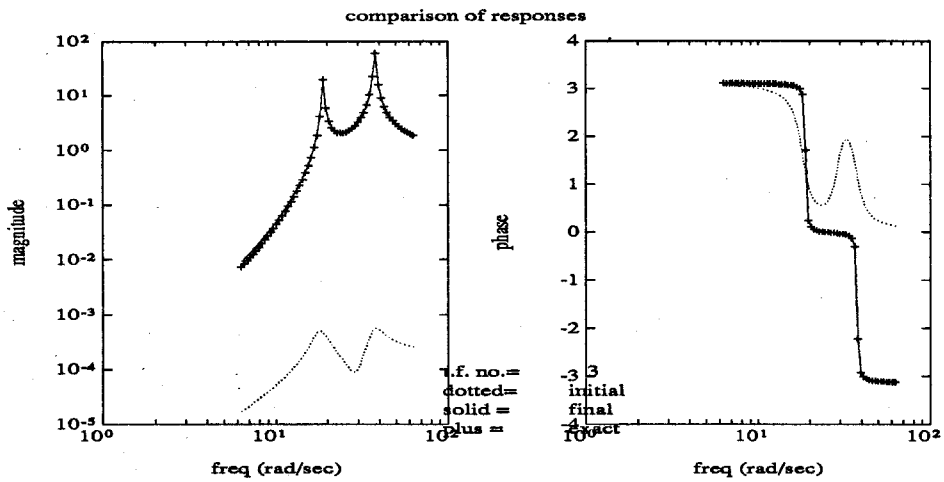

Figure 3.5 - MIMO Transfer Function Channel 3.

bolted to building structural members[BaD]. The structure hangs so that frequencies of the first few modes could be designed lower, and so that buckling of members due to structure weight could be avoided. The structure is illustrated in Figure 3.7.

The structure has a total height of 2.32 metres (91.34") and has an equilateral triangular cross-section with each side 0.4064 m (16"). The first platform (between bays 1 and 2) is a solid aluminum plate 0.00953m ($\frac{3}{8}$"). The second and third platforms are 0.0064m ($\frac{1}{4}$") thick with a triangular section with side length measuring

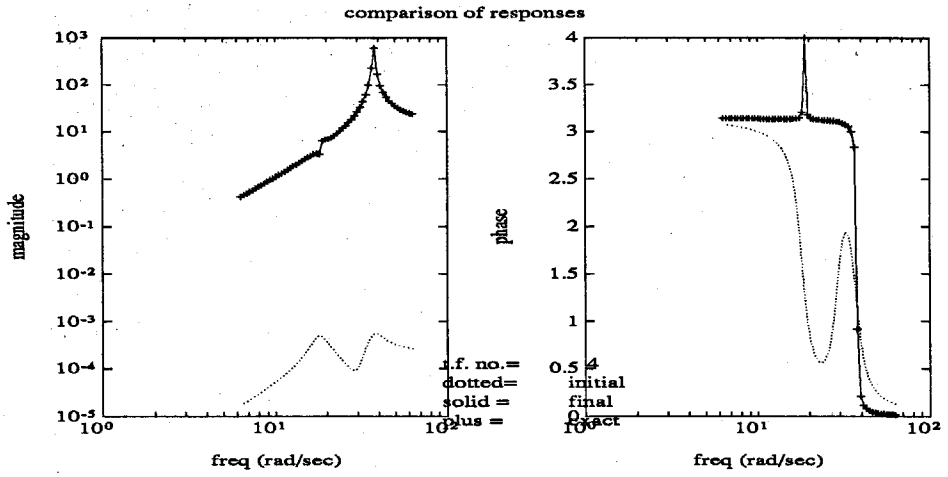

Figure 3.6 - MIMO Transfer Function Channel 4.

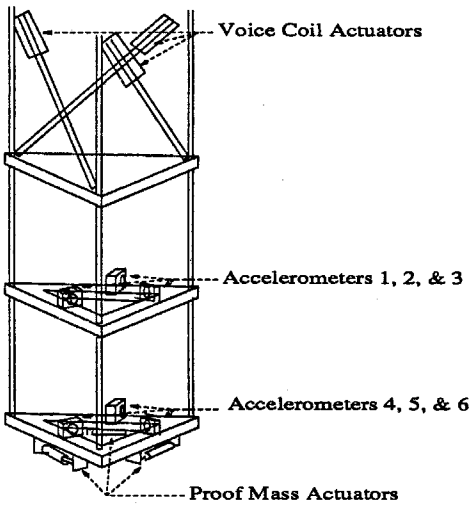

Figure 3.7 - Caltech Prototype Space Structure.
The top of the structure is bolted to the ceiling.

0.3556m (14") cut out. The reduction in mass of plates two and three placed the torsional modes very close to bending modes, thus increasing the challenge of the identification and control problems.

3.4.1. Actuators

The system has two types of actuators, both of which provide no support if power is turned off. One set is the voice coil type. They are rated at $\pm 13.46N$ ($\pm 3lb$) at ± 5 Volts, and have a bandwidth of 60 Hz. They are placed so that when activated, they support or induce all forces passing through the diagonals of the first bay.

3.4.2. Modeling of the Proof Mass Actuators

There are also three proof mass type actuators attached horizontally to the underside of the bottom bay. They act along the directions of the sides of the triangular base. These only impart force to the structure when in motion. Unfortunately, these actuators have nonlinear response to input. At low amplitudes of motion, stiction overwhelms the inductive force trying to move the mass. Here, a large gain is necessary. However, as the motion of the mass increases, the relative effect of friction decreases, so the gain is no longer necessary. Thus a nonlinear controller which gives a large gain at low velocities and a small gain for large velocities is necessary. The linear portion of the controller was designed using classical loop-shaping techniques[DFT]. In [BaD] these features are discussed. The proof masses are rated at approximately $\pm 6.5N$ (± 1.5lb) at ± 5 Volts, and have an effective bandwidth of approximately 5 Hz. Since these actuators are not in the structural load paths, they are only able to add small forces to the system. At low frequencies, they are especially ineffective because very large displacements are necessary to generate decent size forces.

For position sensing of the proof masses, each actuator is equiped with a linear voltage displacement transducer. These are rated as having a linear response in the band of 0.5 Hz to 8 Hz.

The local controllers for the proof masses command displacements, thus additional states were added to the transfer function models to reflect the double differentiation between position of the proof mass and the force generated. This results in what appears as a two zero roll up on log-log plots of magnitude versus frequency for the appropriate transfer function channels. Additionally, the controlled behavior of the proof mass actuators had to be identified. Attempts were made to fit a standard (modal) force input-acceleration output model to the curves generated by these actuators. Because of the displacement command of the local controllers, however, the force-acceleration models were very poor at the higher frequency modes. Thus, two zeroes were added as dynamics for each proof mass

motor. For implementation in a state space model, this required addition of two poles for each actuator also.

The model for the behavior from the proof mass actuators to the accelerometers is then

$$T_{ij}(\omega_k) = \left[\sum_{m=1}^{M} \frac{c_i^{(m)} b_j^{(m)} (-\omega_k^2)}{(f_m^2 - \omega_k^2) + 2\sqrt{-1} f_m \zeta_m \omega_k} + b_j^r c_i^r\right] \left[\frac{m_j(-\omega_k^2)}{(\sqrt{-1}\omega_k + p_1)(\sqrt{-1}\omega_k + p_2)}\right]$$

where the additional terms are m_j for the j^{th} actuator gain, and p_1 and p_2 as poles to keep the model proper. The m_j terms were also added to the list of parameters to be determined by the iteration scheme.

3.4.3. Sensors

Structural behavior is sensed through 6 uniaxial Sunstrand QA700 accelerometers placed on the second and third platforms half way between the longerons. They are oriented to be along one structure axis and at $\pm 45°$ to this axis. Frequency response of the sensors is flat and has very low noise between 0 and 200 Hz. Signals from these are conditioned by a 4 pole Butterworth filter with a 100 Hz cutoff frequency before being fed into the data acquisition /control system. Because of the high quality of these accelerometers, it was not considered necessary to explicitly model dynamics of these devices.

3.4.4. Data Acquisition and Control System

Structure excitation and data acquisition are controlled by a Masscomp 5400 computer with digital to analog (D/A) and analog to digital (A/D) boards. Outputs from the D/A converters are passed through amplifiers which feed into the voice coil and proof mass actuators. The system has been set up so that during data acquisition or control the processor is dedicated to the control task.

3.5 Modal Properties of the Structure

3.5.1. Excitation

To obtain a frequency response function of the system the structure was excited with an amplitude modulated sine sweep (chirp) with frequency between

0.2 and 20.0 hz. The modulation is carried out by a sine squared envelope in the time domain. Thus, the excitations were computed as

$$\sin^2\left(\frac{t\pi}{T}\right)\sin\left(\int_0^t \omega_i e^{\frac{t}{T}\ln\left(\frac{\omega_f}{\omega_i}\right)}dt\right), \tag{3.13}$$

where ω_i and ω_f are the initial and final frequencies of the sweep and t and T are the current time and the total sweep time. The Fourier transform of this signal is shown in Figure 3.8.

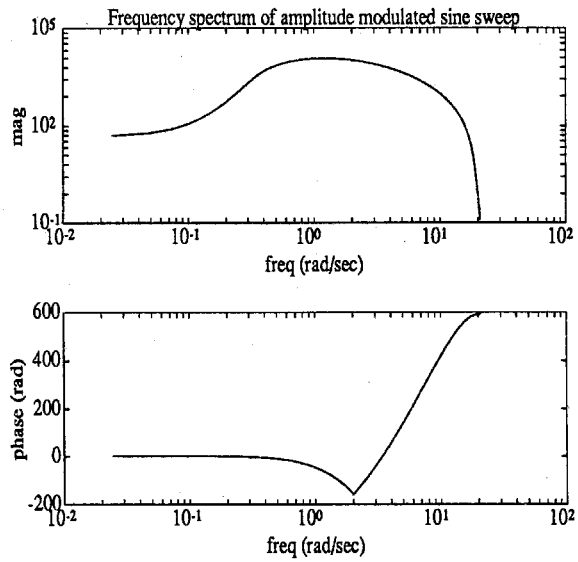

Figure 3.8 - Fourier Transform of Sine Sweep: .2 to 20. hz.
This signal is chosen because it is quite smooth in the time domain and in the frequency domain (both amplitude and phase). Most of the energy in the signal is concentrated in the region where the structure has modes.

With nonlinear controllers holding the proof mass actuators in their zero positions (centered), the structure was excited through one voice coil actuator at a time for 40.96 seconds at a sampling rate of 200hz. Similarly, the structure was excited through the controlled proof mass actuators, with a zero voltage sent to the voice coils. The time domain data from the six sensors and from the excitation were then Fourier transformed.

The FFT's of the sensor outputs were then divided by the FFT's of the input signal. Thanks to the smoothness of the FFT of the excitation (Figure 3.8),

the resulting data are quite smooth. The result of the division is taken as the transfer function (or FRF) from the single input. In the experiment, each excitation experiment was repeated three times, and the resulting transfer functions were averaged in the frequency domain. More averaging results in smoother results.

Other excitations, such as pseudo-random noise and impulses were tested; however, the amplitude modulated chirp gave the smoothest transfer functions. The pseudo-random signal gave amplitude results of the same quality as the chirp, but the phase results were of lesser smoothness. Impulses were not used because of difficulty with reproduction of excitations. Also, there was no control with the energy spectrum of impulse signals, whereas the chirp and the pseudo-random signal could be tailored to place energy in certain frequency bands. Windowing for the FFTs was not necessary since the initial and final signals of the chirp were zero.

3.5.2. Curve Fit

For creation of a MIMO problem, the SIMO FRF's were assembled is such a way that the curve fit program could keep track of the channel correspondences. Initial estimates for modal frequencies and dampings were made by looking at plots of magnitude versus frequency. Estimates for the input and output weight matrices were made from observation of the real and imaginary vs. frequency plots. In development of the estimates, user experience was very important.

Parameter values were improved by iterating first with a SIMO problem. Here, the user helped the iteration by pushing values into the region where they gave the best fit. Once a good SIMO estimate was obtained, the resulting parameters were applied to the MIMO problem. The parameters obtained from the SIMO fit (frequencies, dampings, input weights for one input, a full set of output weights, and some static weights) were held constant. The only values allowed to change were modal and quasi-static input weights for the new inputs. Once good fits had been obtained with the restricted problem, all parameters were allowed to vary simultaneously. This improved the curve fits further.

Figure 3.9 presents the root mean square sums of all the response functions of the LSS (dashed line), of the identification model (solid line), and of the errors in each of the 36 channels (dotted line). That is, the synthesized FRF's from the three

voice coil actuator and the three proof mass actuator inputs to the six accelerometer outputs were squared and added at each frequency. Magnitude versus frequency and phase versus frequency plots for the response of a middle bay accelerometer (#1) to one of the voice coil actuators (#1) are also shown with the corresponding response of the model (Figure 3.10). The phase, as plotted, has apparently large discrepancies, but these are due to the 2π non-uniqueness of the phase calculating procedures. When plots of real and imaginary parts of the responses versus frequency are observed, the phase discrepancy is not seen.

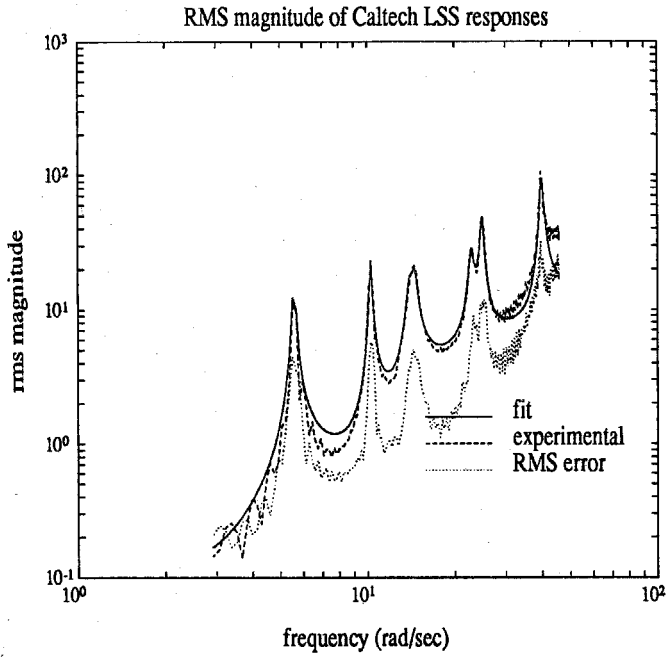

Figure 3.9 - RMS Responses of Structure, Model, and Error.
There are 36 channels of data compressed into each of these curves (3 voice coil inputs plus 3 proof mass actuators to 6 accelerometer outputs). The increase in magnitude with frequency is due to dynamics in the proof mass actuators which are tracking commanded displacements. The error looks large because it is the RMS sum of all errors in all channels. It can be seen that the model catches all the modes.

The main features to note about Figure 3.10 are the appearance of only six peaks. These fully represent nine modes. For example, the peak at 5.5 rad/sec contains two bending modes. The transfer function response presented is for a sensor and an actuator that are separate from the location where the second structure is to be attached.

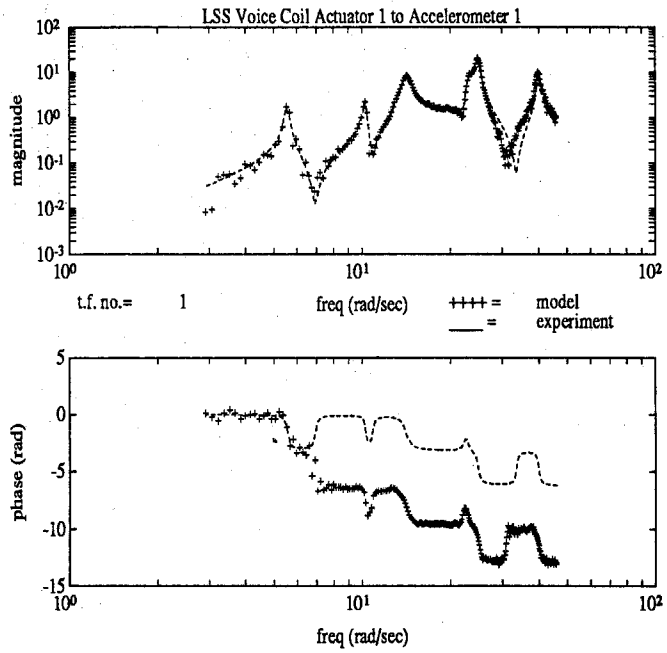

Figure 3.10 - Caltech Structure and Model Response for Actuator 1 to Accelerometer 1.
Both the peaks and the valleys of the amplitude are fit well. The phase appears off by multiples of 2π radians because of the algorithm which computes the phase.

A little work was needed to find the proper placement of the poles p_1 and p_2 for the proof mass actuator controllers. The first estimate was that the poles were above the frequency range of interest for the global modal structural responses. This placement gave good quality curve fits at all modes except the last one. Upon looking carefully at the plots of the real and imaginary parts of the experimental and model frequency response functions due to the proof mass actuators, it was noticed that there was a 90° phase shift between the modal system and the experiment between modes eight and nine. By shifting one of the additional poles for the proof mass actuator dynamics to the region between the eighth and ninth modes, the model became able to describe this phase shift. Thus, the curve fit was significantly improved. The cause of the phase shift is the local controllers (which roll off between the eighth and ninth structural modes) for the proof mass actuators.

3.5.3. Finite Element Estimates

Finite element models (FEM) were also developed to obtain estimates of the frequencies and mode shapes. The level of discretization of these models was

quite rough; however, there were certain features pointed out by these results. The main conclusion from the numerical analysis is that different FEM packages deliver somewhat different results. For example, NASTRAN placed the first torsional mode at a higher frequency than the group of second bending modes. ABAQUS and experiments located this mode between the first global bending and second global bending modes. It is thought that the main reason for these discrepancies is the differences in the beam models used by the FEM packages. The difference may also be due to an element used in ABAQUS to model sliding members (voice coil actuators in this case), which was not available in NASTRAN. In NASTRAN the voice coil actuators were modeled by a constraint in the degrees of freedom of the node such that it could only move along the axis of the actuators. Results of the FEM analyses are compared with experimental results for the modal frequencies in Table 3.3.

The most probable explanations for the differences in the frequencies between the FEM results and the experiment is the boundary conditions at the joints and the low level of discretization of the models. In the FEM implementations, the joints were assumed to be rigid. On the structure, the rods were shrink fit and welded to mating brackets which were then bolted to the platform plates. Although quite stiff, these are not rigid connections. Another source of error was that flexibility of the plates was neglected - they were modeled as lumped masses and lumped rotational inertias. The proof mass actuators were also modeled as lumped masses.

Mode	FEM Package Freq. ($\frac{rad}{sec}$)		Experimental		Mode
No.	NASTRAN	ABAQUS	Frequency ($\frac{rad}{sec}$)	Damping	Shape
1	4.784	5.0301	5.557	1.18%	Bending
2	4.784	5.0301	5.602	1.07%	Bending
3	11.563	11.943	10.2577	1.11%	Torsion
4	10.852	12.239	14.04	1.90%	Bending
5	10.852	12.239	14.50	1.90%	Bending
6	21.34	22.52	22.81	1.86%	Torsion
7	26.02	26.58	24.75	1.32%	Bending
8	26.02	26.58	24.88	1.35%	Bending
9	51.58	54.401	39.99	1.51%	Torsion

Table 3.3 - Identified and Finite Element Frequencies and Dampings. The finite element estimates vary in quality. Notice that the NASTRAN estimates place the first torsional frequency above the second bending modes.

3.5.4. Closely Spaced Modes

The biggest difficulty in the identification was finding the frequencies and mode shapes for modes 1 and 2. Because of discrepancies between finite element models and experiments such as deviations from symmetry of the experimental setups, it was first thought that there was a mode at 5.6 rad/sec and one at 6.1 rad/sec. These estimates were made because of the presence of a large bump at 5.6 rad/sec and a small one at 6.1 rad/sec in the FRFs. After many iterations, several of the curve fit channels looked as good as those for Channel 3 in Figure 3.11 for modes 1 and 2. However, other channels still looked like Channel 2 in Figure 3.11, where the fit is nowhere nearly as good.

Several attempts were made to improve the estimate using the 5.6 and 6.1 rad/sec frequencies, but they failed. The modes were then isolated, and a trial was made with two modes at 5.6 rad/sec. After some variations in the input and output weights, the program converged, and the fits of all the input/output channels resulted as well as those for Channel 3 in Figure 3.12. Note that Channel 2 is presented in both Figure 3.11 and Figure 3.12, although in Figure 3.12 it has a much better fit. The fit for the Channel 3 in Figure 3.12 also improved with the overlapping modal frequencies.

To check the robustness of this result, the frequency of one of these modes was moved back to 6.1 rad/sec. After a few iterations, the frequency moved back to about 5.60 rad/sec.

The input weights were then used to excite the structure. Multiple point excitations of pure sinusoids scaled by the ratios determined by the curve fits were used for all modes. With the input weights and frequencies from the overlapping frequency fit, the modes were very cleanly and distinctly excited. As expected for the model with the slightly separated frequency fit, one mode was excited cleanly but the other was not.

3.6 Conclusions

Identification of modes with practically the same frequency but with different mode shapes can be carried out in experimental settings. Using multiple input

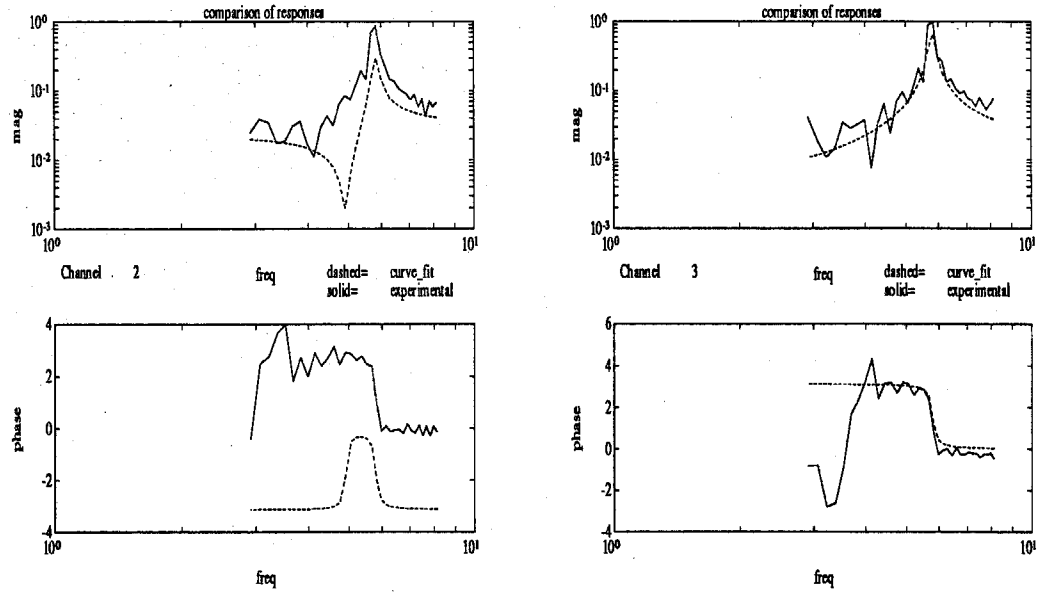

Figure 3.11 - Transfer Functions 2 and 3: Modes at 5.60 and 6.23 rad/sec.
In the model for transfer function 2 (left), the phase is off by π radians, while the fit is good for transfer function 3 (right).

multiple output data, distinct modes whose FRF's appear single peaks can be distinguished from their input and output weights. When the peak is modeled with a single mode, some input/output channels may have good peaks, but others will not. Addition of more modes, and use of multiple input data results in good fits for all channels if indeed the system behaves in a linear modal manner. These results were obtained experimentally on the Caltech structure.

3.7 References for Chapter 3

BaD: Balas, Gary J., and Doyle, John C., (1990), "Collocated versus Non-collocated Multivariable Control for Flexible Structure." *Proceedings of the 1990 American Controls Conference,* San Diego, California, 1923-28.

BeB: Beck, R.T., and Beck, J.L., (1985), "Comparison Between Transfer Function and Modal Minimization Methods for System Identification." *Earthquake Engineering Research Library,* EERL 85-06. California Institute of Technology, Pasadena, California.

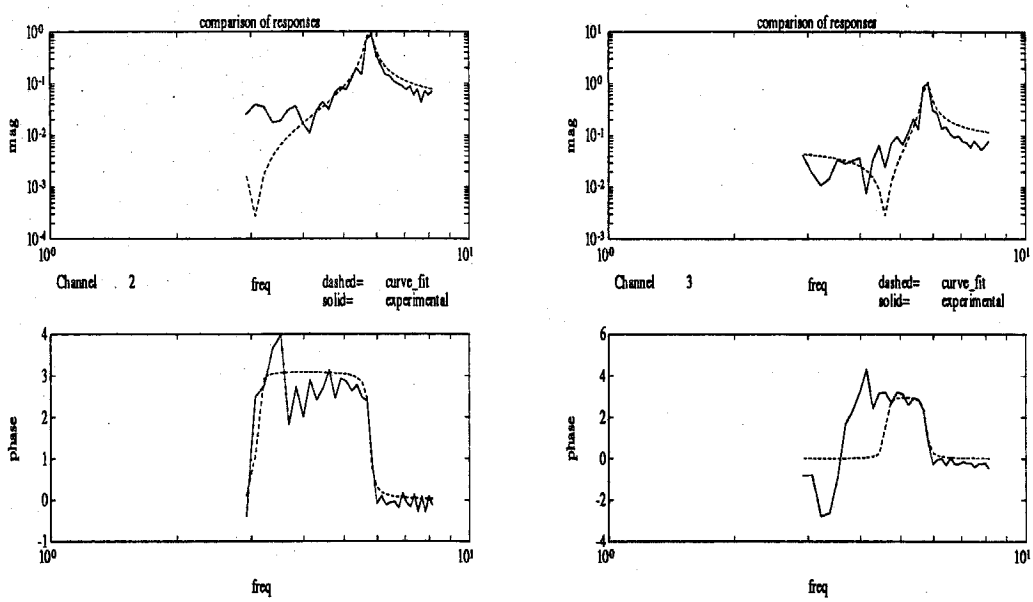

Figure 3.12 - Transfer Functions 2 and 3: Modes at 5.56 and 5.60 rad/ sec.
Here, the phase values are good for both transfer functions (#2 on the left, and #3 on the right). This indicates that the model could fit the two closely spaced modes correctly

Bra: Brandon, John A., (1988), "On the robustness of algorithms for the computation of the pseudo-inverse for modal analysis." *Proceedings of the 6th International Modal Analysis Conference,* Orlando, Florida, 397-400.

CaV: Caughey, T.K., Vakakis, A.F., and Moser, A.N., (1990) "Modeling of Modal Interference for a System with Closely Spaced Modes." *Proceedings of the 8th International Modal Analysis Conference,* Orlando, Florida, 1410-16.

DBM: Dongarra, J.J., Bunch, J.R., Moler, C.B., and Stewart, G.W., (1979), **LINPACK User's Guide,** Society for Industrial and Applied Mathematics, Philadelphia.

DFT: Doyle, J., Francis, B., and Tannenbaum, A., (1992), **Feedback Control Theory,** Macmillan Publishing Co., New York.

EbI: Ebersbach, P., and Irretier, H., (1989), "On the Application of Modal Parameter Estimation using Frequency Domain Algorithms," *International Journal of Analytical and Experimental Modal Analysis,* (4) 4, pp. 109-116, October.

Ewi: Ewins, D., (1984) *Modal Testing : Theory and Practise.* London: Research Studies Press Ltd.

GoV: Golub, G., and Van Loan, C., (1983), *Matrix Computations.* Johns Hopkins University Press.

Ibr: Ibrahim, S., (1985), "Modal Identification Techniques: Assessment and Comparison," *Proceedings of the 3rd International Modal Analysis Conference,* Orlando, FL, January.

IsK: Isaacson, E., and Keller, H., (1966), *Analysis of Numerical Methods.* John Wiley and Sons.

Mcv: McVerry, G., (1979) "Frequency Domain Identification of Structural Models from Earthquake Records." *Earthquake Engineering Research Library,* EERL 79-02. California Institute of Technology, Pasadena, California.

McB: McVerry, G., and Beck, J., (1983), "Structural Identification of JPL Building 180 Using Optimally Synchronized Earthquake Records." *Earthquake Engineering Research Library,* EERL 83-01. California Institute of Technology, Pasadena, California.

Nat: Natke, H.G., (1978), "Survey on Identification of Mechanical Systems," *Road Vehicle Systems and Related Mathematics Workshop,* Turin, Italy, June.

PaW: Papalambros, Panos Y., and Wilde, Douglas J., (1988), *Principles of Optimal Design, Modeling and Computation*, Cambridge University Press.

RRR: Reklaitis, G.V., Ravindran, A., and Ragsdell, K.M., (1983), *Engineering Optimization Methods and Applications*, John Wiley and Sons.

Sag: Sage, A.P., (1982), "System Identification History, Methodology, Future Prospects," *System Identification of Vibrating Structures-Mathematical Models from Test Data,* ASME Winter Annual Meeting, pp. 1-21.

Str: Stroud, R.C., (1987), "Excitation, Measurement, and Analysis Methods for Modal Testing," *Sound and Vibration,* pp. 12-27, August.

VKR: Vold, H., Kundrat, J., Rocklin, G.T., and Russel, R., (1982), "A Multi-Input Modal Estimation Algorithm for Mini-Computers," SAE Paper #820194.

Chapter 4. Response Mode Synthesis using Linear Fractional Transformations and Identified Models

4.1 Introduction

With the development of optimal control methodologies[DGK], the most sensitive step in structural controller synthesis has become development of a good model of the structure. Without accurate models, performance and stability of the actively controlled structure are greatly decreased.

Usually the control designers will have models generated using the finite element method (FEM), but because of insufficient knowledge of material properties, nonlinearities, and other quantities, this model will be inaccurate. When the structure is built, its behavior will differ from that predicted by the finite element method model. The structure may be experimentally identified, and the FEM model can be modified to better match the structure's behavior. However, because of lack of uniqueness in identifiable parameters ([Ber], [Cau]), the changes made to the model might not correspond to what is really happening to the system. There are several possible parameter values for the FEM model that will give the same behavior.

The alterations made to the model will not degrade performance of the predictions until information about more modes or alterations of the structure are needed. Since the analyst will have a good idea of how they want to change the

system, the FEM model is usually changed to reflect these desired changes. However, the lack of correlation between the altered FEM model and the actual system may lead to an incorrect prediction of the modified structure.

If instead, the experimental model (transfer functions) can be changed to account for the modifications, it should be possible to obtain the model that is closest to reality with the minimum effort. On structural systems, this is possible using linear fractional transformations (LFT), which are the equations that result from feedback between two systems. The method presented here results in a $2n$-space version of response mode synthesis ([Bla], [CKR], [Dok], [GLM], [HEN], [Hur], [SBC]) which fits nicely with current optimal robust control synthesis methodologies. It has the traits deemed desirable by Craig [Cra] and Ewins [Ewi] in their reviews of the various substructure assembly methods, and it points out particular values that need to be identified carefully. The approach is similar to (but possibly more general than) the mechanical impedance method proposed by [Sku]. (An extensive review of previous theoretical and experimental results of response mode synthesis may be found in [Bla]).

This chapter presents LFTs as a general tool for structural dynamics work. The LFTs in state space format ([DGK], [Kai], [KwS]) allow change of identified models of structures without theoretical knowledge of the system. For one-dimensional or chain-type structures, this application of LFTs is straightforward and exact. For more complex systems, there are restrictions that could be difficult to meet, and there are required parameters which might be difficult to identify exactly. The main advantages of the proposed method are
i) non-colocated sensor-actuator (S/A) geometries can be used,
ii) there is no need to obtain generalized displacements from accelerometer data[Bla],
iii) conversions from voltages to physical parameters are not needed, that is, this is a purely input/output method, (compatibility of individual component models is easily obtained) and
iv) locally controlled actuators may be used without direct knowledge of the forces the actuators apply to the structure.

The main motivation of this work is synthesis of controllers for modified structures. For example, during docking of two actively controlled structures, the current approach involves shutting off the controller on each structure during docking. Once

the systems have combined, a new controller based on the coupled behavior is applied. With robust optimal control synthesis techniques such as H_∞/μ-synthesis [Bmu], [DFT], [DGK] it is possible to design a controller which works for both the separate systems and the docked system. This makes it possible to keep the system actively controlled during the entire mating procedure. Controller synthesis theory and experimental results for combined structures will be presented in Chapters 6and 7.

Section 2 of this Chapter presents the basic theory of LFTs. Section 3 applies the state space LFT method to modifications of a spring-damper-mass system, and shows the equivalence to basic equations of motion. More complex multidimensional systems and some of the limitations of the method due to rotational motions are discussed in Section 4. Section 5 gives a summary of the advantages of using LFTs for structural assembly. Numerical and experimental results are presented in Chapter 5, along with recommendations for improvement of the experimental portions of the procedure.

4.2 Linear Fractional Transformations - Basic Definition

The linear fractional transformation used herein is a multivariable extension of the standard LFT used in complex analysis. In this setting, the LFT is the result of applying one system to another, such as a controller connected to a plant. Working in the frequency domain using transfer functions, the LFT

$$\mathcal{F}_l(G,K) \equiv G_{11}(s) + G_{12}(s)K(s)[I - G_{22}(s)K(s)]^{-1}G_{21}(s), \quad (4.1)$$

(where $s = j\omega$, $j = \sqrt{-1}$, ω is frequency,) is equivalent to the block diagram in Figure 4.1. The subscript l (for *lower*) in $\mathcal{F}_l(G,K)$ denotes that the fractional transformation connects the last set of inputs and outputs of G system to the outputs and inputs of K as in Figure 4.1.

Each transfer matrix G_{ij} can be represented in state space by the quadruple

$$\left(\begin{array}{c|c} A & B_j \\ \hline C_i & D_{ij} \end{array}\right)$$

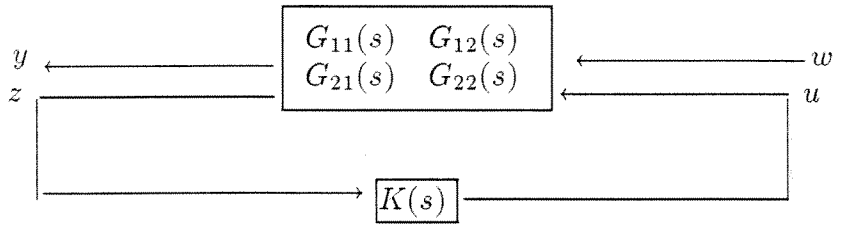

Figure 4.1 - Basic LFT Structure.

such that $G_{ij}(s) = C_i(sI - A)^{-1}B_j + D_{ij}$. C_i contains the i^{th} output/sensor participation factors, B_j is a matrix of the j^{th} input/actuator participation factors, A is the dynamic behavior matrix, and D_{ij} has the static behavior information from inputs j to outputs i. In the time domain, this realization represents the system

$$\dot{\underline{x}} = A\underline{x} + B_j\underline{u}_j$$
$$\underline{y_i} = C_i\underline{x} + D_{ij}\underline{u}_j$$

where $\underline{x}$ is the state vector, $\underline{u}_j$ denotes the j^{th} vector of inputs, $\underline{y}_i$ represents the i^{th} output signal vector, and the dot superscript symbolizes differentiation with respect to time.

The main feature of LFTs is that addition of signals, cascading of systems, and feedback set-ups are easily constructed. Straightforward matrix multiplications and linear algebra are the only operations necessary to obtain models for these linear time invariant system operations [Bmu], [Kai].

4.3 Spring-Damper-Mass System

A series of simple spring-damper-mass (SDM) systems can be assembled using the LFT concepts in a very straightforward manner. A simple SDM system is modeled by the equation $m\ddot{x} + d\dot{x} + kx = f(t)$. In state space form this is shown as in Figure 4.2.

Outputs may be chosen as comprised of displacement x, velocity $\dot{x}$, or acceleration $\ddot{x}$.

$$\begin{pmatrix} x \\ \dot{x} \end{pmatrix} = \begin{bmatrix} 0 & 1 \\ -\frac{k}{m} & -\frac{d}{m} \end{bmatrix} \begin{pmatrix} x \\ \dot{x} \end{pmatrix} + \begin{bmatrix} 0 \\ \frac{1}{m} \end{bmatrix} f(t)$$

$$\begin{pmatrix} \text{displacement} \\ \text{velocity} \\ \text{acceleration} \end{pmatrix} = y = \begin{pmatrix} 1 & 0 \\ 0 & 1 \\ -\frac{k}{m} & -\frac{d}{m} \end{pmatrix} \begin{pmatrix} x \\ \dot{x} \end{pmatrix} + \begin{pmatrix} 0 \\ 0 \\ \frac{1}{m} \end{pmatrix} f(t)$$

which can represented in state space as

$$= \left(\begin{array}{cc|c} 0 & 1 & 0 \\ -\frac{k}{m} & -\frac{d}{m} & \frac{1}{m} \\ \hline 1 & 0 & 0 \\ 0 & 1 & 0 \\ -\frac{k}{m} & -\frac{d}{m} & \frac{1}{m} \end{array}\right) = \left(\begin{array}{c|c} A & B \\ \hline C & D \end{array}\right)$$

Figure 4.2 - State Space for Spring-Damper-Mass System.

The equations of motion for two SDM systems in series are

$$\begin{aligned} m_1\ddot{x}_1 + d_1\dot{x}_1 + d_2(\dot{x}_1 - \dot{x}_2) + k_1x_1 + k_2(x_1 - x_2) &= f_1(t) \\ m_2\ddot{x}_2 + d_2(\dot{x}_2 - \dot{x}_1) + k_2(x_2 - x_1) &= f_2(t). \end{aligned} \tag{4.2}$$

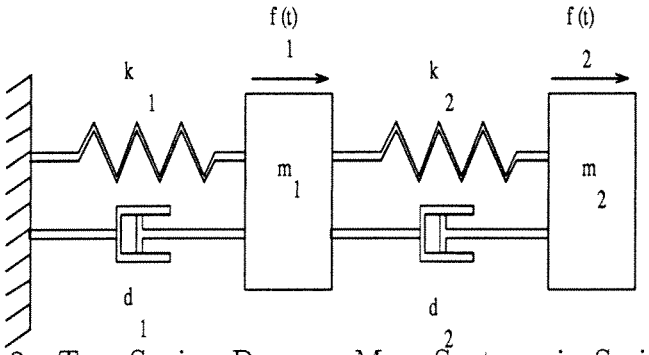

Figure 4.3 - Two Spring-Damper-Mass Systems in Series.

Supposing that the two systems have been independently identified, they can be assembled in the configuration in Figure 4.3 by feeding the displacement and velocity from each system into the other as follows. First, transform the equations of motion so that only the simple SDM system equations appear on the left side of the equation:

$$\begin{aligned} m_1\ddot{x}_1 + d_1\dot{x}_1 + k_1x_1 &= -k_2(x_1 - x_2) - d_2(\dot{x}_1 - \dot{x}_2) + f_1(t) \\ m_2\ddot{x}_2 + d_2\dot{x}_2 + k_2x_2 &= -k_2x_1 - d_2\dot{x}_1 + f_2(t). \end{aligned} \tag{4.3}$$

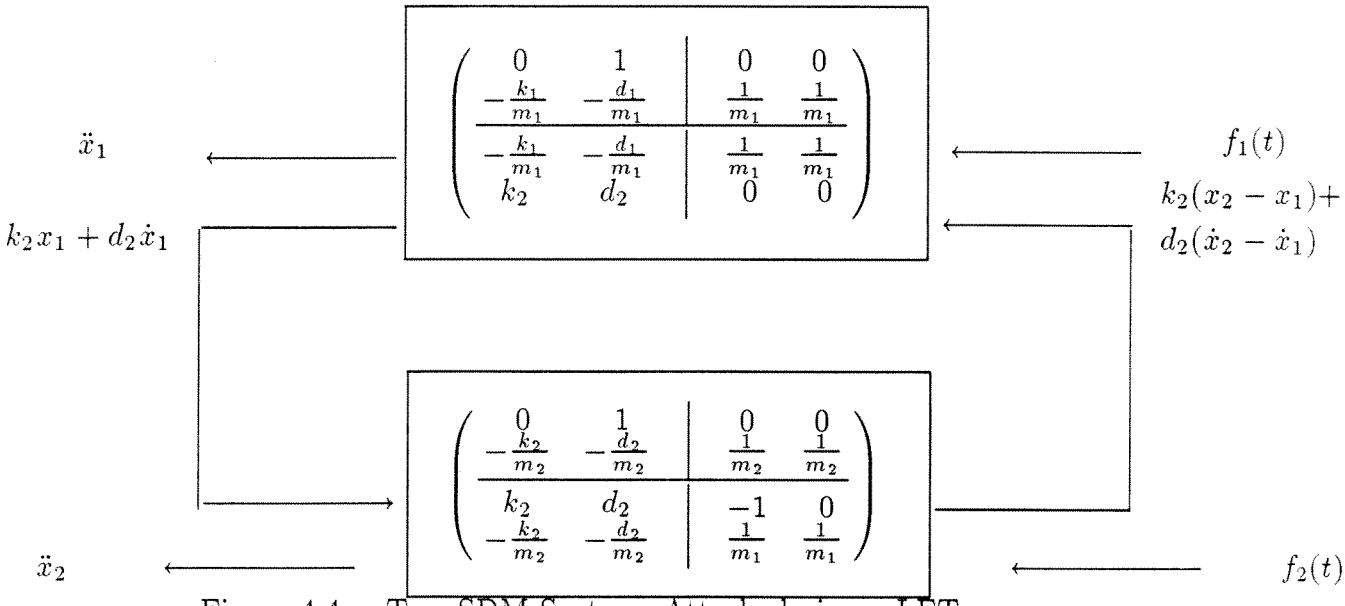

Figure 4.4. - Two SDM Systems Attached via an LFT.
For construction of these systems, it is necessary to know the stiffness and damping of springs and dampers connecting the subsystems.

Then the appropriate outputs from each system may be fed to the other one as shown in Figure 4.4. The connection of these systems looks like a feedback connection, widely used in control theory. This technique can be extended to any length series of SDM systems using the element in Figure 4.5.

Note that during identification of each system, the values $1/m_i$, k_i/m_i, and d_i/m_i must be found. From these, m_i, k_i, and d_i can be derived. Derivation of these values, however, may be quite sensitive to the quality of the identification.

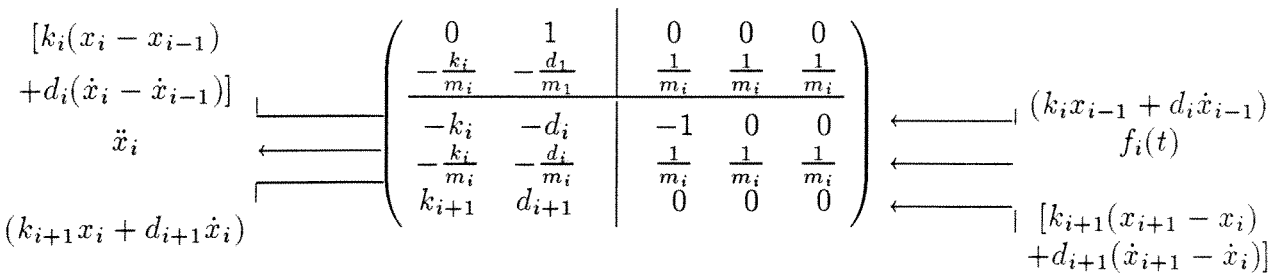

Figure 4.5. - General Series Spring-Damper-Mass Block.
These can be cascaded with any number of SDM systems. Computation of the resulting model is quite straightforward.

More commonly, there will be a need to alter an identified system by the addition of a mass, damping, or stiffness element. It is quite easy to do this using the above technique. For the addition of mass, the equation of motion is

$$(m + m_2)\ddot{x} + d\dot{x} + kx = f(t), \tag{4.4}$$

which is transformed to

$$m\ddot{x} + d\dot{x} + kx = f(t) - m_2\ddot{x}. \tag{4.5}$$

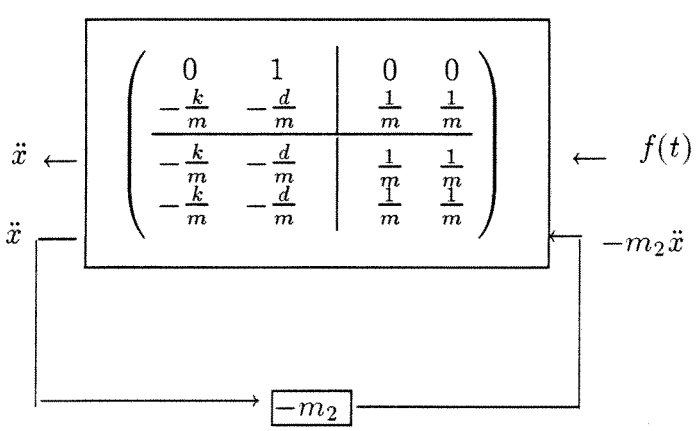

Figure 4.6. - LFT for Addition of Mass.
This is equivalent to the standard equations of motion for mass addition.

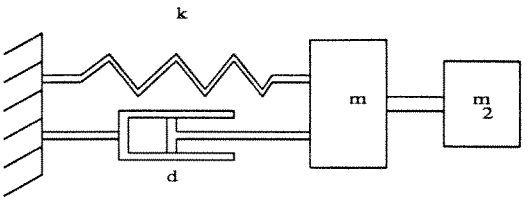

Figure 4.7 - Addition of a Mass to Identified System.
m_2 is added to the rest of the system.

This is represented by Figure 4.7. Change of the system via addition of stiffness or damping is done by replacing $\ddot{x}$ and m_2 with x and k_2 or $\dot{x}$ and d_2 respectively.

4.4 A More General System

4.4.1. A Plate Attached to a Beam

The interconnection method will now be extended for use with multidimensional systems. As a point of departure, a plate at the end of a beam will be treated. The plate is allowed to move essentially in the plane perpendicular to the beam. Thus, the beam experiences one torsional and two transverse bending modes. The axial and other modes may be treated similarly, but for this analysis they are considered negligible. Also, the mass of the beam is ignored. It is assumed that single axis accelerometers are mounted on a plate of mass M and moment of inertia $\mathcal{I}_r$ about the beam (mounted at the center of gravity of the plate). The accelerometers' axes are mounted at angles θ_i to the x-axis of the system. Each sensor is positioned at a distance r_i from the center of gravity (c.g.) with an angle ϕ_i from the x-axis. Motions of the c.g. are denoted by x_{cg}, y_{cg}, and ϕ_{cg}. This mounting scheme allows the sensors to pick up the bending and the torsional models. The expressions for multiaxis accelerometers mounted at the c.g. with torsional sensors are less involved. Figure 4.8 presents this setup.

Motion sensed by each accelerometer will consist of the participation of each mode in the direction of sensitivity of the sensor. It is assumed that the accelerometer is rigidly attached to the plate. The expression for the acceleration sensed by the i^{th} accelerometer in its direction of sensitivity is obtained from a geometric analysis.

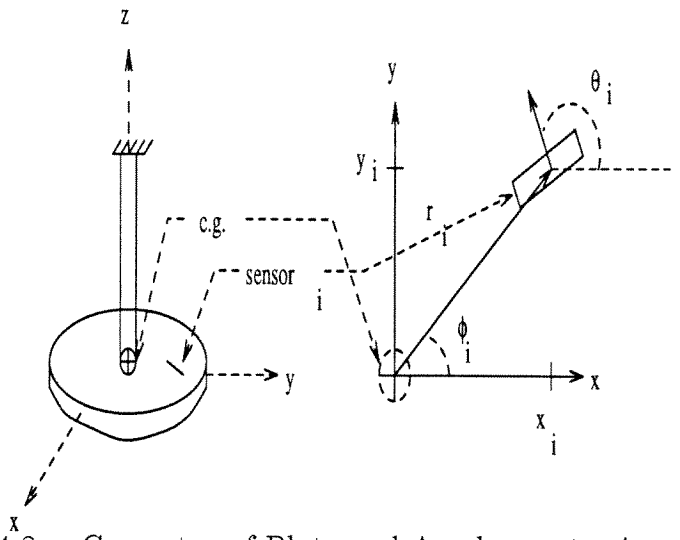

Figure 4.8. - Geometry of Plate and Accelerometer i.
In general, several single axis sensors are mounted on portions of structures in arbitrary configurations as shown. The various motions of the system can be deduced if the geometrical relations are known between the various sensors.

$$\begin{aligned} a_i =& \ddot{x}_{cg}\cos\theta_i + \ddot{y}_{cg}\sin\theta_i + r_i\ddot{\phi}_{cg}\sin(\theta_i - \phi_i - \phi_{cg}) \\ & - r_i\dot{\phi}_{cg}^2\cos(\theta_i - \phi_i - \phi_{cg}). \end{aligned} \tag{4.6}$$

Since motions are considered small, this can be linearized with respect to ϕ_{cg} as

$$\begin{aligned} a_i =& \ddot{x}_{cg}\cos\theta_i + \ddot{y}_{cg}\sin\theta_i + r_i\ddot{\phi}_{cg}\sin(\theta_i - \phi_i) \\ & - r_i\dot{\phi}_{cg}^2\cos(\theta_i - \phi_i). \end{aligned} \tag{4.7}$$

The system has vibrations in the x_{cg}, y_{cg}, and ϕ_{cg} directions represented by the expressions

$$\begin{aligned} M_x\ddot{x}_{cg} + D_x\dot{x}_{cg} + K_x x_{cg} &= \sum_j f_{xcg_j}(t) \\ M_y\ddot{y}_{cg} + D_y\dot{y}_{cg} + K_y y_{cg} &= \sum_j f_{ycg_j}(t) \\ \mathcal{I}_r\ddot{\phi}_{cg} + D_r\dot{\phi}_{cg} + K_r\phi_{cg} &= \sum_j \tau_{cg_j}(t), \end{aligned} \tag{4.8}$$

where M_x and M_y are the mass of the structure; $\mathcal{I}_r$ is the rotational moment of inertia; D_x, D_y, and D_r are the dampings; K_x, K_y, and K_r are the stiffnesses;

and f_{xcg_j}, f_{ycg_j}, and τ_{cg_j} are the forces/moments applied at point j affecting the c.g.

Then, assuming that a linear actuator is placed at position j which is capable of applying a force f_j with orientation θ_j to the x-axis, the i^{th} accelerometer output is

$$\begin{aligned} a_i(s) &= \cos\theta_i \frac{s^2}{M_x s^2 + D_x s + K_x} \sum_j f_j \cos\theta_j \\ &+ \sin\theta_i \frac{s^2}{M_y s^2 + D_y s + K_y} \sum_j f_j \sin\theta_j \\ &+ r_i \sin(\theta_i - \phi_i) \frac{s^2}{\mathcal{I}_r s^2 + D_r s + K_r} \sum_j f_j r_j \sin(\theta_j - \phi_j) \\ &- r_i \cos(\theta_i - \phi_i) \Big[\frac{s}{\mathcal{I}_r s^2 + D_r s + K_r} \sum_j f_j r_j \sin(\theta_j - \phi_j)\Big]^2. \end{aligned} \tag{4.9}$$

The only source of torques is the linear actuator.

The last term of this expression is due to the effect of radial acceleration on a linear sensor. It is a quadratic term corresponding to $\dot{\phi}_{cg}^2$. Because of this quadratic dependence on f_j, this system cannot, in general be described by linear transfer functions. Fortunately, there are two cases where it is possible to apply linear models and the LFT model modification technique:
i) If $(\theta_j - \phi_j) = k\pi$, $k \in$ integer, the $\sin(\theta_j - \phi_j)$ term is zero, so the quadratic terms are removed. This corresponds to forcing geometries which do not excite the torsional mode. In general, external forces will affect torsion, so this special case is not of interest.
ii) If $(\theta_i - \phi_i) = \frac{(2k+1)\pi}{2}$, $k \in$ integer the $\cos(\theta_i - \phi_i)$ term is zero. This corresponds to aligning the axes of the accelerometers so that they do not sense any radial acceleration. By placing the sensors in directions orthogonal to their radial position lines, this can be accomplished.

With condition ii) satisfied, the transfer function from force j to accelerometer i becomes

$$T_{ij}(s) = \cos\theta_i \frac{s^2}{M_x s^2 + D_x s + K_x} \cos\theta_j + \sin\theta_i \frac{s^2}{M_y s^2 + D_y s + K_y} \sin\theta_j + r_i \sin(\theta_i - \phi_i) \frac{s^2}{\mathcal{I}_r s^2 + D_r s + K_r} r_j \sin(\theta_j - \phi_j). \qquad (4.10)$$

with $sin(\theta_i - \phi_i) = \pm 1$.

The state space description for this system is then as shown in Figure 4.9.

$$\left(\begin{array}{cccc|c} 0 & 1 & & & 0 \\ -\frac{K_x}{M_x} & -\frac{D_x}{M_x} & & & \frac{1}{M_x}\cos\theta_j \\ & & 0 & 1 & 0 \\ & & -\frac{K_y}{M_y} & -\frac{D_y}{M_y} & \frac{1}{M_y}\sin\theta_j \\ & & 0 & 1 & 0 \\ & & -\frac{K_r}{\mathcal{I}_r} & -\frac{D_r}{I_r} & \frac{1}{\mathcal{I}_r} r_j \sin(\theta_j - \phi_j) \\ \hline \cos\theta_i[-\frac{K_x}{M_x} & -\frac{D_x}{M_x}] & \sin\theta_i[-\frac{K_y}{M_y} & -\frac{D_y}{M_y}] \quad r_i \sin(\theta_i - \phi_i)[-\frac{K_r}{\mathcal{I}_r} & -\frac{D_r}{\mathcal{I}_r}] & \frac{\cos(\theta_i - \theta_j)}{M} + \frac{r_i \sin(\theta_i - \phi_j) r_j \sin(\theta_j - \phi_j)}{\mathcal{I}_r} \end{array}\right) = \left(\begin{array}{c|c} A & B \\ \hline C & D \end{array}\right)$$

Figure 4.9. - State Space Description of Plate System.
Only one mode is assumed in each direction of motion. When multiple modes are present, this form generalizes.

4.4.2. Addition of a Mass to a System

If a mass m_2 is added at a distance $\bar{r}$ from the c.g., the setup is represented by Figure 4.10 where

$$C_2 = \begin{pmatrix} -\frac{K_x}{M_x} & -\frac{D_x}{M_x} & & \\ & & -\frac{K_y}{M_y} & -\frac{D_y}{M_y} \\ & & -\frac{\bar{r}K_r}{\mathcal{I}_r} & -\frac{\bar{r}D_r}{\mathcal{I}_r} \end{pmatrix} \quad B_2 = \begin{pmatrix} 0 & & \\ \frac{1}{M_x} & & \\ & 0 & \\ & \frac{1}{M_y} & \\ & & 0 \\ & & \frac{\bar{r}}{\mathcal{I}_r} \end{pmatrix}$$

$$D_{12} = CB_2 \quad D_{21} = C_2 B \quad D_{22} = C_2 B_2. \qquad (4.11)$$

It may be noted that $-m_2[I_n]$ is placed in the lower block of the LFT. Here I_n is the identity matrix of size n, where n is the number of dimensions of motion measured (3 in this case). When more dimensions are used, this size needs to be increased (up to six per connection location).

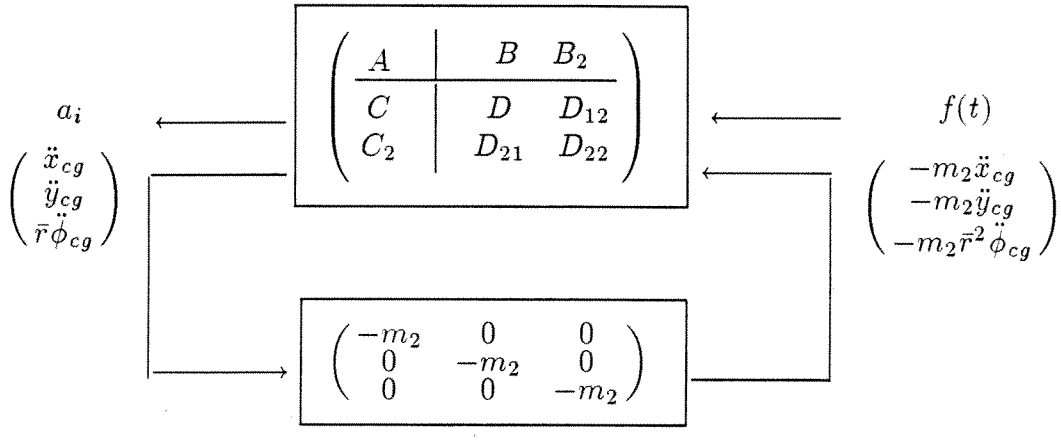

Figure 4.10. - Adding a Mass to a Plate.
Only three directions of motion are assumed in this setup. In a more general situation, there may be six directions of motion, so the lower matrix will be six by six.

Similar changes in stiffness or damping can be made using this formulation. The outputs in those cases then need to be changed to the differences in distance or velocity (respectively) between the points at which the changed elements are attached. Then, inputs will be forces applied at those points.

4.4.3. Connection of Systems with Dynamics

For addition of dynamics a relationship similar to the LFT may be set up. There are two derivations for this: one is based on the LFT; the other is based on Lagrange undetermined coefficients (constraints) as used in [CKR]. First, the transfer function from force input to acceleration output for a mass m is $\frac{1}{m}$. In the above LFT, the lower block is $-m$. Generalizing to a system with dynamics, then a negative inverse of the system dynamics could be placed in the lower block. That is, suppose the identified model for a certain system (force input; acceleration, velocity or displacement output) is represented by K, which is assumed invertible.

K^{-1} corresponds to the transfer function from sensors to actuators (the inverse of the actual plant). The attachment LFT to a system P is then

$$\mathcal{F}_l(P, -K^{-1}) = P_{11} - P_{12}K^{-1}[I + P_{22}K^{-1}]^{-1}P_{21}.$$

Because of invertibility of K, then

$$\mathcal{F}_l(P, -K^{-1}) = P_{11} - P_{12}[K + P_{22}]^{-1}P_{21}. \tag{4.12}$$

The last part of this expression is convenient because the model K does not need to be inverted. On identified models, this inversion is undesirable since it can be very sensitive numerically.

The derivation of this relation using constraint variables is shown next. More general connection types can be derived with this procedure. It is assumed that transfer function models (in state space, for example) are used to describe each structure to be connected. The models may come from theoretical analyses or from identification procedures. Each system will be taken as 2-input, 2-output where the inputs or outputs may be vectors of signals. Expressions are given in state space for computation of the combined system model. Without loss of generality, the derivation will be done for the connection of two structural systems.

Let the first system (structure I) be modeled as

$$P = \begin{bmatrix} P_{11} & P_{12} \\ P_{21} & P_{22} \end{bmatrix} = \left(\begin{array}{c|cc} A & B_1 & B_2 \\ \hline C_1 & D_{11} & D_{12} \\ C_2 & D_{21} & D_{22} \end{array}\right)$$

$$\begin{pmatrix} z_1 \\ z_2 \end{pmatrix} = \begin{bmatrix} P_{11} & P_{12} \\ P_{21} & P_{22} \end{bmatrix} \begin{pmatrix} f_1 \\ f_2 \end{pmatrix}$$

and let the second system (structure II) be denoted by

$$K = \begin{bmatrix} K_{11} & K_{12} \\ K_{21} & K_{22} \end{bmatrix} = \left(\begin{array}{c|cc} E & F_1 & F_2 \\ \hline G_1 & H_{11} & H_{12} \\ G_2 & H_{21} & H_{22} \end{array}\right).$$

$$\begin{pmatrix} z_3 \\ z_4 \end{pmatrix} = \begin{bmatrix} K_{11} & K_{12} \\ K_{21} & K_{22} \end{bmatrix} \begin{pmatrix} f_3 \\ f_4 \end{pmatrix}$$

It is required that force input to sensed output transfer functions be available for both structures at the attachment locations. In this case, structure I's attachment is located where f_2 is applied and z_2 is measured. structure II's connection point is at f_3 and z_3. When the systems are connected at these points, the effects of f_2 and f_3 will be the same on z_2 and z_3. If z_2 and z_3 measure the same quantity with the same gain, then they should be equal. For these relations to be met, the transfer functions from f_2 to z_2 must be made equal to those from f_3 to z_3.

For the second derivation, the two independent systems are diagonally augmented as

$$\underline{z} = \begin{pmatrix} z_1 \\ z_2 \\ z_3 \\ z_4 \end{pmatrix} = \begin{bmatrix} P_{11} & P_{12} & & \\ P_{21} & P_{22} & & \\ & & K_{11} & K_{12} \\ & & K_{21} & K_{22} \end{bmatrix} \begin{pmatrix} f_1 \\ f_2 \\ f_3 \\ f_4 \end{pmatrix} = T\underline{f}.$$

Addition of constraints may be done by choosing a constraint matrix R, and constraint coefficients λ so that $R^*\underline{z} = \underline{0}$. The * superscript denotes complex conjugate transpose, although in this case R is real. For the case of setting constraints equal, R is chosen such that $R = [0\ R_1^*\ R_2^*\ 0] = [0\ I_{z_2}\ -I_{z_3}\ 0]$, where $I_{z_2} = I_{z_3}$ is the identity matrix of size of the number of signals in the attachment outputs. $R\lambda$ will be the necessary forces of constraint to impose the desired connections. Assuming that T is invertible (symbolically) the constraint forces are added to create the system

$$\begin{bmatrix} T^{-1} & R \\ R^* & 0 \end{bmatrix} \begin{pmatrix} \underline{z} \\ \lambda \end{pmatrix} = \begin{pmatrix} \underline{f} \\ \underline{0} \end{pmatrix}.$$

By solving for λ and substituting back into the equations for $\underline{z}$, the transfer functions in Figure 4.11 are obtained for the combined system. When $R_1 = I$, and $R_2 = -I$ these transfer functions simplify via straightforward identities to Figure 4.12.

In state space, this transfer matrix is computed as shown in Figure 4.13. The only inversion necessary is that of Q, which contains the static response of the system and the effects of the unmodeled modes. As seen here, and discussed by Ewins [Ewi], these terms need to be identified quite well, especially if they are of small magnitude. Otherwise, when inverted, errors will appear in all transfer functions.

$$\hat{T} = \begin{bmatrix} P_{11} - P_{12}R_1B^{-1}R_1^*P_{21} & P_{12} - P_{12}R_1B^{-1}R_1^*P_{22} & -P_{12}R_1B^{-1}R_2^*K_{11} & -P_{12}R_1B^{-1}R_2^*K_{12} \\ P_{21} - P_{22}R_1B^{-1}R_1^*P_{21} & P_{22} - P_{22}R_1B^{-1}R_1^*P_{22} & -P_{12}R_1B^{-1}R_2^*K_{11} & -P_{12}R_1B^{-1}R_2^*K_{12} \\ -K_{11}R_2B^{-1}R_1^*P_{21} & -K_{11}R_2B^{-1}R_1^*P_{22} & K_{11} - K_{11}R_2B^{-1}R_2^*K_{11} & K_{12} - K_{11}R_2B^{-1}R_2^*K_{12} \\ -K_{21}R_2B^{-1}R_1^*P_{21} & -K_{21}R_2B^{-1}R_1^*P_{22} & K_{21} - K_{21}R_2B^{-1}R_2^*K_{11} & K_{22} - K_{21}R_2B^{-1}R_2^*K_{12} \end{bmatrix}$$

$$\text{such that } \begin{pmatrix} z_1 \\ z_2 \\ z_3 \\ z_4 \end{pmatrix} = \hat{T} \begin{pmatrix} f_1 \\ f_2 \\ f_3 \\ f_4 \end{pmatrix} \text{ and } B = [R_1^*P_{22}R_1 + R_2^*K_{11}R_2]$$

Figure 4.11. - Combined System Transfer Functions.
Information on how the two systems are connected to each other (rigidly, through springs, etc.) is contained in R. This is the general form of the attachment formulation.

$$\begin{pmatrix} z_1 \\ z_2 \\ z_3 \\ z_4 \end{pmatrix} = \begin{bmatrix} P_{11} - P_{12}B^{-1}P_{21} & P_{12}B^{-1}K_{11} & P_{12}B^{-1} * K_{11} & P_{12}B^{-1}K_{12} \\ K_{11}B^{-1}P_{21} & K_{11}B^{-1}P_{22} & P_{22}B^{-1}K_{11} & P_{22}B^{-1}K_{12} \\ K_{11}B^{-1}P_{21} & K_{11}B^{-1}P_{22} & P_{22}B^{-1}K_{11} & P_{22}B^{-1}K_{12} \\ K_{21}B^{-1}P_{21} & K_{21}B^{-1}P_{22} & K_{21}B^{-1}P_{22} & K_{22} - K_{21}B^{-1}K_{12} \end{bmatrix} \begin{pmatrix} f_1 \\ f_2 \\ f_3 \\ f_4 \end{pmatrix}$$

$$B \text{ simplifies to } [P_{22} + K_{11}]$$

Figure 4.12. - Combined System Simplified Transfer Functions.
The transfer functions from f_2 to z_2 and from f_3 to z_3 have been set equal. This corresponds to connection at locations 2 and 3.

The result is a state space transfer function model which can be used directly to generate frequency responses or to synthesize controllers. If the modes of the new system are desired, an eigenvalue and eigenvector computation of the A-matrix of the new system is required. It is easy to check that the transfer functions from f_2 to z_2 are equal to those from f_3 to z_3.

For every degree of freedom that is connected, one mode (2 states) will drop out of the above system. Removal of these modes from the realization can be done using one of various model reduction methods [Bmu]. The main restriction this procedure has in state space is that Q must exist. For this to happen the static

$$\left(\begin{array}{cc|cccc} A - B_2QC_2 & -B_2QG_1 & B_1 - B_2QD_{21} & -B_2QH_{11} & -B_2QH_{11} & -B_2QH_{12} \\ -F_1QC_2 & E - F_1QG_1 & -F_1QD_{21} & -F_1QD_{22} & -F_1QD_{22} & F_2 - F_1QH_{12} \\ \hline C_1 - D_{12}QC_2 & -D_{12}QG_1 & D_{11} - D_{12}QD_{21} & -D_{12}QH_{11} & -D_{12}QH_{11} & -D_{12}QH_{12} \\ -H_{11}QC_2 & -D_{22}QG_1 & -H_{11}QD_{21} & -H_{11}QD_{22} & -H_{11}QD_{22} & -D_{22}QH_{12} \\ -H_{11}QC_2 & -D_{22}QG_1 & -H_{11}QD_{21} & -H_{11}QD_{22} & -H_{11}QD_{22} & -D_{22}QH_{12} \\ -H_{21}QC_2 & G_2 - H_{21}QG_1 & -H_{21}QD_{21} & -H_{21}QD_{22} & -H_{21}QD_{22} & H_{22} - H_{21}QH_{12} \end{array}\right)$$

$$Q = [D_{22} + H_{11}]^{-1}$$

Figure 4.13. - State Space Representation of Combined Systems.
It is easy to see that the state space relations for the transfer functions at locations 2 and 3 are equal.

contributions of the two structures must be nonzero. Unfortunately, this restricts the procedure to acceleration output models. On actual structures, this is not a significant restriction, since accelerometers are easy to implement.

It is still possible to apply the connection scheme using displacement or velocity sensing. The velocity or displacement models can be easily modified to acceleration models by modifying the state space descriptions. Similarly, the computations may be done with polynomials or with other realization setups.[Kai]

4.4.4. Restrictions of the Connection Method

Physically, there is a large restriction to this method: The system's behavior must only be changed in a linear-fractional way. This limitation also exists in previous approaches to response mode synthesis. For bending modes, the limitation is not a problem. However, torsional modes, because of Coriolis and centrifugal forces may give trouble. As with the beam-disk problem shown above, the resulting implementational limitations are stated easily: the axes of rotation of the torsional modes must not be significantly altered by the assembly of the substructures; and radial acceleration must not be sensed. For exact results, the axes of rotation (a.r.) must not be moved at all. If the axes of rotation move, the radii from the a.r. to the attached mass become unknown. Since these quantities appear as r^2, the changes will give a nonlinear modification. In general, however, the method will give good linear re-analyses to systems.

4.5 Conclusion

The method, as presented in this chapter is a generalization to state space of response/component mode synthesis. Given, the proper models, the connection scheme involves inversion of only the static components of the system models. The state space and LFT framework points out the restrictions of the method quite clearly and presents the needs for information to be identified. Chapter 5 further discusses identification of the necessary parameters, and presents examples of implementation of the method explained in this chapter.

4.6 References for Chapter 4

Bmu: Balas, G., *et al.*, (1991),**μ-Analysis and Synthesis Toolbox,** MUSYN, Inc., and The Math Works, Inc., Natick, Massachusetts.

Ber: Berman, A., (1984), "System Identification of Structural Dynamics Models-Theoretical and Practical Bounds," AIAA Paper # 84-0929.

Bla: Blackwood, G.H., (1988), "Experimental Component Mode Synthesis of Structures with Joint Freeplay," Report SSL#16-88, Space Systems Laboratory, Massachusetts Institute of Technology, Cambridge, Massachusetts.

CaO: Caughey, T.K., and O'Kelley, M.E.J., (1965), "Classical Normal Modes in Damped Linear Dynamic Systems," *Journal of Applied Mechanics,* Vol. 39, No. 3, pp. 583-588

Cau: Caughey, T.K., (1982), "Structural Dynamics Analysis, Testing, and Correlation," JPL Publication 81-72, Pasadena, CA.

Chi: Chiatti, G., and Sestieri, A., (1979), " Analysis of Static and Dynamic Structural Problems by a Combined Finite Element-Transfer Matrix Method," *Journal of Sound and Vibration* 67(1), pp. 35-42.

Cra: Craig, R.R., Jr., (1985), "A Review of Time-Domain and Frequency-Domain Component Mode Synthesis Methods," **Combined Experimental/Analytical Modeling of Dynamic Structural Systems,** ASCE/ ASME Mechanics Conference, AMD, Vol. 67, pp. 1-30.

CKR: Crowley, J.R., Klosterman, A.L., Rocklin, G.T., and Vold, H., (1984), "Direct Structural Modification Using Frequency Response Functions," *Proceedings of the 2^{nd} International Modal Analysis Conference,* Union College, Schenectady, NY, pp. 930-936.

Dok: Dokainish, M.A., (1972), "A New Approach for Plate Vibrations: Combination of Transfer Matrix and Finite Element Techniques," *ASME Journal of Engineering in Industry,* pp. 526-530.

DFT: Doyle, J., Francis, B., and Tannenbaum, A., (1992), **Feedback Control Theory,** Macmillan Publishing Co., New York.

DGK: Doyle, J., Glover, K., Khargonekar, P., and Francis, B., (1989), "State Space Solutions to standard H_2 and H_∞ Control Problems," *IEEE Transactions on Automatic Control* Vol. AC 34, pp. 831-847.

DGF: Doyle, J., Glover, K., Khargonekar, P., and Francis, B., (1988), "State Space Solutions to standard H_2 and H_∞ Control Problems," *Proceedings of the American Controls Conference,* Atlanta, GA.

Ewi: Ewins, D.J., (1985), "Modal Test Requirements for Coupled Structure Analysis Using Experimentally Derived Component Models," **Combined Experimental/Analytical Modeling of Dynamic Structural Systems,** ASCE/ASME Mechanics Conference, AMD, Vol. 67, pp. 1-30.

Fla: Flashner, H., (1986), "An Orthogonal Decomposition Approach to Modal Synthesis", *International Journal for Numerical Methods in Engineering* 23, p. 471-493.

GLM: Gwinn, K.W., Lauffer, and J.P., Millar, A.K., (1988), "Component Mode Synthesis using Experimental Modes Enhanced by Mass Loading", *Proceedings of the 6^{th} International Modal Analysis Conference,* Kissimmee, FL, pp. 1088-1093

HEN: Hedges, T., Elliot, S.J., and Nelson, P.A., (1988), "The Active Simulation of Structural Frequency Response Functions" *Proceedings of the 6^{th} International Modal Analysis Conference,* Kissimmee, FL, pp. 67-72

Hur: Hurty, W.C., (1965), "Dynamic Analysis of Structural Systems using Component Modes," *AIAA Journal,* Vol 3, No. 4, pp. 678-685.

Kai: Kailath, T., (1980), **Linear Systems**, Prentice-Hall, Englewood Cliffs, New Jersey.

KwS: Kwakernaak, H., and Sivan, R., (1972), **Linear Optimal Control Systems**, Wiley-Interscience, New York.

Lar: Larsson, P.O., (1989), "Dynamic Analysis of Assembled Structures using Frequency Response Functions: Improved Formulation of Constraints," *International Journal of Analytical and Modal Analysis,* 5(1): pp. 1-12.

MdE: M^{c}Daniel, T.J., and Eversole, K.B., (1989), "A Combined Finite Element-Transfer Matrix Structural Analysis Method," *Journal of Sound and Vibration,* 51(2), pp. 157-169.

Mos: Moser, A.N., and Caughey, T.K., (1991) "Some Experience with Identification of the Caltech Experimental Space Structure." *Proceedings of the 1991 American Controls Conference,* Boston, Massachusetts.

SBC: Sadeghipour, K., Brandon, J.A., and Cowley, A., (1985), "The Receptance Modification Strategy of a Complex Vibrating System," *International Journal of Mechanical Sciences*, 27 (11/12), pp. 841-846.

Sku: Skudrzcyk, E., (1968), **Simple and Complex Vibratory Systems**, Pennsylvania State University Press, Pennsylvania.

SpT: Spanos, J.T., and Tsuha, W.S., (1989), " Multibody Dynamics: Modeling Component Flexibility with Fixed, Free, Loaded, Constraint, and Residual Modes," *Proceedings of the 3rd Annual Conference on Aerospace Computational Control,* JPL Publication 89-45, Pasadena, CA, pp. 761-777.

StF: Strang, G., and Fix, G.J., (1973), **An Analysis of the Finite Element Method** Prentice-Hall Inc., Englewood Cliffs, New Jersey.

Tsu: Tsuei, Y.G., and Yee, E.K.L., (1988), "An Investigation to the Solution of Component Modal Synthesis," *Proceedings of the 6th International Modal Analysis Conference,* Kissimmee, FL, pp. 383-396

Wan: Wang, J.H., and Liou, C.M., (1989), "Experimental Substructure Synthesis with Special Consideration of Joint Effects," *International Journal of Analytical and Experimental Modal Analysis,* 5(1): pp. 13-24.

Chapter 5. Numerical and Experimental Applications of the Assembly Methodology

5.1 Introduction

In this chapter, the methods explained in Chapter 4 are applied to numerical and experimental systems. In the first section, implementational details relating to what information must be experimentally obtained for the procedure are discussed. Section 3 presents a method to identify these parameters for systems with noncolocated sensor/actuator (sensor/actuator) geometries. A numerical example of the entire procedure follows in Section 4. The experimental connection, which involves comparisons of the responses of the physically attached systems with the predictions based on the proposed method, is given in Section 5. This is followed by discussions of the experimental results (Section 6) and suggestions for improvement of the experiments (Section 7). The final section gives a brief conclusion.

Many of the features which make this method so valuable are used for the experiments: The two structures are excited by actuators that are not colocated with the sensors or the connection point for the systems. Some of the actuators are locally controlled to follow a given displacement command. Models are developed from input and output voltages from accelerometers and actuators sampled by a data acquisition system. Thus absolute physical information of the structure is not used (except for some geometrical relations between sensors). And finally, the two structures have different sensor/actuator (hardware) combinations so that the basic system input/output models are incompatible for connection.

5.2 Necessary Information from Identification

If the procedure is to be used, there are several parameters that need to be identified besides those identified for transfer function models. These parameters have to do with normalization/uniqueness of the models and with compatibility of the substructures' models.

The models for two systems will be immediately compatible if the same actuators and sensor are used on both structures and if there are enough sensors and actuators colocated at the attachment points. The transfer functions from inputs to outputs at the connection locations are then known and are normalized correctly for both structures. In this case, the procedure is identical to previous response/ component mode synthesis approaches[Ewi]. When different sensors and actuators are used, if accurate conversion factors are known from one set of transfer functions to the other, the necessity of using the same actuators and sensors is reduced, but the models must be normalized appropriately. The colocated sensor/actuator requirement means that all significant directions of motion (degrees of freedom to be connected) are sensed and excited at the connection points of the systems. With an identified model for the colocated case, the transfer functions to be constrained can be obtained from straightforward manipulation of the realizations using the known geometries of the sensors and actuators. A reference coordinate system should be chosen on each system based on the geometry of the attachment procedure.

5.3 Systems with Noncolocated Sensor/Actuator Geometries

For systems where colocated sensor/actuator geometries are not available at the attachment point, or where the sensor/actuator sets are not identical (i.e., sensor and actuators on the two systems have different sensitivities and gains,) an indirect method can be used to determine the parameters necessary for modal synthesis. The procedure requires two physical identification experiments for each system: a full identification, and a partial identification. First, the structure is excited and fully identified in its basic form. For force input, acceleration output structures a model of the form

$$T_{ij}(\omega_k) = \sum_{m=1}^{M} \frac{c_i^{(m)} b_j^{(m)} (-\omega_k^2)}{(f_m^2 - \omega_k^2) + 2\sqrt{-1} f_m \zeta_m \omega_k} + b_j^{(r)} c_i^{(r)}. \qquad (5.1)$$

as described in Chapter 3 can be used. For displacement or velocity sensing, the numerator term $-\omega_k^2$ can be changed to 1 or $\sqrt{-1}\omega_k$, respectively and the residual terms are removed. The functional dependence of the transfer functions on ω_k is assumed, and is left out of the notation.

5.3.1. Uniqueness of Identified Modal Models

This type of model is unique to within one parameter per mode, i.e.,

$$[\alpha^{(m)} c_i^{(m)}][b_j^{(m)} \frac{1}{\alpha^{(m)}}] = \hat{c}_i^{(m)} \hat{b}_j^{(m)}$$

for all m, i, and j. $\alpha^{(m)}$ can be thought of as a normalization factor, but it will be referred to herein as the *modal weight* since each mode's input and output participation factors needs to be mass-normalized for the attachment procedure to work.

5.3.2. Systems with Actuator Dynamics

Actuator dynamics can also be added. For example, if the actuator at input j has a local controller for displacement tracking, a term of the form

$$\left[\frac{m_j(-\omega_k^2)}{(\sqrt{-1}\omega_k + p_1)(\sqrt{-1}\omega_k + p_2)}\right] \tag{5.2}$$

can multiply equation (5.1). This term is included only for transfer functions relating to the controlled input.

5.3.3. Modal Assumption

In structural systems, for every mode and every location on the structure, the input eigenvectors have the same shape as the output eigenvectors. The input and output participation factors for the models are obtained from these eigenvectors. Since the basic identification procedure is unable to determine the modal weight parameters $\alpha^{(m)}$, another procedure is needed. The second experiment and the partial identification mentioned above do this. In the LFT for mass attachment, the only unknown parameters (in the non-ideal case) are the input participation factors at the attachment location. These can be assumed, from basic structural theory, to be multiples of the output participation factors at that point, i.e., $b_i^{(m)} = \alpha^{(m)} c_i^{(m)}$.

The factors $\alpha^{(m)}$ may then be determined from the following partial identification procedure: The base model obtained from the original identification is used with data from experimental excitations of the structure with the known mass attached to it. That is, a mass of known size is attached to the structure at the connection location, and the system is excited. The resulting data is then used for an identification procedure based on the model developed for the unmodified structure. A gradient search, for example, can be made on the response of the LFT for a structure with a known mass attached to it. The search is done for the $\alpha^{(m)}$ parameters which appear in the input participation factors for the attachment point $b^{(m)}_{attach} = \alpha^{(m)} c^{(m)}_{attach}$.

To describe the transfer function for the partial identification, an example for two-dimensional motion is given. A coordinate frame must be chosen, and geometric relations between the sensors and the coordinates must be determined (as in the plate at the end of the beam example in Chapter 4). Letting the directions of motion for the two-dimensional example be x and y, T_{ix} will denote the transfer function from a force in the x-direction to sensor i, T_{xj} denotes effects of input j to an artificial sensor in the x-direction, and T_{xx} represents the motion sensed by an x-direction sensor by an x-direction force. Forces and accelerations in the y-direction are denoted similarly. Then, the transfer matrix of a structure modified by a known mass $\hat{m}$ is computed as in Figure 5.1.

$$T_{ij}^{(modified)} = T_{ij} + \begin{bmatrix} T_{ix} & T_{iy} \end{bmatrix} \begin{bmatrix} -\hat{m} & 0 \\ 0 & -\hat{m} \end{bmatrix} \left\{ \begin{bmatrix} 1 & 0 \\ 0 & 1 \end{bmatrix} - \begin{bmatrix} T_{xx} & T_{xy} \\ T_{yx} & T_{yy} \end{bmatrix} \begin{bmatrix} -\hat{m} & 0 \\ 0 & -\hat{m} \end{bmatrix} \right\}^{-1} \begin{bmatrix} T_{xj} \\ T_{yj} \end{bmatrix}$$

Figure 5.1. - Modified Transfer Function.
Only two directions of motion are considered in this representation.

For linear structures with torsion, the torsional modes may be assumed independent of the bending modes, thus translational direction forces will not excite torsional modes. Letting

$$Q(m,k) = \frac{-\omega_k^2}{(f_m^2 - \omega_k^2) + 2\sqrt{-1} f_m \zeta_m \omega_k},$$

the individual transfer functions for the x-direction are computed as

$$T_{ix} = \sum_{m=1}^{M} c_i^{(m)} c_x^{(m)} \alpha^{(m)} Q(m,k)$$

$$T_{xj} = \sum_{m=1}^{M} c_x^{(m)} b_j^{(m)} Q(m,k)$$

$$T_{xx} = \sum_{m=1}^{M} c_x^{(m)} c_x^{(m)} \alpha^{(m)} Q(m,k).$$

Other directions are computed similarly.

When the identifications of the $\alpha^{(m)}$'s is done for each structure, the resulting parameter set includes enough information to set up models for structure coupling. The modal mass properties are known. Different masses $\hat{m}$ may be used on the different systems, but for compatibility, the relationships between the mass sizes must be known. The relation is used for a normalization which involves multiplying all the modal weight parameters on one structure by the ratio of the two masses used. In essence, the above procedure produces a generalized physical input which can be identified without the use of an actual physical actuator. This results in the main advantage of this method which is that conversion of measured voltages to physical quantities is not necessary. In other words, amplifier gains, sensor resolutions, and equipment voltage conversion factors need not be known. Another major advantage is that actuators with local feedback controllers can be used since the actuator dynamics do not affect the generalized force input created by the added mass.

5.4 Numerical Example

A simple numerical example consisting of two SDM systems with two modes each is given to assist presentation of the concepts. The basic set for each system matches that in Figure 5.3. The properties of each structure for this example are shown in Table 5.1.

A mass of .3 (30% of m_1 on structure I) was added to each system's m_2 to modify it. Theoretical and LFT models were set up for the modification. The LFT procedure was verified by comparison of the resulting LFT models with the theoretical models of the two modified SDM systems. Various internal realizations

quantity	Structure I	Structure II	quantity	Structure I	Structure II
m_1	1.0	5.0	m_2	2.0	7.0
d_1	0.001	0.002	d_2	.002	.003
k_1	1.0	4.0	k_2	3.0	8.0
ω_1	0.5365	0.5294	ω_2	2.2830	1.8063
ζ_1	2.553×10^{-4}	1.266×10^{-4}	ζ_2	8.160×10^{-4}	3.584×10^{-4}

Table 5.1 - Numerical Examples: 2SDM Systems: Basic Properties.
Units on mass, stiffness, and damping are not specified. They must be compatible, but the curve fit method does not select units.

were set up to test the generality of the method. (The $[A, B, C, D]$ state space internal realization is equivalent to $[S^{-1}AS, S^{-1}B, CS, D]$, where S is a similarity transformation. Then, using S, the realization can be transformed into various forms (for A) including diagonal and block modal form.) The LFT mass addition procedure was then performed on the block modal realization and on the original full realization. As expected, the LFT model responses were identical to the theoretical responses regardless of the internal realization of the input/output transfer functions. Results of these tests were then compared with theoretical input/output models. No difference appeared as seen in Table 5.2. Frequency responses from all inputs to all outputs were also compared: they were exactly equal.

quantity	Structure I	Structure II	quantity	Structure I	Structure II
m_1	1.0	5.0	m_2	2.3	7.3
d_1	0.001	0.002	d_2	.002	.003
k_1	1.0	4.0	k_2	3.0	8.0
Theo. ω_1	0.5084	0.5215	Theo. ω_2	2.2436	1.7995
LFT ω_1	0.5084	0.5215	LFT ω_2	2.2436	1.7995
Theo. ζ_1	2.411×10^{-4}	1.245×10^{-4}	Theo. ζ_2	8.068×10^{-4}	3.567×10^{-4}
LFT ζ_1	2.411×10^{-4}	1.245×10^{-4}	LFT ζ_2	8.068×10^{-4}	3.567×10^{-4}

Table 5.2 - Numerical Examples: 2SDM Systems: Properties when Modified.
The theoretical and the LFT connections give exactly the same results. This shows that the method extends to multi degree of freedom systems.

The frequency responses for the original and modified systems were then used for the full and partial identification procedures as outlined above. The experiment was set up in a form where information on the modal weight parameters was not directly obtainable (only the FRFs were used). Since this data was numerically

generated, when the necessary curve fits for parameter identification were carried out, very small errors resulted between the identified and theoretical models. Further iterations of the identification procedures would have resulted in removal of all error between the models and the numerically generated data. Magnitude versus frequency plots for the two structures from f_1 to $\ddot{x}_1$ in each one are presented in Figure 5.2. The responses of the models are also shown.

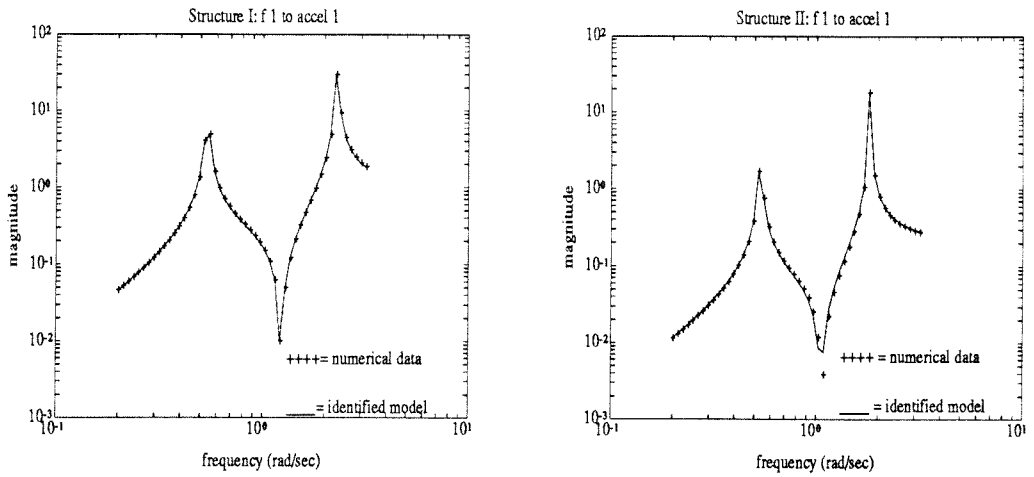

Figure 5.2. - Unmodified SDM Systems: Full Identification.
The only error visible is in structure II at the zero between modes. Further iterations removes this error, but it is left in to check robustness of the connection method.

In Table 5.3, the modal weight parameters from the modified system identification procedure are presented for the two SDM structures. The modification mass was placed on each structure at the location where the two systems were to be joined (mass 2). As a check of the theory, the mass was then placed on each structure's mass 1. When this identification was done, it was found that the modal weight quantities were independent of the mass attachment location. (Small differences were found, but these are due to errors in the original identification procedures.)

Magnitude plots of f_1 to $\ddot{x}_1$ for the modified independent systems (addition at mass 2) are presented in Figure 5.3. It is encouraging to note that the fits are of the same quality as those for the original system. The change from the original response to the mass modified one is parametrized by one value per mode.

quantity	Attachment Mass #	Structure I	Structure II
α_1	1	4.054	17.330
α_1	2	4.056	17.308
α_2	1	1.325	6.891
α_2	2	1.325	6.887

Table 5.3 - Numerical Examples: 2SDM Systems: Identified Modal Weights.
Invariance of modal weights with respect to modification location is demonstrated here. The differences are due to errors in the identification of the base structures.

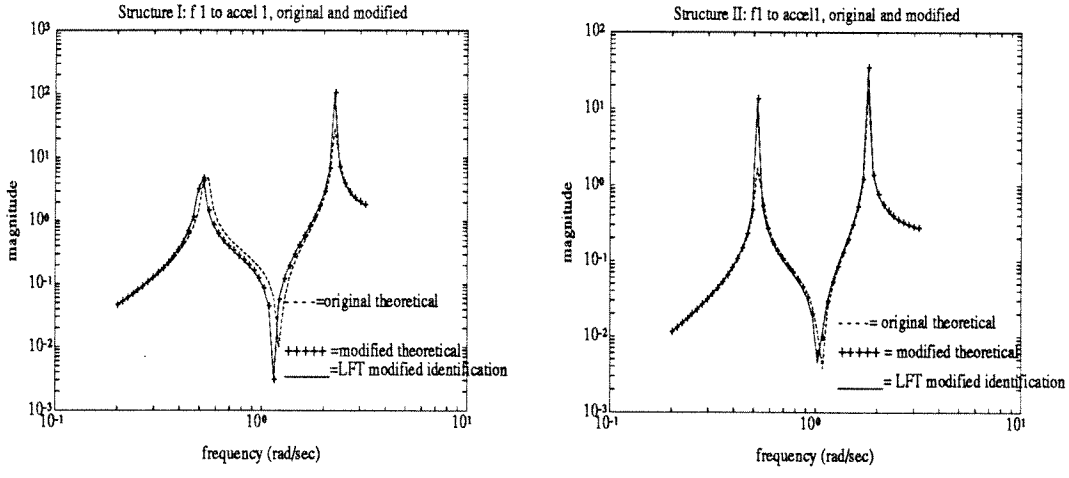

Figure 5.3. - Mass Modified Spring-Damper-Mass Systems.
The original responses (dashed) are presented to show that the modifications are quite small. From these small differences in responses, it is still possible to identify the necessary values for the connection procedure.

The attachment procedure was then used to join the two structures at m_2 of each system. Results for frequencies and dampings of the response synthesis procedure are compared in Table 5.4 to those of the same system generated from basic principles. Plots of the previously shown transfer functions are also presented for the combined system and the exact three mode system. These plots demonstrate that the dynamics of both original systems appear clearly where they did not previously appear. That is, modes due to Structure II appear in responses of Structure I's masses and vice-versa.

5.5 Experimental Connection of Two Lightly Damped Structures

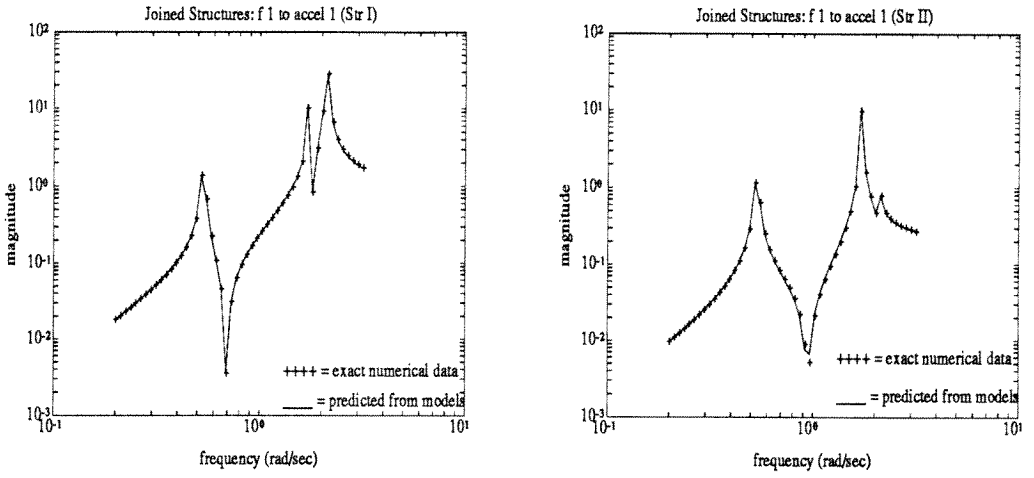

Figure 5.4. - Coupled Spring-Damper-Mass Systems.
The only visible error between the LFT connection procedure and the exact theoretical response is at very small amplitudes. This is caused by the error in the base system identification. The LFT method works quite well.

quantity	Exact Theoretical	From Combined Systems
ω_1	0.5309	0.5309
ζ_1	1.541×10^{-4}	1.543×10^{-4}
ω_2	1.7135	1.7120
ζ_2	3.797×10^{-4}	3.750×10^{-4}
ω_3	2.0987	2.0994
ζ_3	7.363×10^{-4}	7.204×10^{-4}

Table 5.4 - Numerical Examples: 2 Coupled SDM Systems: Predicted and Exact.
The values resulting from the two methods are quite close. Differences may be attributed to errors in the identification procedures. These discrepancies can be removed through further iterations.

As a true test of the methodology, two structures were connected experimentally, and their models were attached theoretically (as above). Information on the shape and identification of the larger of the two systems (the Caltech Flexible Structure) is found in [Mos] and in Chapter 3 of this thesis.

For the partial identification procedure (to find the $\alpha^{(m)}$'s) the structural transfer functions were put in an LFT framework based on attachment of a mass at a particular location. Gradient searches were then performed to determine the modal mass parameters.

5.5.1. Secondary Structure to be Attached

A simple single mode beam-like structure was built to experimentally test the validity of the response synthesis method as proposed. This system consists of two steel masses connected to each other through thin aluminum strips. For brevity, this structure is referred to as "Str2". The placement of the strips allows for one direction (the x-direction) to have a low frequency mode (about 12 rad/sec when the structure hangs with the upper mass clamped). The y-direction has only rigid body motions in the frequency range of interest (5.0 to 40.0 rad/sec).

Identification of the rigid body properties of this structure was necessary for accurate combination of the models. Unfortunately it was not possible to excite the structure freely in an environment with gravity. Thus, several excitation configurations were tested to determine which would give the most accurate model for response synthesis. The structure was hung on a flexible wire attached to the ceiling. Excitation was provided by a voice coil actuator with a displacement-command following controller attached to a laboratory table.

This system is about 0.38m (15") long with a total mass of 1.48kg (3.25lb). Therefore, its mass is about 19% the size of the primary structure's mass of approximately 7.78kg (16lb). Sensing is carried out by two NOVA Sensors accelerometers model NAS-002G. These have a range of ± 2g and have a resolution of 1.25 Volts/G. The signals from these devices are passed through differential amplifiers with gains of 20, and are filtered by 100hz, 4 pole Butterworth filters before being fed into the data acquisition system.

5.5.2. Identification of Secondary System

Excitation of the secondary structure was carried out by a single voice coil actuator. Because of friction in the actuator it was necessary to place a local feedback controller on the system. This improved the response at low and high frequencies. An LVDT was used to sense the location of the push-rod; therefore, the controller commanded the position of the actuator rod, rather than the force generated. The controller was designed using loop-shaping techniques [DFT].

The following excitation and identification procedure was used: The structure was excited by a chirp signal with frequencies ranging from .1 to 15 hz. Data

for the excitation and the sensor signals were stored at 200hz. Fourier transforms were taken of both the inputs and outputs, and the output responses were divided frequency by frequency by the input frequency response. Then, the response of the LVDT on the actuator was also divided out from the accelerometer transfer functions. This resulted in transfer function responses from the actuator displacement to acceleration. Finally, a parameter search was done in the frequency domain [Mos] to fit the model

$$T_{ij}(\omega_k) = \left[\sum_{m=1}^{M} \frac{c_i^{(m)} b_j^{(m)} (-\omega_k^2)}{(f_m^2 - \omega_k^2) + 2\sqrt{-1} f_m \zeta_m \omega_k} + b_j^r c_i^r \right] \left[\frac{m_j (-\omega_k^2)}{(\sqrt{-1}\omega_k + p_1)(\sqrt{-1}\omega_k + p_2)} \right]$$

The last term here is due to actuator dynamics when the actuator rod is rigidly connected to Str2. If the rod is connected to Str2 through a spring or flexure, this term drops out.

A schematic drawing of both the Caltech LSS and this secondary structure is given in Figure 5.5. (These figures are not to scale.) Since only two accelerometers were available for the modal tests, it was necessary to change the system configuration to align the accelerometers in the direction of excitation. Each accelerometer's mass was only 10g, so this was not a significant change.

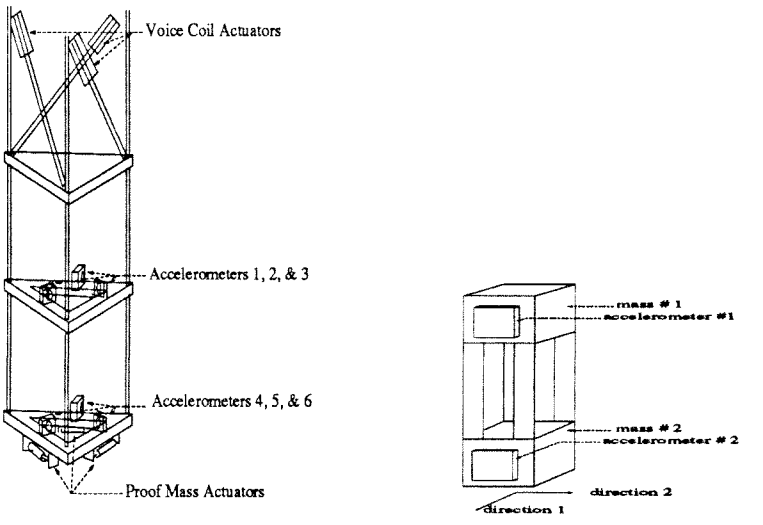

Figure 5.5. - Caltech LSS and Secondary Structure.
Drawings are not to scale. The second structure is connected to the bottom of the Caltech structure.

The modes for which identification was desired were the rigid body translations and rotation modes for both directions 1 and 2, and the bending mode in direction 1. The rigid body modes are important since they contain information on the mass and inertia properties of the system. Unfortunately, it was not possible to identify these for two major reasons:
i) It was not possible to suspend the structure in mid-air: That is, it was necessary to hang the structure from a cable. This modified the rigid body modes making them pendulum modes; and
ii) At low frequencies, accelerations were very small even for reasonably sized displacements; thus, the sensor signals were overwhelmed by noise at the low frequencies.
With these restrictions, the only possible approach was to hang the structure (with the cable attached to mass #1), and to identify pendulum modes as if they were rigid body modes.

Various connectors were also used between the actuator and the structure. Each of these resulted in slightly different structural responses since they modified the system's boundary conditions. Among the connections used were steel threaded rod, a spring, and flexures made of .066 cm (0.026") "o-ring" stock. The flexures were used so that pendulum modes would be minimally affected. For stronger excitation of the flexible modes, the solid rod was used. Finally, a test was done with a spring whose displacement was measured with an LVDT so that the force to acceleration curves could be directly obtained.

All of these connections were tested with the actuator acting on either mass #1 or mass #2. The length of the suspension wire had to be changed when the excitation location was changed. This changed the behavior of the structure and thus restricted the procedure to using only data from excitations at one of the masses. Identification using data from excitations at both masses then was not possible.

Data from two sets of experiments with Str2 are presented to demonstrate the experimental issues. The first set, referred to as "Case 1" used a flexure with o-ring stock and excitations at mass #2. This set of data is useful for developing insight into the connection process. Case 2 used a steel threaded rod connection that joined the actuator to mass #1. Results from the spring connection were similar to those from Case 1, so they are not presented.

Figure 5.6 presents data for directions 1 and 2 for Case 1, with the identified model overlayed. The data is for accelerometer 2. Similarly, Figure 5.7 shows accelerometer 2 data and model response for Case 2. In this case, it was very important to fit the quasi-static/residual terms of the model accurately. These residual components balance the actuator controller dynamics.

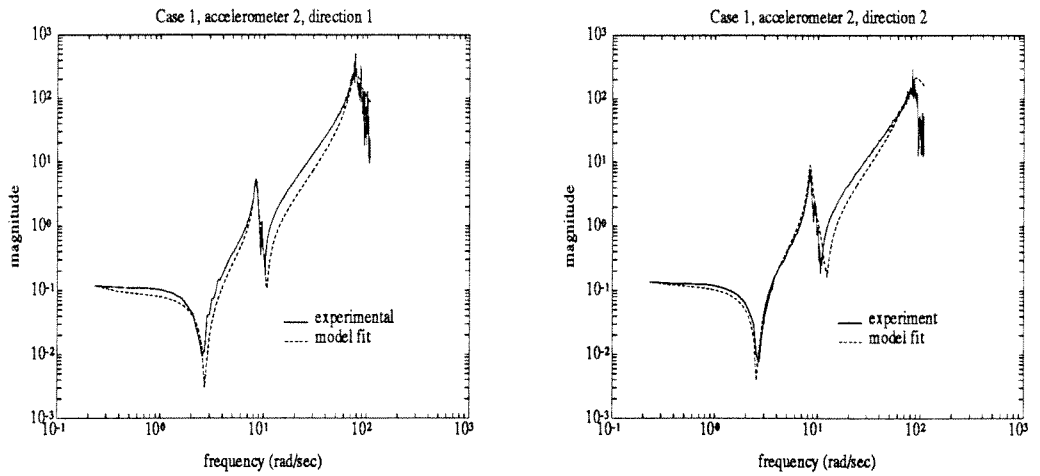

Figure 5.6. - Str2, Case 1, Accel. 2, Directions 1&2.
There is a very low frequency mode in these models due to the first pendulum mode. Because of the flexure, actuator dynamics are not needed in the model.

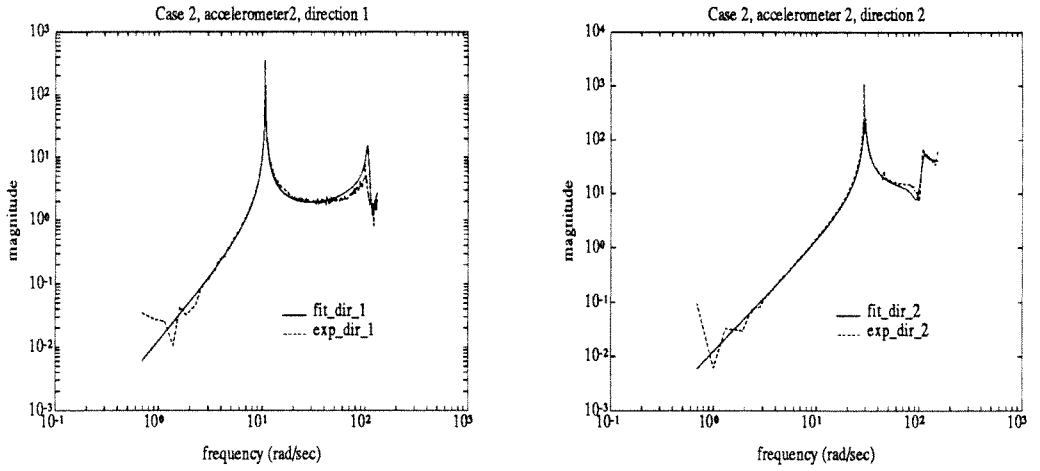

Figure 5.7. - Str2, Case 2, Accel. 2, Directions 1&2.
A displacement tracking actuator was used here. The modes at around 100 rad/sec are due to the clamps which held down the actuator.

5.5.3. Identification of Modal Masses

Once these models were obtained, the search for the $\alpha^{(m)}$'s was conducted. On the Caltech LSS, a mass of .953kg (2.10lb) was placed in the center of the bottom plate. This was the location were the second structure was attached later in the procedure. Str2 had a mass of .614kg (1.35lb) attached at mass #1 for Case 1 and to mass #2 for Case 2. In both of these Str2 cases the actuator and the attachment locations were different. When the actuator and the mass were colocated, the displacement tracking controller removed the effect of the modification mass, making it impossible to accurately identify the $\alpha^{(m)}$'s.

Str2 was attached to the Caltech LSS at Str2's mass #1, thus it was necessary to use invariance to modification location of the $\alpha^{(m)}$'s for Case 2. That is, the connection to the LSS was done through mass #1, but the partial identification was done with the modification at mass #2. Figure 5.8 presents plots of the rms sums of the responses of the unmodified system, the response of the modified system, and the response of the LFT based identified modification models for the Caltech LSS, Case 1, and Case 2. In Table 5.5, modal frequencies of the original and mass-modified systems are shown. These values resulted from the $\alpha^{(m)}$ partial identification.

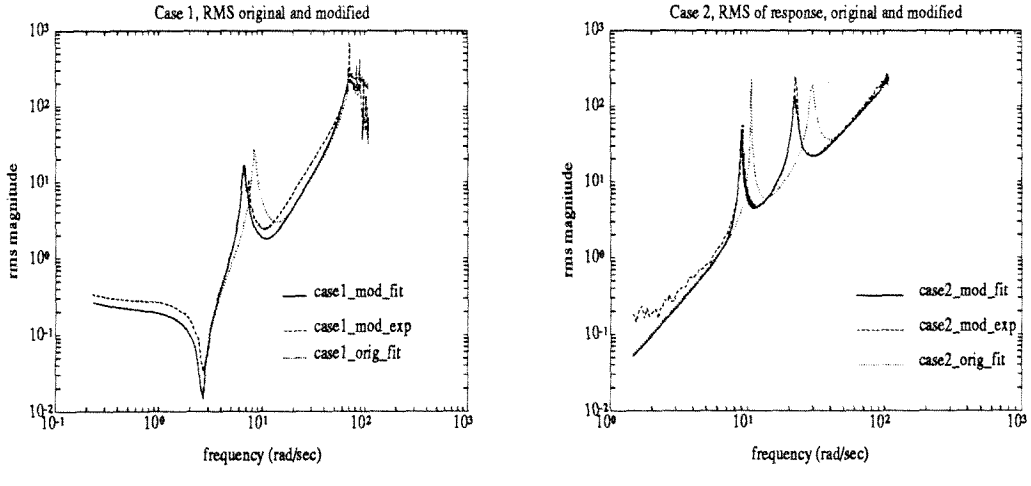

Figure 5.9 - RMS Magnitude, Modified Str2: Case 1, Case 2.
The solid lines show the modified fit which comes from performing an LFT mass modification on the original systems' models (dotted lines).

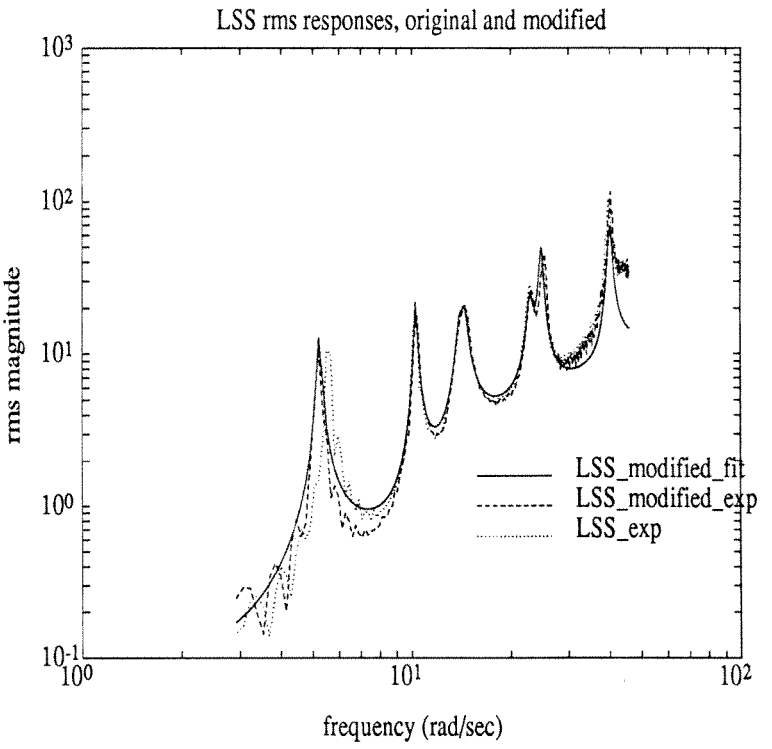

Figure 5.8. - Modified and Original Caltech LSS, RMS Responses. The modification of responses due to addition of a mass on the bottom bay are shown here. Using the differences between the original model and modified responses, the modal weights are found.

5.5.4. Results of Connection of the Structures

Models were then set up for connection of Str2 to the Caltech Flexible Structure, and MATLAB was used to compute the state space relations previously discussed for the model of the combined structures. Table 5.6 gives the modal frequencies for the original systems and for the predicted combined systems. The values are located in the table to try to demonstrate where each mode of the combined system comes from. The rms sums of all relevant channels of the frequency responses for the original LSS, the experimentally combined system, and the predicted systems are given in Figure 5.10.

5.6 Discussion of Experimental Results

Success of the structure connection method can be measured by the following two criteria:

i) There are some modes which are greatly affected by the attached structure, and

Caltech LSS		Case 1	
Original frequency rad/sec	Modified frequency rad/sec	Original frequency rad/sec	Modified frequency rad/sec
5.558	5.203	0.113	0.113*
5.607	5.278	0.085	0.085*
10.267	10.301	8.347	6.600
13.972	14.023	8.347	6.935
14.488	14.478	77.78	72.981
22.777	22.965	87.78	85.791
24.766	24.810	Case 2	
24.868	24.875	10.637	8.969
39.878	40.133	105.0	94.745
		29.71	22.172
		110.9	110.9

*Not enough data at low frequencies to fully identify

Table 5.5 - Original and Mass-Modified Systems: Caltech LSS, Case 1, and Case 2.
The changes in Str2 due to different excitation clamping fixtures can be observed from the differences between Case 1 and Case 2. Values in this table are from the models for the original and the modified systems.

---

some which are not. For those which are significantly moved, agreement between experimental and predicted frequency locations and participations indicates success. ii) Dynamics will be added to each structure by the other. Thus, it is important that the modes which are caused by the secondary appear in the response of actuators and sensors from the primary structure, and vice-versa.

In these experiments, the significantly altered modes are the lowest frequency ones. This is indicated first by the amounts of change in these modes caused by addition of a mass at the attachment location. The two closely spaced, first bending modes (5.5 and 5.6 rad/sec) were moved to about 4.7 rad/sec by the second structure. Additional dynamics in the combined structure were found at 11.0 rad/sec, where the flexible mode in Str2 appeared quite strongly in the experimental data (Figures 5.10and 5.11).

5.6.1. Case 1

Case 1, which used the soft flexure and excitation at mass #1, will be discussed first. The lowest predicted LSS modes appear as though they were moved

Case 1			Case 2		
Original frequency rad/sec	Combined frequency rad/sec	Origin	Original frequency rad/sec	Combined frequency rad/sec	Origin
0.084	*	Second	5.558	4.970	LSS
0.113	*	Second	5.607	3.211	LSS
5.558	0.1134	LSS	10.267	10.267	LSS
5.607	0.7913	LSS	10.637	10.628	Second
8.347	5.963	Second	13.972	14.103	LSS
8.347	6.056	Second	14.488	14.446	LSS
10.267	10.267	LSS	22.777	22.777	LSS
13.972	14.008	LSS	24.766	24.862	LSS
14.488	14.491	LSS	24.868	24.900	LSS
22.777	22.776	LSS	29.710	28.081	Second
24.766	24.799	LSS	39.878	39.878	LSS
24.868	24.878	LSS	105.0	95.402	Second
39.878	39.878	LSS	110.9	110.91	Second
77.78	65.287	Second			
87.78	83.472	Second			

*Removed by model reduction

Table 5.6 - Joined System Predicted Modes: Case 1, and Case 2. From the plots of the RMS responses, the indication is that Case 2 gives better predictions than Case 1. The fourth mode in Case 2 is obscured in the plots.

---

to higher frequencies (5.9 and 6.0 rad/sec) in the response plots. However, a better explanation is indicated in Table 5.6, where the lowest modes were shifted to very low frequencies. Then, the two secondary structure pendulum modes moved from 8.3 rad/sec down to the 5.9 and 6.0 rad/sec values. Simple one-dimensional modal theory explains that frequencies of vibratory modes (for one-dimensional systems) are bounded by other modes in the system. For example, the frequency of the second mode of a system cannot become higher than the third, or lower than the second when the structure is physically modified. Usually, when physical changes are applied, all the modes will move. Thus, it is plausible to explain the motion of the low modes in Case 1 as insufficient change in the first modes of the Str2 (at 8.3 rad/sec), rather than as negative change (frequency increase) in the fundamental frequencies of the primary structure (5.5 and 5.6 rad/sec).

This error is also caused by the fixturing system which could not be factored out of the Str2 behavior before the connection procedure. Thus the theoretical connection procedure acted as though it was connecting Str2, the flexure connection,

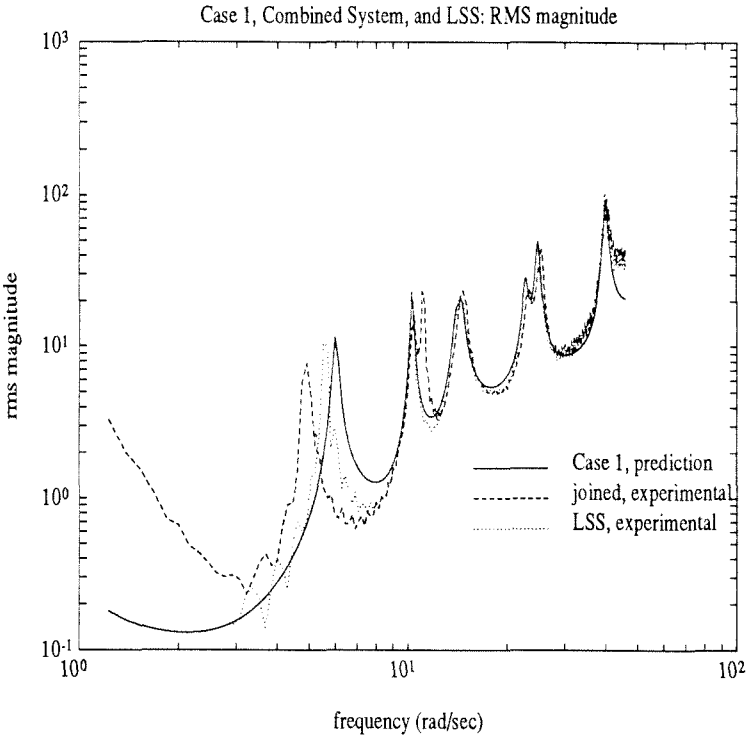

Figure 5.10 - RMS Sums of Combined Behavior: Case 1.
This plot presents the response of the original Caltech LSS (dotted), the response of the combined structures (dashed), and the prediction using Case 1 (solid). While the first modes are shifted to lower frequencies in the experimental response, the prediction appears to move them to higher frequencies. Similarly the additional mode between the LSS first torsional and second global bending does not appear in the prediction. All 36 input/output channels are presented here.

and the hanging wire to the LSS. Proper modification of the fundamental modes was then not calculated.

Additional modes did not appear in the predicted behavior of the primary structure when combined with the secondary. One explanation for this is that since pendulum modes in Str2 were easily excited, motion of the flexible mode was not detected. That is, the motion of Str2 was dominated by pendulum modes which obscured motions of the flexible mode when this was tested independently of the LSS. The pendulum modes were constrained by the connection bolt between the system, thus becoming fundamental modes of the combined system. The primary motion of Str2 then became flexible modes, which had not been detected.

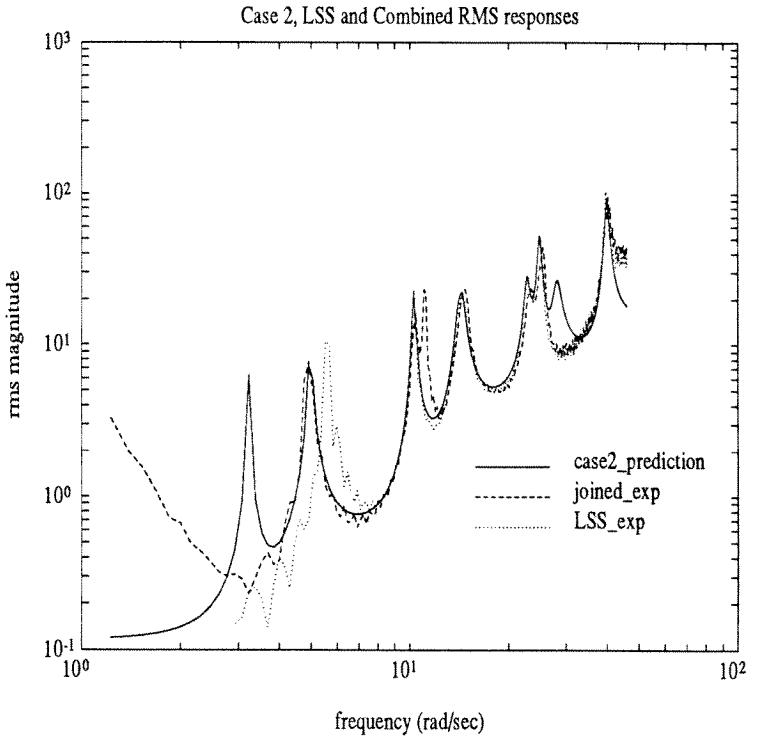

Figure 5.11 - RMS Sums of Combined Behavior: Case 2.
This presents the same data sets as the previous plot, except using the model from Case 2 fixturing. The lowest modes are predicted at lower frequencies, although one of them is shifted down too far. The added mode (at 11 rad/sec) appears in the prediction at 10.62 rad/sec, so it is obscured by the LSS torsional mode.

The other reason that the additional flexible mode does not appear in Case 1 is that rotational motion about axis 2 of Str2 was not measured. When the structure connection was carried out, these motions could not be theoretically constrained to match the behavior of the Caltech LSS. The prediction then corresponds to connecting Str2 to the LSS through a hinge rather than a bolt. These errors would have been reduced significantly if rotation about the axis for direction 2 for both structures had been measured at the attachment locations. Connecting the structures without constraining this direction (and other rotations) incorrectly models the bolt joint between the systems. Unfortunately, rotational sensors were not available.

Appearance of primary structure behavior in the combined Str2's sensors indicates good identification of the LSS and validity of the method. Figure 5.12 shows the transfer functions (experimental and predicted) from voice coil #1 on the LSS to accelerometer #2 on Str2 along directions 1 and 2. Although the amplitudes

of the predicted responses are incorrect by almost one order of magnitude at lower frequencies in the transfer functions presented, it can be seen that modes from the LSS appear in the response of Str2's sensors. Other transfer functions had better correlation of the predicted behavior and the experimental response. At 11 rad/sec there was a lack of a flexible mode in Case 1. These results were encouraging, but they indicated that the fixture for the experimental excitations was not a good one for testing the secondary structure.

It is also worth noting that the transfer functions from actuators to sensors on the original Str2 had magnitude approximately one order of magnitude higher than those of the LSS. Some of the responses at accelerometer #2 of Str2 still came out too small at the lower frequencies. This indicated poor identification of the static properties of the attached system.

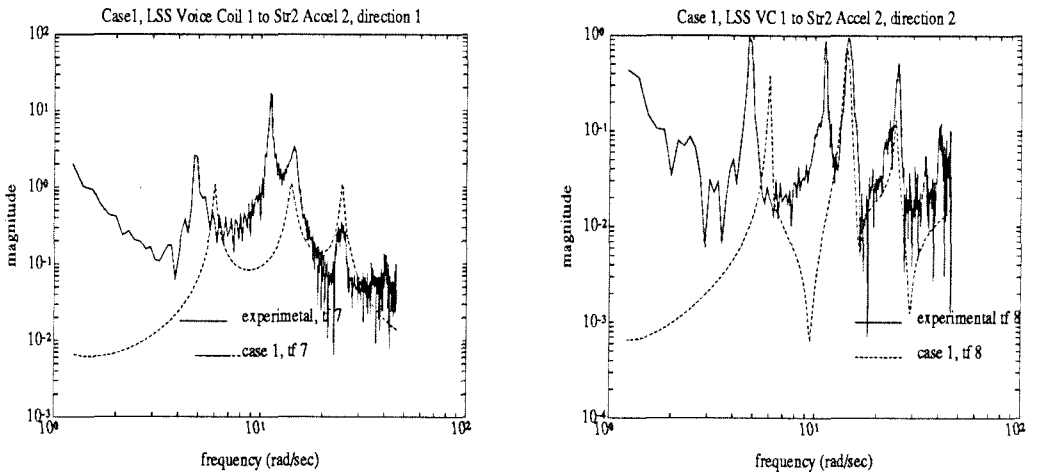

Figure 5.12. - Transfer Functions from VC #1 to Accelerometer #2 on Str2: Case 1.
Results here are not great, but they are encouraging. Many of the modes due to the LSS appear in the response of the sensor from Str2. Unfortunately, Case 1 did not properly catch the flexible mode in Str2, so it does not appear here. Also, the first LSS torsional mode does not appear in the predicted behavior through Str2. This is because rotational motions are not used in the constraint procedure and the accelerometers are very close to the center of rotation for this mode.

5.6.2. Case 2

Case 2 resulted in a significantly better prediction of the behavior of the combined structure. Here, a rigid connector was used between the actuator and Str2. This prevented most of the pendular responses. The fundamental mode of the LSS shifted down to 4.9 rad/sec in the prediction, as in the combined experiment. Unfortunately, the second first-bending mode (not the originally lower frequency first first-bending) shifted too far (to 3.2 rad/sec). The conclusion that this was the 5.6 rad/sec (and not the 5.5 rad/sec) mode came from the eigenvectors. Predicted and measured responses were viewed channel by channel, and it was determined that the behavior of the 3.2 rad/sec mode matched that of the 5.6 rad/sec one. This shift may be attributed to experimental error: The identification of direction 2 of Str2 was dominated by a mode at 28 rad/sec, which did not appear in the combined experimental response. It is believed that this was not a structural mode; rather, since the actuator was not rigidly connected to ground for the tests, the mode was likely a result of motion of the whole actuator/structure assembly. Parameters related to direction 2 were changed to check their effect on the modification of the 5.6 rad/sec mode. When properly changed, the quality of the predicted combined behavior improved significantly. The conclusion is that poor identification of these parameters led to the large change of the 5.6 rad/sec mode.

The flexible mode identified in direction 1 of Str2 appears in the combined structure, although it is obscured by the LSS first torsional mode at 10.26 rad/sec. This mode, as seen in Table 5.6 is shifted from 10.63 rad/sec to 10.62 rad/sec. In Figure 5.13, the transfer function from voice coil actuator 1 to accelerometer #2 shows this mode clearly, although with too small a magnitude. Also appearing in the predicted behavior are the LSS modes. These appear with much more accurate participation levels. In this case, the excitation of the secondary system is much more accurate because of the connection scheme. The bending mode at 28 rad/sec, which was considered non-structural, does not appear in the experimental response of the system, although it appears in the prediction. In particular, it shows up in the response direction #2. This would confirm that this mode was not structural.

Several possibilities exist which explain the small predicted participation of the bending mode in direction 1 and the large response in the experiments. Because of difficulty exciting the small structure properly, the flexible mode was not fully set in motion. Also, the fixture for the identification procedure altered the modes too

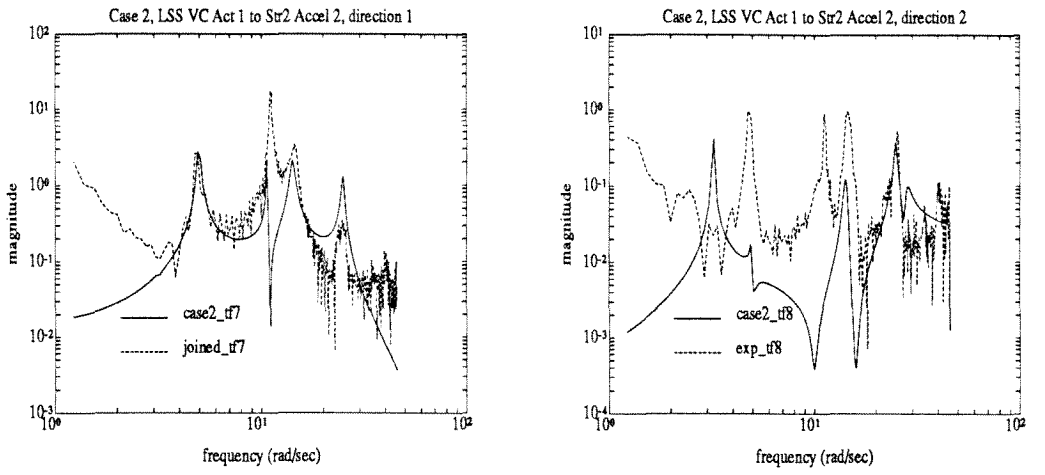

Figure 5.13. - Transfer Functions from VC #1 to Accelerometer #2 on Str2: Case 2.

These results are significantly better than Case 1. Once again, most of the LSS modes appear in the predicted response through Str2. In particular, LSS mode 1 appears in the exactly correct location in direction 1. The added mode from Str2 appears in direction 1 also, although at a frequency 0.5 rad/sec too low. In direction 2, LSS mode 2 appears at too low a frequency. The experimental data (dir. 2) also picks up a peak at 11 rad/sec: Had this peak been due to the torsional mode, it would have been at a slightly lower frequency. The torsional mode does not appear in the predicted behavior since rotations of the two systems are not constrained to be equal. The best explanation for this peak is that it is due to cross-axis sensitivity of the accelerometer (which then picks up the bending mode perpendicular to its sensitivity direction).

much. For example, the suspension wire might have absorbed much of the energy from the mode, resulting in smaller sensed accelerations. Another explanation, which has more to do with the large response of the joined system experiment, is that the accelerometer on Str2 measured radial accelerations due to the LSS torsional mode at 10.26 rad/sec. This would cause a large response in torsion, which because of closeness to the bending mode would give a large base upon which the bending mode response would appear. (This is a phenomenon of closely spaced modes.) The implementation used in these cases assumed that the secondary structure sensors were at the center of the bay. In this configuration, torsional modes are not predicted. In Figure 5.13, direction 2, this mode appears again at 11 rad/sec. Here, it could be due to torsion, although then it should be at a lower frequency. More likely, the appearance in direction 2 was due to cross-axis sensitivity of the accelerometer.

As with Case 1, measurement of rotations of mass 1 about direction 2 were not used for the connections. The rod that connected Str2 to its excitation actuator significantly constrained this direction for Case 2. Better predictions would have probably been obtained with proper sensing and theoretical constraint of the rotational motions.

5.6.3. *A Posteriori* Improvement of Case 2

In Figure 5.14, the results of the a *posteriori* improved models for Case 2 are presented. The improved models were obtained by adjusting parameters in the models to obtain better agreement between the predicted and the experimental combined structure responses. Here, the low frequency mode location is corrected, and the 11 rad/sec mode is visible, although its magnitude is a little small. Improvement in mode 2 was due to changes in the quasi-static components in the model of Str2. The 11 rad/sec mode was corrected by changing the frequency and output participation factor of mode 1 for direction 1 in Str2's model.

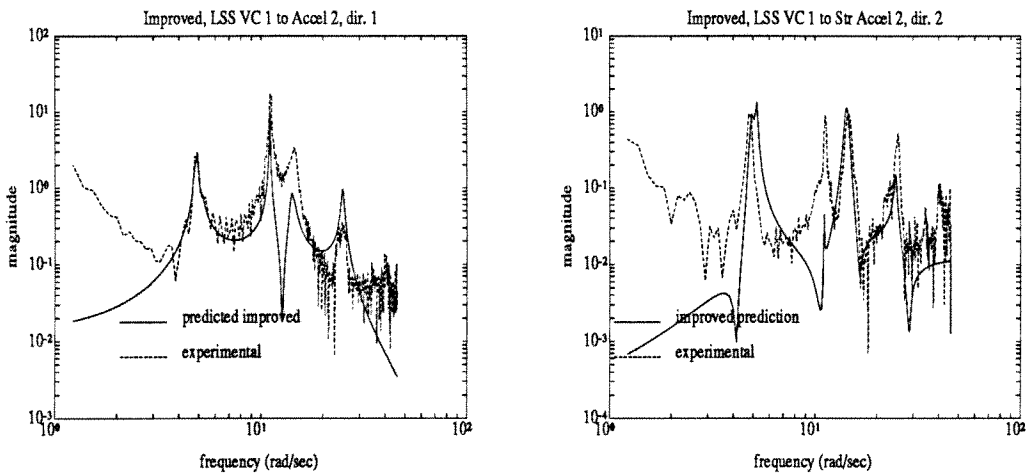

Figure 5.15. - Transfer Function from VC #1 to Accelerometer #2 on Str2: Improved.
Here, the LSS modes appear correctly in the individual transfer functions to Str2. The mode due to bending of Str2 also appears nicely in direction 1, as visual observations indicated. Better fixturing of Str2 and more sensors would have given results of this good quality.

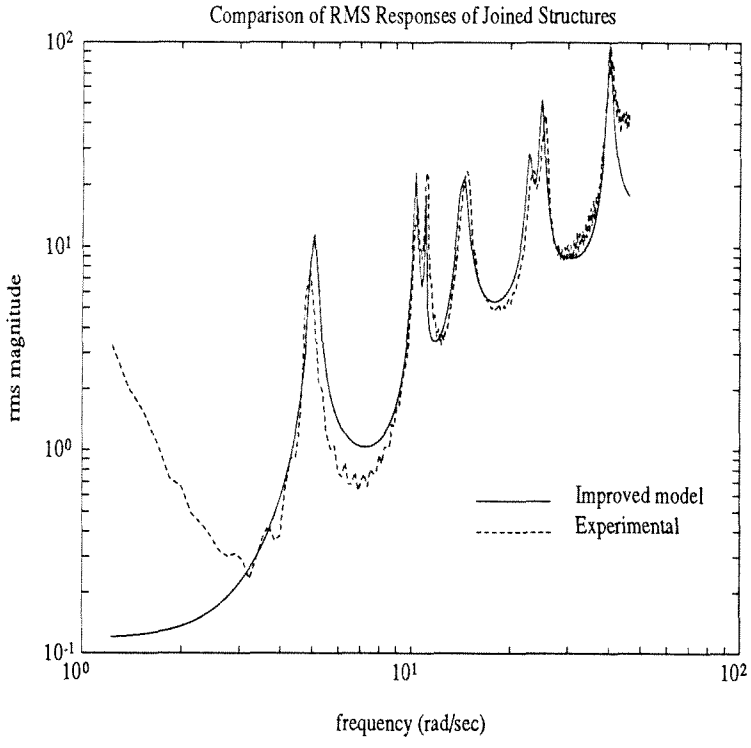

Figure 5.14. - Experimental and Predicted RMS Behaviors for Connected Structures.
Model Improved by Altering Parameters.

The first bending modes and the additional mode appear in the combined responses quite well here. Case 2 data was changed as follows: The residual participation of direction 2 was reduced, thereby shifting LSS mode 2's frequency less. Str2's mode 1 frequency was moved from 10.63 to 11.0 rad/sec, thereby moving it out from behind the LSS torsional mode. Also the participation of Str2's mode 1 was increased so that it would match the experiment better.

5.7 Observations and Suggestions for Experimental Improvements

Overall, these experiments were a quite successful demonstration of the method. In particular, Case 2 pointed out areas in the experimental procedure which greatly affected the quality of the overall fit. First, it was very important to properly identify the quasi-static components of the structural behavior. These were due to static properties and higher frequency modes not explicitly modeled. The fit was done using residual participation terms in the full identification model for each system and with a residual modal weight in the partial identification for the modified systems ($\alpha^{(res)}$). If $\alpha^{(res)}$ is negative (as the curve fit program sometimes

gave,) the method predicted unstable poles. Since the final system was passive, this was incorrect.

To avoid the problems with fixturing, the best approach is to fully sense all directions of motion at the attachment locations. By properly accounting for these motions in the connection procedure, the physical joints are modeled correctly.

Another concept developed from these results is that larger changes in modes reduced the apparent size of the system. That is, when the modal weights were determined as being larger, the modifications to the other system resulted smaller. Thus the $\alpha^{(m)}$ are really like inverses of the modal masses.

Controlled actuation also added some difficulties to the procedure. The magnitude of the actuator dynamics (m_j in the describing transfer function) over-parametrized the model since it could multiply the modal participation factors. Thus, it was possible that the modal gain components traded-off with the actuator dynamics to improve the fit of the model. Then, the input and output components multiplying the modal weight values would be incorrect. This problem is avoided through use of an actuator which does not require feedback control to give good performance. Because of the model forms, the modal weight parameters were not affected by this phenomenon.

Other suggestions for improvement of the test procedure include testing the secondary system in a gravity-free environment and testing the system with fixtures that do not allow for pendulum modes. The first of these ideas is quite expensive to implement, but should lead to better identification of the rigid body properties of the system since it will be free of any constraints. A support system which does not allow pendulum modes will probably have dynamics of its own which then have to be removed from the models. More study will definitely be beneficial for the determination of the best testing setups.

5.8 Conclusions

A quite general approach to response mode synthesis has been presented in the previous two chapters. The main advantages of this approach are:
i) the procedure can be done using input-output experimental data alone (no reference to physical quantities is needed);

ii) noncolocated sensor/actuator geometries are allowed (in some cases, even preferred);
iii) acceleration sensing can be used directly (there is no need to synthesize displacement data from accelerometers); and
iv) locally controlled actuators can be used to excite the structure (as long as their effect can be modeled).
The procedure involves first, a basic identification experiment of each substructure; second, a partial identification of each subsystem after modification (to make the models of the systems compatible); and finally, theoretical assembly of the various component models.

The linear fractional transformation framework was also presented as a general tool for linear structural dynamic analysis. Theoretical and experimental results were given for input/output identification and interconnection of structural systems. Limitations of the method because of experimental difficulties were presented along with suggestions for improvement of the procedure. In Chapter 7, an application of the LFT connection method is given where the attached structure is used as an uncertainty description for active controller design.

5.9 References for Chapter 5

DFT: Doyle, J., Francis, B., and Tannenbaum, A., (1992), **Feedback Control Theory,** Macmillan Publishing Co., New York.

Ewi: Ewins, D.J., (1985), "Modal Test Requirements for Coupled Structure Analysis Using Experimentally Derived Component Models," **Combined Experimental/Analytical Modeling of Dynamic Structural Systems,** ASCE/ASME Mechanics Conference, AMD, Vol. 67, pp. 1-30.

Mos: Moser, A.N., and Caughey, T.K., (1991) "Some Experience with Identification of the Caltech Experimental Space Structure." *Proceedings of the 1991 American Controls Conference,* Boston, Massachusetts.

: Please also see the references for Chapter 4

Chapter 6. Structural Control Using H_∞/μ-Synthesis

6.1 Introduction

In this chapter, a discussion is given of the steps necessary for design of H_∞/μ-optimal controllers. In particular, the setup used to specify the synthesis problem for the Caltech Flexible Structure (CFS) is presented in detail. In Chapter 7, results of application of controllers resulting from the synthesis setup are given.

This chapter is organized as follows: Section 2 discusses some of the difficulties of active control of structures. In Section 3, the mathematical formulation of the H_∞/μ-synthesis procedure is presented. The theoretical framework is followed by Section 4, which contains a discussion of application of the method including some of the computational issues involved in implementation of H_∞/μ-synthesis. The models used for controller design for the unmodified structure are also explained in this section.

The term *open loop* in this and the following chapter refers to the uncontrolled system without any compensator dynamics. *Closed loop* refers to the system with full controller dynamics and feedback.

6.2 Difficulties with Structural Control

The achievable closed loop performance of a structure depends on the desired levels of stability, robustness, and effort of a synthesized controller. These properties are specified by models in a mathematical control problem formulation. The mathematical problem specification for optimal controller synthesis, hereafter

referred to as the *synthesis setup*, consists of a model of the system to be controlled, descriptions of the uncertain quantities in this model, specifications of the desired performance, and ideas on the qualities of the controller that make it more successful. For H_∞/μ-synthesis the models for all these properties consist of state space realizations of input/output transfer functions.

Modeling of the base (open loop) system may be done analytically/ numerically, experimentally, or by some combination of these methods. Analytical/ numerical modeling for structures is primarily carried out using the finite element method (FEM). Accurate results require very complex and exact information on each structural component, each joint in the structure, and each sensor and actuator to be mounted on the system. Information with the necessary level of precision is almost never obtained. Thus, the basic analytical/numerical model of the system will be inaccurate.

Experimentally identified models require less prior information on the components of the system. The system, however, must be tested in its working environment in order for the descriptions to be appropriate for controller design. Therefore, controller synthesis cannot be done until the system has been deployed. Errors in these models are caused by phenomena such as experimental noise, variation of material properties over time, and incomplete knowledge of what kind of model to use. A combination of theoretical and experimental procedures which consists of using experimental results to improve theoretical models can also be used. This is probably the approach that will be used for future missions, although certain uniqueness of model issues exist with this procedure.

The main effect of modeling errors on the controlled system is performance reduction, possibly to the level of instability. A phenomenon known as the *water bed effect*, where the controller redistributes energy in the system from frequencies where performance is desired to other frequencies, occurs when the system is being controlled. If certain modes or other system dynamics are left out of the system model, the controller may shift energy in such a manner that these unmodeled effects are excited, thereby causing degradation of performance or instability. Instability may be avoided by specifying where the system's behavior is poorly known. The controller will then either achieve less performance or will avoid shifting energy into these regions. With better knowledge of the system, greater performance can be obtained.

The desired performance objective for most structures consists of increasing the system's stiffness. For example, displacements will have to be kept in the micron range for systems such as NASA's large optical interferometer (which will be on the order of 50 meters long). Experimental identification is difficult because of very close spacing of very lightly damped modes. Theoretical analysis is hindered by incomplete knowledge of joint and material properties, by partial data on the damping of each mode, and by poor understanding of the interactions between the structure and the sensors and actuators. Nonlinear behavior of the system which shall not be discussed here, introduces another level of errors in the modeling and control.

6.3 H_∞/μ-Synthesis: Theory

The control synthesis procedure used for this work is H_∞/μ-synthesis, which consists of H_∞-optimal synthesis, μ-analysis, and D-scaling, nested in an iterative scheme[Bmu], [DFT], [DGK], [Pac]. This section gives a sketch of the process, leaving out some of the mathematical rigor necessary for a complete description. This description is intended as an overview of the motivation behind the procedure known as μ-synthesis.

First, the synthesis setup is used to compute an H_∞-optimal controller. In the notation used here, this is known as the *K-iteration.* At this point, uncertainties modeled in the setup act as scalings on the performance of the system. Once the control algorithm has been computed, the loop is closed around it (i.e., interaction of the controller and the synthesis system is computed via the Redheffer Star product [Kai]) producing a model of the controlled structure. Effects of the uncertainty on the stability and performance of the closed loop system are then calculated to produce a value known as μ, which is discussed in greater detail later. Information from μ on the worst case uncertainty (which degrades the stability and performance of the system the largest amount) is then incorporated into descriptions known as *D-scales.* (This step is referred to as the *D-iteration.*) The D-scales are then collapsed into the synthesis setup thereby changing the performance objective so that the controller is robust to the worst case uncertainties during the next K-iteration. Combination of D-scaling and K-synthesis is denoted by *D-K iteration*, and results in the technique known as μ-synthesis. The procedure is repeated so as to obtain the controller which gives the best performance in an H_∞setting and which has the best robust stability and performance in a μ-analysis sense. The feature about

this procedure that makes it so effective is that for all the systems in the family generated by the model and uncertainties (the synthesis setup), the controller is guaranteed to be stable and to achieve the desired performance for values of $\mu \leq 1$.

6.3.1. H_∞-Optimal Control

A brief description of H_∞-optimal control is given here. The system realization framework used is state space, which, for linear systems gives descriptions in both the time and frequency domains. Denoting the states of a system as $\underline{x}$, the control inputs to the system as $\underline{u}$, the outputs to be minimized by the procedure as $\underline{z}$, the unmeasured disturbances as $\underline{w}$, and the measured signal for control as $\underline{y}$, the evolution of the system to be controlled is described by

$$\begin{aligned} \dot{\underline{x}} &= A\underline{x} + B_1\underline{w} + B_2\underline{u} \\ \underline{z} &= C_1\underline{x} + D_{11}\underline{w} + D_{12}\underline{u} \\ \underline{y} &= C_2\underline{x} + D_{21}\underline{w} + D_{22}\underline{u}. \end{aligned} \tag{6.1}$$

Since these signals may be transformed between time and frequency domains easily, the same notation shall be used for both domains. The dot superscript represents differentiation with respect to time. Subscripts on transfer matrices denote output and input locations.

Upon transformation to the frequency domain, this system is given by

$$\begin{pmatrix} \underline{z} \\ \underline{y} \end{pmatrix} = \begin{bmatrix} P_{11} & P_{12} \\ P_{21} & P_{22} \end{bmatrix} \begin{pmatrix} \underline{w} \\ \underline{u}, \end{pmatrix} \tag{6.2}$$

where $P_{ij} = C_i(sI - A)^{-1}B_j + D_{ij}$, $s = \omega\sqrt{-1}$, and ω is frequency. Dependence on frequency of the P's is assumed, and thus left out of the notation. For structural systems, the C matrices contain the output participation factors and information on the sensing type (e.g., velocity or acceleration), the B matrices consist of the input participations, the A matrix incorporates the modal frequencies and damping values, and the D matrices are the static input/output components.

In H_∞-optimal control, the input and output signals ($\underline{w}, \underline{u}, \underline{z}$, and $\underline{y}$) are all $\mathcal{L}_2$-norm bounded, that is the 2-norm of all of these signals, $\|\underline{\cdot}\|_2^2 = \int_0^\infty |\underline{\cdot}^2| dt < \infty$. Using norm bounds, the H_∞norm results because $\|\underline{z}\|_2^2 = \|T_{zw}\underline{w}\|_2^2 \leq \|T_{zw}\|_\infty^2 \|\underline{w}\|_2^2$, so the induced norm from a signal $\underline{w} \in \mathcal{L}_2$ to a signal $\underline{z} \in \mathcal{L}_2$ is the ∞-norm of the transfer function T_{zw}. To get the smallest response of the performance signal

$\underline{z}$ to the worst case disturbance $\underline{w}$, the goal becomes to minimize $\|T_{zw}\|_\infty$ over all controllers K with the property that $\underline{u} = K\underline{y}$. In mathematical notation, the H_∞-optimal controller achieves

$$\min_K \max_{\|\underline{w}\|_2<1} \|T_{zw}\|_\infty. \tag{6.3}$$

Appendix 1 presents a constructive partial motivation for the formulas leading to the optimal controller as presented originally in [DGK] and in [DGF].

The synthesis setup consists of, as previously mentioned, a system model, performance specifications, and uncertainty specifications. These are assembled into the state space realization in Equation 6.1. When synthesized, the controller K will manipulate the measured outputs $\underline{y}$ resulting in the controlled inputs $\underline{u}$ which alter the dynamics of the system. The effects of the control inputs $\underline{u}$ on the measurement outputs $\underline{y}$ are given for the open loop system by the transfer function P_{22}. The transfer matrix P_{11} consists of uncertainty descriptions and performance specifications; P_{12} contains information which is used to shape the controller effort most directly; and P_{21} details effects of disturbances and uncertainties on the sensed signal.

6.3.2. μ-analysis

The robustness of stability and performance can be quantified with the structured singular value, or μ, which is defined as

$$\mu_\Delta(M) = \frac{1}{\min_{\Delta\in\Delta}\{\overline{\sigma}(\Delta) \,:\, \det(I+M\Delta)=0\}}. \tag{6.4}$$

The Δ in this value corresponds to a structure of interactions between the uncertainty signals, the M represents the closed loop controlled synthesis setup, $\overline{\sigma}(\ )$ is the largest singular value, and det( ) is the determinant. Since M is a function of frequency, $\mu_\Delta(M)$ is taken as the largest value over all frequencies. Uncertainties are put in a format which uses linear fractional transformations through the Δ block. These blocks denote families of matrices with particular specifiable shapes (structures). For example, Δ may be chosen as block diagonal consisting of full complex matrices of size $m \times n$ or as diagonal complex matrices of size $n \times n$. The form of the blocks characterizes the interactions between the inputs and the different outputs.

The value of μ specifies the norm of the smallest matrix (in the family) Δ which destabilizes the closed loop synthesis problem. The Δ-block is partitioned so that both uncertainty and performance blocks are included. $\mu > 1$ means that the controller will not achieve the specified performance for the uncertainties described by the setup, that the controlled system will not be stable for the particular uncertainties, or a combination of failure of performance and stability. A value of $\mu \leq 1$ means that the controller will meet the specified performance with the given modeled uncertainties. The performance/stability boundary of 1 results from the formulation of linear fractional transformations. Figure 6.1 graphically presents the connection of components which leads to M and μ. The linear fractional notation $\mathcal{F}_l(P, K)$ denotes that the last outputs of P are fed into the first inputs of K, and that the first outputs of K are fed into the last inputs of P. Thus, if P is partitioned as in Equation 6.2, $M = P_{11} + P_{12}K(I - P_{22}K)^{-1}P_{21}$.

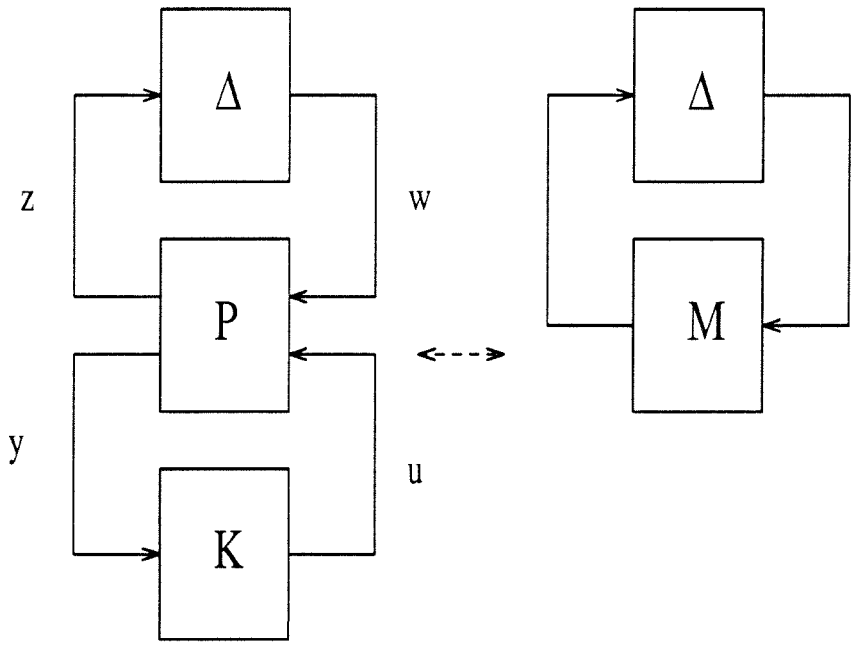

Figure 6.1 - Linear Fractional Transformations Leading to M and μ. P is the synthesis plant setup, K is the compensator, and M is the closed loop controlled synthesis system. Robustness is thus measured with respect to specified performance and robustness.

The characteristic dynamics of this system are dominated by $M\Delta(I + M\Delta)^{-1}$. This system will be stable (well behaved) when $\det(I + M\Delta) \neq 0$, that is, when $\overline{\sigma}(M\Delta) \leq 1$. Stability of M is guaranteed by the H_∞-synthesis procedure when a controller for the particular setup exists.

In a more practical sense, the performance and uncertainty descriptions are the components of M that interact with the Δ. For the value $\mu = 1$ to be reached, P must be modified through the performance and uncertainty specifications. If $\mu < 1$ the controller may be designed to either achieve more performance or to be robust to greater uncertainty. This will increase the gains in P. When $\mu > 1$ the gains in P must be decreased, either reducing the desired performance or the achievable robustness to uncertainty. If $\mu \approx 1$, a trade-off exits: larger uncertainties mean that less performance can be achieved; more performance reduces robustness to uncertainty.

6.3.3. D-scaling

The D-scale iteration results from steps necessary to compute μ, which cannot be calculated directly [Pac]. Current implementations of the calculation shall be discussed here. Upper and lower bounds for μ can be computed as

$$\max_{Q \in \mathcal{Q}} \rho(QM) \leq \mu_\Delta(M) \leq \inf_{D \in \mathcal{D}} \overline{\sigma}(DMD^{-1}), \qquad (6.5)$$

where $\rho(\ )$ is the largest eigenvalue, Q is a set of appropriately structured unitary matrices ($Q^*Q = I$, where * denotes complex conjugate transposition), and $\mathcal{D}$ is the set of appropriately structured invertible matrices. A power iteration is carried out to find the Q which maximizes $\rho(QM)$ at each frequency of interest. For each submatrix in Δ (and in D), the D-scales which maximize the maximum singular value are obtained through a generalization of Osborne's balancing method[Bmu]. The maximum singular values at the sampling points may be assembled to give frequency-varying descriptions which can be modeled by curve fitting. Currently this is done using minimum phase rational polynomials fit to the curves described by the maximum singular values for each submatrix in Δ. The order of the curve fit is chosen by the control designer. The polynomials are then converted to state space and assembled to give *approximate* D-scales. Approximation is a result of the curve fitting.

6.3.4. μ-synthesis

The D and its inverse D^{-1} are then collapsed back into the P in the open loop synthesis setup (D-iteration). The performance objectives of the problem are thus changed so that avoidance of the worst case uncertainties is incorporated into the disturbances. Since $\min_{\Delta \in \mathbf{\Delta}}(\overline{\sigma}(\Delta)) \leq \overline{\sigma}(DMD^{-1})$ specifies the D's, the scaling is guided by μ. In the next K-iteration, the best controller under the worst case disturbances, which now include the worst case uncertainties (from the perspective of the prior controlled system M) is synthesized.

In the first D-K iteration, the D-scales are chosen as identities. Thus, the first controller is guaranteed to be stable to perturbations of size

$$\overline{\sigma}(\Delta) \leq \frac{1}{\overline{\sigma}(M)}. \tag{6.6}$$

As the D-K iterations proceed, $\overline{\sigma}(DMD^{-1})$ is usually reduced, thus the controllers achieve more robustness and more performance. They are stable when perturbed by larger uncertainties (larger $\overline{\sigma}(\Delta)$).

There are two main features about the method which require caution. First, the D-K iteration procedure is not guaranteed to converge globally. It is possible that the μ will decrease the first few steps, and then it will increase. Since the goal is to reduce μ, the K from the iteration with the smallest value of μ should be used. Secondly, the guarantees on performance and stability are valid only for the model of the system as presented in the synthesis setup. Errors in the base descriptions and lack of conservativeness in the uncertainty models can lead to controllers which when implemented lead to an unstable or poorly performing system. So, the controller will only be as good as the model.

6.4 Implementational Issues of H_∞/μ-Synthesis

This section presents examples of the various components in the synthesis setup, discusses the particular choices for the problem specifications, and reviews descriptions used for design of robust optimal controllers for the Caltech Flexible Structure (CFS). Results of the application of these control algorithms will be given in the next chapter. This portion of the paper also contains discussions of some of the computational and implementational issues of H_∞/μ-synthesis using the MATLAB Musyn Toolbox [Bmu]. Much of this work was pioneered by G. Balas [Ba2].

6.4.1. Nominal Model

The most important component in the synthesis setup is the basic model of the (open loop) system to be controlled, referred to herein as the *nominal model.* This is the best (in some mathematical sense) description of the effects of commanded inputs on sensed outputs. It is most often determined either by theoretical analysis such as FEM code [StF], or by identification using one of the various methods available [CKR], [Mos]. The result of the identification or theoretical analysis must be put into state space form for H_∞-controller synthesis. Chapter 3 discusses modeling of the CFS.

The CFS is a good example of a space structure for several reasons: it has many closely spaced, lightly damped modes, it is set up for both colocated and noncolocated control experiments, and it has both structural (active member, such as voice coil) actuators and nonstructural (inertial, such as proof mass) motors. More information on the identification of this system may be found in [Ba2], and [Mos].

6.4.2. Specification of Desired Performance

Desired performance of the controller may be specified in many ways. The basic goal is to reduce $\|T_{zw}\|_\infty$ below 1.0, thus reducing the effect of the disturbance $\underline{w}$ on the controlled signal $\underline{z}$. In most cases, the disturbance inputs and the performance outputs must be scaled in P_{11} in the synthesis setup to obtain signals with magnitude near 1.0. As the magnification of these signals is increased more performance is specified.

The norm $\|T_{zw}\|_\infty = \sup_\omega \overline{\sigma}(T_{zw}(\omega\sqrt{-1}))$. In the frequency domain, the H_∞-optimal controller therefore reduces the peaks in magnitude over the entire frequency spectrum. In modal systems, such as structures, modal responses create the transfer function peaks when force inputs and acceleration outputs are modeled. This type of actuation and sensing has no inherent integration or differentiation which would appear as a rollups or rolloffs on the magnitude Bode plot. Figure 6.2 presents two transfer functions for an artificial two mode system: one with force input and acceleration sensing, and one with force input and displacement sensing. This figure illustrates the inherent rolloff in displacement sensed systems. Systems such as structures with force input and displacement sensing have representations which are strictly proper. These have inherent rolloff in magnitude as the frequency increases. That is, the magnitude of the transfer functions will generally decrease by

20 dB for each decade of increase in frequency for every pole that takes the system past being proper (i.e., for every unit of relative degree). Therefore, the maximum magnitude dynamics will generally be at low or zero frequencies. At higher frequencies, the response of the system will be very small. The infinity norm peak is then obtained at the low frequencies, thereby specifying low frequency performance. If performance is desired at higher frequencies, the disturbance input of the performance output should be differentiated so that the H_∞-norm of T_{zw} achieves its maximum where performance is desired. Scalings on the disturbance and the performance may take any (state space realizable) form since they do not alter the nominal transfer function P_{22}. That is, they modify the synthesized controller, but they do not change the basic system to be controlled.

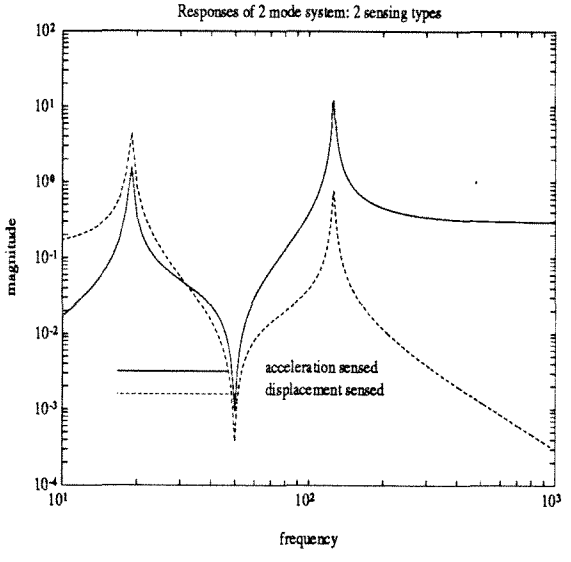

Figure 6.2 - Comparison of Sensing Types to Show Inherent Rolloff. The displacement sensed signal's magnitude rolls off with frequency, while the acceleration sensed signal remains generally flat. If performance is specified with these signals, mode 2 of the acceleration specified signal will be affected significantly more than the displacement sensed mode 2, but mode 1 of the displacement sensed will be attenuated much more than that for mode 1 of the acceleration sensed. The displacement signal has been multiplied by a scalar so that its magnitude matches that of the acceleration sensed signal.

There are two main ways to specify the performance through P_{11}: as noise rejection or as disturbance rejection. Noise rejection involves creating a frequency weight signal (like a filter) which scales an input whose effect is added at the system output. That is, the noise signal is fed directly to the performance output instead of through the system. The controller will then try to minimize the effect of noise or disturbances acting directly at the performance location. This type of performance is not very effective for modal systems since the controller must shift energy to regions outside the performance region which may be quite large. Figure 6.3 presents the block diagrams for noise and disturbance rejection.

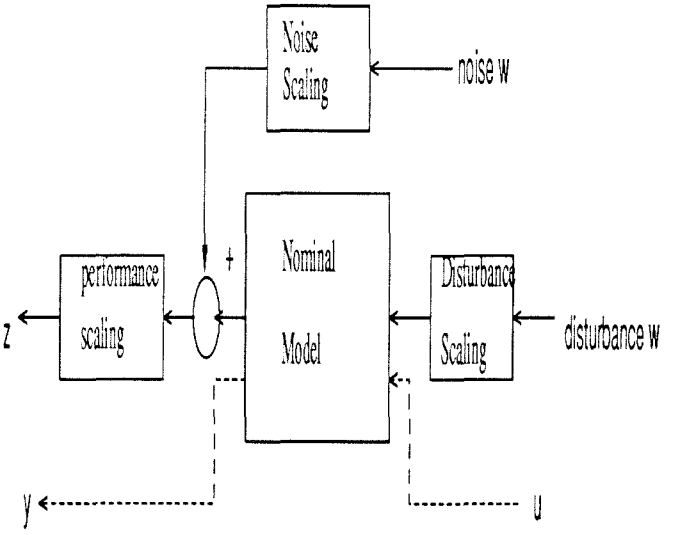

Figure 6.3 - Noise and Disturbance Rejection for Performance Specification.
Increasing the noise scaling will generally increase robustness of the controller since this will specify larger noises. Since the controller can only modify the plant (not external noises), increasing the disturbance scaling will increase the controller effort, thereby reducing robustness.

Placing the disturbance at the inputs to the nominal system means that the controller will alter the system so that it responds less at the open loop peaks. This is significantly more effective for systems such as structures because the controller then shifts energy from peaks of transfer functions to the valleys which are at nearby frequencies.

In the case of the CFS, the primary performance specification uses disturbances acting at the nominal model inputs and performance signals from the system

outputs. This means that all structure motions are considered as composed of sums of motions of the individual modal responses. The goal is to reduce motions, thus modal responses are to be removed. In the H_∞framework, this means reducing the response peaks so that the system behaves like a rigid structure. For an ideal system, optimal control produces a system with a flat response over the frequency band of interest (i.e., no peaks/poles and no valleys/zeroes).

Various combinations of input disturbances and output locations are chosen for performance of the CFS. The main objective is to reduce the effects of disturbances at the bottom bay on sensors at the same location (proof masses to accelerometers). Control is done by the voice coils at the top of the system. The other setup presented here aims to minimize the effects of disturbances at the voice coils on motions of the bottom bay, with control by the proof mass actuators.

It is possible to specify performance at only one accelerometer on the bottom bay of the CFS. The sensor picks up several bending modes and torsion modes, but is uniaxial. Motions in the direction of sensing are reduced quite nicely, but movements in other directions are not attenuated significantly. In some cases, energy is redirected to directions where performance is not specified thereby pushing the system closer to instability for these motions. Therefore, it becomes necessary to specify performance at multiple accelerometers covering various directions of motion.

With multiple locations specifying performance it becomes possible to specify which locations are most important for control and what kinds of disturbances are expected. On the CFS, different levels of performance are placed on disturbances coming from the proof masses and the voice coils, and on vibration reduction at the bottom bay or at the second platform. The disturbances acting at the proof masses have to be scaled by a single or a double integration so that the controller effort is placed at the lowest modes. This counteracts the rollup caused by the actuator dynamics (which places the maximum amplitudes of the transfer functions at higher frequencies). This weight is presented in Figure 6.4 along with scaled and unscaled responses at a bottom bay accelerometer to a proof mass. The scaled response is used to specify performance.

6.4.3. Controller Shaping

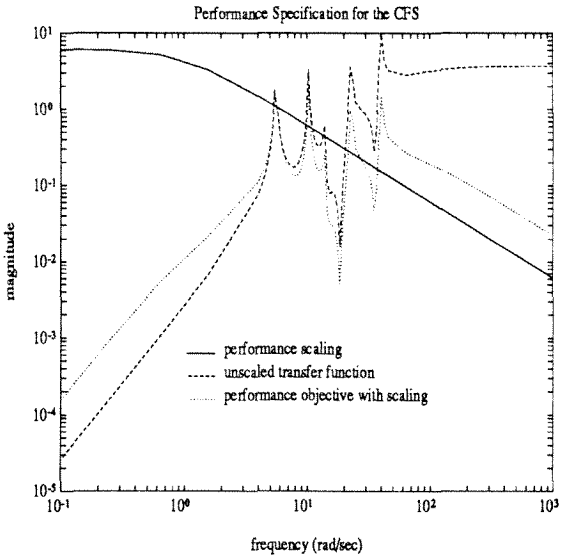

Figure 6.4 - Performance Specification for the CFS.
The unscaled transfer function (dashed) results in controllers which nicely control the higher frequency modes, but do not affect the lowest modes. When the scaled objective (dotted) is used, effort is placed to control all the modes.

Experimental control synthesists often know general properties that make the controller more effective. These include maximum allowable controller gains and frequency ranges of small effort. Characteristics of this type are incorporated into the controller in order to avoid phenomena like actuator and sensor saturation, destabilization of unmodeled high frequency modes, and aliasing due to finite frequency bandwidths of implementation hardware. Three general methods exist to shape the controller in μ-synthesis: performance specifications, uncertainty descriptions, and controller effort weighting.

Performance specification, which is discussed in the previous subsection is very indirect. By choosing levels of necessary performance in particular frequency bands in the synthesis setup, the designer will, in general, obtain controllers which place more or less effort at the particular regions. There are still many cases where because of the complexity of the performance and uncertainty specifications, the controller will have significant effort in regions where little performance is necessary. This is caused by energy redistributions the controller causes from regions where significant performance is desired to those where levels are less important. Thus, this tool for controller shaping is not very direct.

Use of uncertainty descriptions to affect the synthesized controller is a recommended method. The various uncertainty description types will be discussed in more detail in the next subsection. Since uncertainty indicates to the synthesis mathematics that large control efforts at certain frequencies may destabilize the system, the resulting controller will not greatly affect the uncertain regions. Similarly, the control algorithm will distribute energy from frequencies where significant performance is required to regions other than those with large uncertainties. For systems where destabilization of unmodeled modes are a great danger, uncertainty shaping of controllers is useful.

The most direct controller shaping method is scaling of the transfer function from control effort to performance P_{12}. In essence, this is what uncertainty descriptions at the inputs do. Since the goal of H_∞-synthesis is to reduce all transfer functions to below magnitude 1.0, the control signal can be scaled through P_{12} by a frequency dependent scaling which has the shape of the inverse of the desired controller (magnitude) form. For example if a controller with maximum gain of 10.0 is desired, the transfer function P_{12} may be chosen as $1/10.0 = 0.1$. Generally, however, the synthesis setup has many conflicting objectives, so the ability to obtain the controller shape features is traded off with other goals. That is, the multiple objectives compete against each other; thus, the resulting controller may have features not directly expected.

Mathematically, the transfer functions in P_{12} must be nonzero in order to prevent controllers with infinite gain. This can be shown using basic loopshaping concepts of robustness[DFT], where the sensor signal is defined as noisy. If the controller has very large gains, the effects of sensor noise will be greatly magnified. The transfer functions from sensor noise to the performance outputs (with unity scaling on P_{12}) are calculated by $(I + KP)^{-1}K$. Larger K's will then, in general, result in larger gains in this component, particularly when KP results with small magnitude.

In order to prevent controllers with zeroes which cancel plant poles, the disturbance signal must also be included in the synthesis setup. The unscaled transfer functions for disturbances through the controlled plant to the performance measure is $(I + PK)^{-1}P$. Thus, the poles of the plant will still add cost to the mathematical problem even if $PK \approx 1$ through pole-zero cancellation.

A comment must be made about controller magnitude rolloff: In order for the controller magnitude to decrease at higher frequencies, it must have poles where controller rolloff is first desired. These poles, however, will change the phase of the compensator. If the phase change is too rapid (as when quick rolloff is desired), the controller rolloff may end up destabilizing the plant. Therefore, controller rolloff must not be carried out too quickly.

In the CFS synthesis setup, the controller is weighted directly by a constant scaling which aims to keep the maximum gain below 10. This maximum desired value is determined from experimental experience. The desired controller rolloff (to avoid destabilization of unmodeled higher frequency modes) is specified by uncertainties which are described in the following subsection.

6.4.4. Uncertainty Descriptions

Uncertainty in systems is modeled by weights on Δ-blocks which were described in Subsection 6.3.2. The Δ-blocks are defined as members of a set of norm bounded matrices. When they are used in system descriptions, they generate a family of system behaviors. The family is selected by weights on the Δs. For μ-synthesis, the standard blocks are taken as matrices of appropriate dimensions with the property that they are in complex mathematical balls of norm 1. For example, a 1×1 complex Δ would include all possible signals δ such that $|\delta| \leq 1$ where $|.|$ denotes absolute value.

There are three common types of uncertainty descriptions which are generated using the Δ-blocks: additive, multiplicative, and parametric. These are discussed in this subsection. Use of the linear fractional transformation framework to create structural uncertainty is presented in Chapter 7. Other specialized forms of uncertainty can also be generated, but these are generally combinations of the three common forms.

Additive Uncertainty

Additive uncertainty is presented schematically in Figure 6.5, where the input to the additive scaling for the Δ-block is a control signal ($\underline{u}$). The output from the Δ-block is fed into the sensed signal $\underline{y}$ which in many cases is also part of the performance measure $\underline{z}$. This places uncertainty on the nominal plant model

transfer function P_{22}. Since neither the inputs nor the outputs of the uncertainty description pass through the system model, additive uncertainty is not directly dependent on the magnitude of the nominal model. Thus, this type of description places uncertainty at all frequencies even where the system has small magnitude. In particular, since identification of system transmission zeroes is difficult, additive uncertainty can be used to compensate for lack of this type of knowledge.

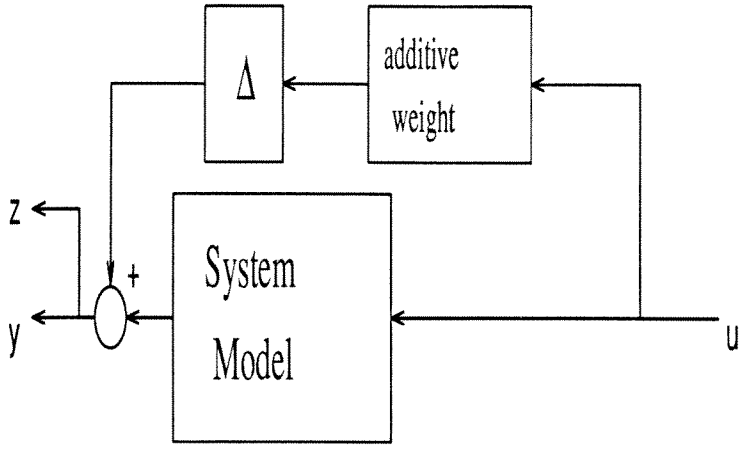

Figure 6.5 - Typical Schematic Form of Additive Uncertainty.
Since this form does not directly depend on the system model, it is most useful to specify uncertainty at system transfer function zeroes.

Because of additive uncertainty, the controller will stay clear of large gains. In the synthesis portion of the D-K iterations, the control signal $\underline{u}$ shaped by the additive weight is part of the transfer matrix to be reduced for performance. Thus, the controller shape will approach the inverse of the frequency weight. For example, when higher frequency modes are not well known, an additive uncertainty whose magnitude is small at low frequencies but large at high frequencies can be used. The controller will then have larger gains at the lower frequencies and low magnitudes at the higher frequency regions. This increases controller magnitude rolloff.

For better computational properties, additive along with all other uncertainty weights should be split between inputs and outputs. For example, if a second order weight is used, one pole should be used at the input weight and the other at the output scaling. Similarly, the magnitudes should be of comparable sizes. Since the connection through the Δ-block does not exist during the K-iteration, these weights specify performance. The inputs and outputs related to these uncertainty weights

interact with the sensor, performance, and disturbance signals through multiple channels. It is therefore a good idea to have well balanced systems. That is, the inputs and outputs should be of similar magnitudes so that important features are not missed because of small weights in the synthesis setup. Another reason to split up the uncertainty weights is that generally the D-scales will not need as many states for the polynomial that fits them. This reduces the number of additional states in the synthesis setup. Computation time and controller state number are thus kept smaller. (Current H_∞methods generate controllers with the same number of states as the synthesis setup.)

In the CFS, uncertainties at lower frequencies of sizes between 3% and 10% are used. For example, with 6% low frequency weight, the input and the output scalings are each

$$\frac{\sqrt{0.06}(s+50)}{(s+250)}. \tag{6.7}$$

The $(s+250)$ term in the denominator specifies the level of higher frequency uncertainty. Since this weight is placed at both the inputs and the outputs for uncertainty, the Δ-block for additive uncertainty is weighted by

$$\frac{0.06(s+50)^2}{(s+250)^2}. \tag{6.8}$$

The Bode magnitude response of this weight is shown in Figure 6.6, where it is overlayed on the structure response of one of the structure channels. As can be seen, this weight places low uncertainty at the zeroes below 50 rad/sec, and places high uncertainty level above 100 rad/sec. The Δ-structure is chosen as a 3×3 full complex block. This additive description is purely *ad hoc* – it is selected based on trials of different controllers.

Multiplicative Uncertainty

Multiplicative uncertainty is represented by Figure 6.7 where the uncertainty block is placed at the output of the nominal system. Here the sensor signal's uncertainty level is generated by the multiplicative weight. Since this description is directly dependent on the nominal system model, uncertainty will be larger in absolute terms when the system has a larger response. In structural systems, this occurs at the modal peaks. Uncertainty at the zeroes will then be very small (or

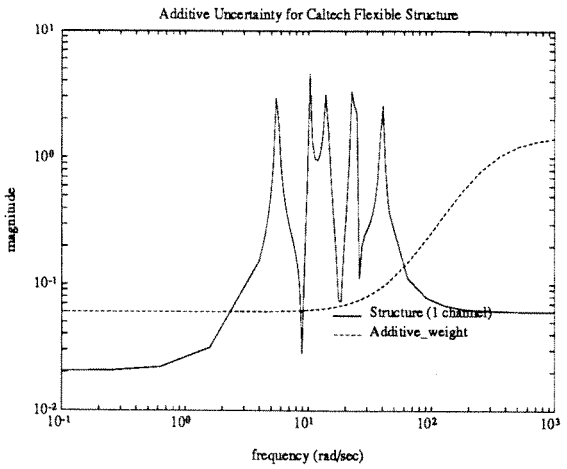

Figure 6.6 - Additive Uncertainty for Caltech Flexible Structure. Uncertainty here has the most effect on the system where the system has low amplitudes. The magnitude increase at high frequencies is used to force the controller to roll off, thereby avoiding unmodeled modes.

zero) since the multiplicative weight scales zero amplitude signals. The multiplicative description may also be placed at the input to the system model to simulate actuator uncertainty.

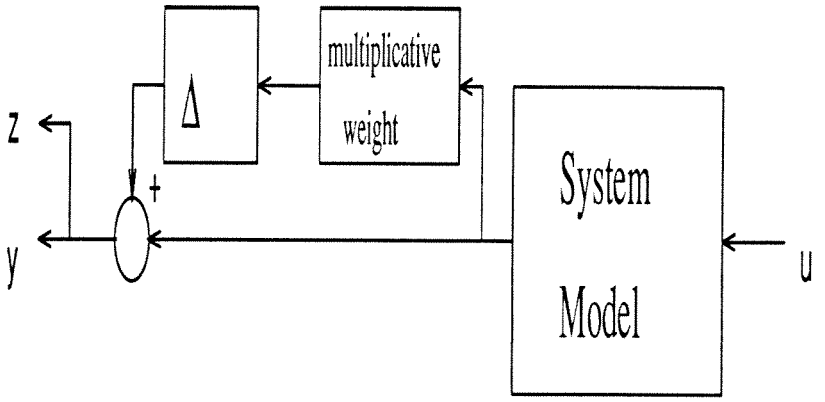

Figure 6.7 - Graphical Representation of Multiplicative Uncertainty. The signal entering the uncertainty description is directly related to the system model. At transmission zeroes, the uncertainty will therefore be very small. At modal peaks, the uncertainty can be quite large in absolute terms.

In terms of controller shaping, multiplicative uncertainty helps prevent pole-zero cancellations. The controller has to be somewhat less aggressive if the exact pole locations and gains are not fully known. As with any type of uncertainty, larger uncertainties result in controllers with less performance.

For structural systems, this type of description will most greatly affect the values of modal frequencies and dampings. They will also affect the modal participation factors (gains). On the CFS, constant weights of 6% are used on the nominal system response output signal. A full 3×3 Δ-block is used. Once more, this level is determined by trial and error.

Parametric Uncertainty

When more tailored uncertainty is desired, parametric uncertainty can be used. This involves isolating a particular uncertain parameter in the model, and feeding uncertainty around it. For example if a modal damping is only known to within a certain level, this may be reflected in the synthesis setup. An example is probably the best way to demonstrate this tool. Suppose that a spring-damper-mass system is modeled by

$$\ddot{x} + 2\zeta_{nominal}\omega\dot{x} + \omega^2 x = f(t), \tag{6.9}$$

but that the damping is only known to be 90% accurate. Thus, with a $-1 \leq \delta \leq 1$, ζ can be described as $\zeta = \zeta_{nominal}(1 + .1\delta)$. The value of ζ is then $.9\zeta_{nominal} \leq \zeta \leq 1.1\zeta_{nominal}$. The equation of motion then becomes

$$\ddot{x} + 2\zeta_{nominal}(1+\delta)\omega\dot{x} + \omega^2 x = f(t). \tag{6.10}$$

Pulling the δ out, and putting the system in state space form,

$$\begin{aligned}
\begin{pmatrix} \dot{x} \\ \ddot{x} \end{pmatrix} &= \begin{bmatrix} 0 & 1 \\ -\omega^2 & -2\zeta\omega \end{bmatrix} \begin{pmatrix} x \\ \dot{x} \end{pmatrix} + \begin{bmatrix} 0 \\ 1 \end{bmatrix} f + \begin{bmatrix} 0 \\ 1 \end{bmatrix} q \\
r &= \begin{bmatrix} 0 & -2\zeta\omega(.1) \end{bmatrix} \begin{pmatrix} x \\ \dot{x}, \end{pmatrix} \\
&\text{with} \\
q &= \delta r.
\end{aligned} \tag{6.11}$$

Unfortunately, this type of uncertainty adds an input and an output to the synthesis setup for every uncertain parameter. Computation of the D-scales then

requires more time because there are more uncertainty blocks to calculate. Similarly, when curve fits of order greater than zero are used for the D-scales, many more states are added to the synthesis setup. This increases the number of states in the controller.

On the CFS, parametric uncertainty is not used. Many of the effects of parametric uncertainty can be modeled with additive or multiplicative uncertainties, although somewhat less exactly. Performance of the controller is reduced somewhat, but since methods do not yet exist for efficient uncertainty identification [NeS], this method can only be used with rule-of-thumb estimates of uncertainty.

6.5 Other Issues in the Synthesis Setup

In addition to the nominal model, the performance specifications, and the uncertainty descriptions, there are several implementation-related components that need to be included in the synthesis setup or that need to be considered during the synthesis procedures. The setup components include such items as control hardware computational details, and sensor and actuator dynamics. Computational difficulties discussed include optimality of the controller and costs associated with calculation of μ.

6.5.1. Computational Delays

When the controller is implemented on digital hardware, there are computational delays which must be accounted for. These effects can lead to instability of dynamics at frequencies above the Nyquist frequency (1/2 the sampling frequency). Controller synthesis using MATLAB is set up for continuous systems so it is necessary to approximate the discrete phenomenon in a continuous setting. For state space relations, the most common method to model delays is the Pade approximation. In the Caltech system, real-time computer control running at 200 Hz is used. A second order Pade approximation is used since most of the dynamics to be controlled are well below the Nyquist frequency. Once the continuous time controller is synthesized, it is converted to a discrete form using a zero-hold approximation. Other transformations can also be used.

6.5.2. Sensor and Actuator Dynamics

Sensors and actuators used in systems have finite bandwidths of effective operation. They also may have significant dynamics, as the controlled proof mass actuators on the CFS have. If these characteristics are not included in the nominal model, they need to be added into the synthesis setup when it is assembled. Compensation for limited response bandwidths may be done using uncertainty, but modeling of significant dynamics should be done in the transfer function P_{22} with accurate models of the behavior. If these effects are neglected, unstable controlled systems may result.

On the experiment with the CFS, the accelerometer and voice coil response losses are at frequencies significantly higher than the region of control interest, thus they are not explicitly modeled in the synthesis setup. The higher frequency additive uncertainty leads to controllers that avoid the devices' limitations. Since behavior of the proof mass actuators is actively controlled, these dynamics are incorporated in the nominal model as described in Chapter 3. Additionally, significant actuator uncertainty (multiplicative uncertainty acting at the input to the nominal model) is needed because the proof masses have nonlinear responses due to friction. Identified models of the proof mass actuator behavior are of lower quality than those for the voice coils.

6.5.3. Optimality of the H_∞ Controller

Computation of the H_∞-optimal controller involves an iterative search for the smallest value γ for which $\|T_{zw}\|_\infty < \gamma$. The problem may be scaled so that $\gamma \approx 1$. Failure of the procedure to meet a particular γ value may occur for one of three main reasons. The first two involve finding solutions of Riccati equations related to the full information (FI - similar to state feedback) problem and the output estimation (OE - output state estimator) problem. The third condition is related to the combination of the FI and the OE results to form the optimal dynamic compensator K. Failure of any of these requirements means that a larger value of γ must be used, i.e., that the closed loop performance of the closed loop system will not have $\|T_{zw}\|_\infty < \gamma$. The solution for the FI Riccati equation is denoted X_∞, and that for the OE is represented by Y_∞.

When controllers which achieve $\|T_{zw}\|_\infty < \gamma$ are achieved, the diagnostics in the MATLAB Musyn Toolbox on the requirement for combination of the FI and OE solutions give a good indication of the level of optimality of the controller. That

is, information is given on how close the controller performance is to the absolute minimum value of γ for the infinity norm of the transfer function from disturbance to performance. When the H_∞-optimal controller is obtained, the largest eigenvalue $\rho(X_\infty Y_\infty)$ is just slightly smaller than 1.0. Smaller $\rho(X_\infty Y_\infty)$ values indicate less optimal controllers. Values greater than 1.0 mean failure of the synthesis.

The mathematically suboptimal controllers will, in most cases, perform better that the optimal ones for several reasons. First, the fully optimal controller will push all of the uncertainty and performance specifications to their limit, and will therefore have infinite bandwidths of effort. To obtain an optimal controller with finite bandwidth, an uncertainty with infinite magnitude at high frequencies is necessary. This, however, specifies infinite performance at higher frequencies – an objective which cannot be met. Therefore, uncertainty and performance descriptions of finite magnitudes are always used. Suboptimal controllers will roll off at the high frequencies since the synthesis procedure is not pushed to work at all frequency regions.

Another major reason to use suboptimal controllers exists with systems which are nonminimum phase (have transmission zeroes with eigenvalues in the right half plane) such as structures. In a loose sense, the optimal feedback will attempt to cancel the open loop zeroes by placing compensator poles near the zeroes. Then if the zeroes are in the right half-plane, the controller will have right half-plane poles, thereby being unstable when not connected to the plant. Unstable controllers have difficulties with robustness, hardware implementation, and model reduction, thus they should be avoided. Robustness is lost because errors always exist between the model and the actual behavior of the system, and because the system's behavior often changes over time. An unstable controller relies on the nonminimum phase zeroes to give a stable closed loop (controlled) system; therefore, variation of these zeroes may lead to instability of the whole system. The primary problem with hardware implementation of unstable controllers is saturation due to large magnitude signals generated by the unstable compensator.

Nonminimum phase zeroes can also be introduced to the synthesis setup by the uncertainty and performance specifications. The controller is guaranteed to result in stable behavior of the controlled synthesis setup. Thus, unstable dynamics in the compensator may be artifices of the synthesis setup (not due to the nominal system). It is therefore a good idea to check the behavior of the controller on a *truth*

model consisting of the nominal description, prior to implementation on the actual system. This will help avoid unstable closed loop behavior caused by mathematical devices.

Model reduction of the compensators is often necessary because of limits on controller size for hardware implementation. Model reduction tools such as Hankel singular value truncation work only for stable systems. Unstable controllers, therefore, cannot be model reduced for proper implementation.

From experience with the Caltech system, a good *rule-of-thumb* for choice of the optimality of the feedback algorithm is to choose controllers with $\rho(X_\infty Y_\infty) \leq 0.45$. Different types of systems will require different optimality choices.

6.5.4. Computation of μ

Computation of the value of μ and of the D-scales also has some features worth noting. As previously mentioned, the value of μ cannot be computed directly from its definition. Instead, upper and lower bounds of the scaled M, the closed loop synthesis setup, are used to guide the value of μ. For each frequency value, μ will have different bounds, thus it is necessary to choose frequencies at which to compute μ. This creates a tradeoff between the resolution of the bounds and the computational time necessary to find the maximum value of μ over all frequencies. If resolution is not high enough, peaks in the value may be missed, leading to overly optimistic estimates of μ (μ too small). That is, frequencies where $\mu > 1$ can be missed. However, larger numbers of frequency points increase computational expense.

The upper and lower bounds for μ are found in certain cases to differ by a significant amount [Bmu]. Use of the upper bound as the value of μ can be extremely conservative if there is a large gap between the bounds. Assuming that μ is larger than actual sacrifices obtainable performance but gives greater robustness. On structural systems, experience is that these bounds differ by less than 10%. Therefore, performance is not greatly sacrificed here because of the inability to directly compute μ.

6.5.5. Using D-scales to Study Interactions in the Synthesis Setup

It is also useful to track the progress of the D-scales as iterations of μ-synthesis proceed. In each D-iteration portion, it is necessary to create approximations to the scalings for the upper bound of μ. The D-scales, when collapsed into the synthesis setup (as D on one side and as D^{-1} on the other) alter the performance specifications so that the next controller synthesized avoids the worst case (in the sense of μ) disturbances. Interactions between the various inputs and outputs of the synthesis system are quite complex, so the D-scales can alter the problem in sometimes unforeseen ways. Therefore, tracking the D-scales can indicate problems with the synthesis setup. In particular, large changes in the average magnitude (over the frequency band of interest) of a D-scale indicate that the H_∞problem is being changed greatly. Figure 6.8 gives an example of characteristics the setups often have with respect to the D-scales.

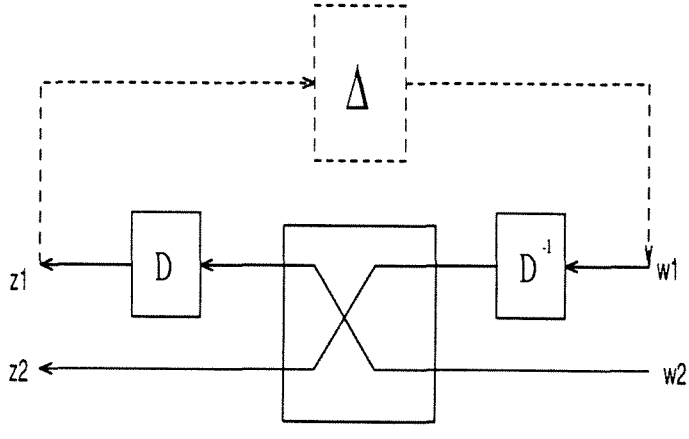

Figure 6.8 - Common Interactions of D-scales in Synthesis Setup.
The solid lines represent connections specified by the controlled synthesis setup. The dashed lines give the closing around the Δ-block. When this loop is closed (for μ-analysis), the D's cancel each other out; however, with the Δ loop open (for the K-iteration) the D's can greatly alter the synthesis specifications.

If D is of very large magnitude, D^{-1} will be of very small amplitude. Then the effect of $w2$ on $z1$ will be greatly increased, while the effect of $w1$ on $z2$ is significantly decreased by the D-scales. This could for example, result in a very small gain controller from the K-iteration. This type of problem is avoided by making sure that $w1$ affects $z1$. Generally this prevents unpredictable scalings of the synthesis setup.

The shape of the D-scales can also be used to get some idea of what the worst case disturbance is. This is done by observing which channels are scaled to large magnitudes by the D-scales, and by noting at what frequencies this occurs.

On the Caltech structure, the interactions in the synthesis setup are replaced when large changes in the D-scale magnitudes occur. The order of the D-scales is kept below 2 to avoid increases in the size of the synthesis setup. For the first step of μ-synthesis, the order of the synthesis setup is approximately 39. For each 3×3 Δ-block, each order for the D-scaling adds six (three for D, and three for D^{-1}) states to the synthesis setup. Therefore, it is desirable to use low order D-scale fits, although this increases the conservativeness of the controller somewhat.

6.5.6. Assembly of the Models

Figure 6.9 presents a typical block diagram of the synthesis setup for a structural system. It contains the features previously mentioned: additive uncertainty, multiplicative uncertainty (at the output), computer delay, controller scaling, a nominal model, performance specifications, and controller shaping. The desired performance results from both the noise and the disturbance inputs affecting the performance output. Weights (acting like filters) can be placed in any branches of this setup except for the loop that links the controller signal to the measured signal. Performance or uncertainty specifications in this loop modify the nominal model thereby changing the controller directly. The compensator will then be incorrect for the unscaled system.

When this setup is actually implemented for controller synthesis, the inputs and outputs to the Δ-blocks are placed as outputs and inputs respectively to the synthesis setup. In Figure 6.10, one of the models for synthesis of the Caltech structure is presented. The solid lines represent interconnections for the K-iteration. The blocks connected to these lines are assembled to form the synthesis setup. Dashed lines represent where the controller and the Δ blocks are connected for μ-analysis.

As described previously, the uncertainty descriptions are split between inputs and outputs. The first (three) inputs and outputs determine additive uncertainty; the next (three) give multiplicative uncertainty; the following (six) specify noise,

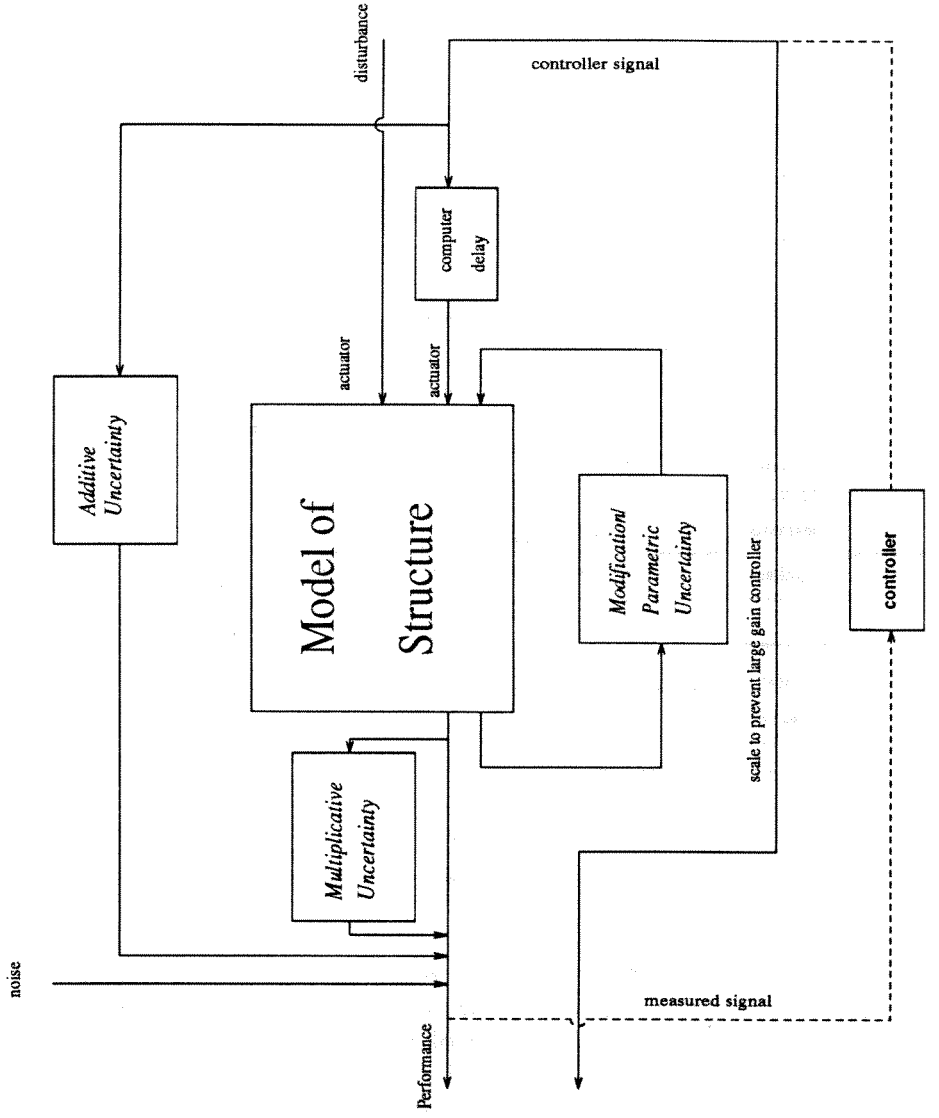

Figure 6.9. - Standard Synthesis Setup.
It is not necessary to include all the various uncertainty blocks. For controller synthesis, the connections through the uncertainty blocks are opened.

disturbance, and performance; and the last (three) give the nominal model. Performance is specified by disturbance and noise inputs and by structural response and control size outputs. This trades off disturbance rejection, noise rejection, and

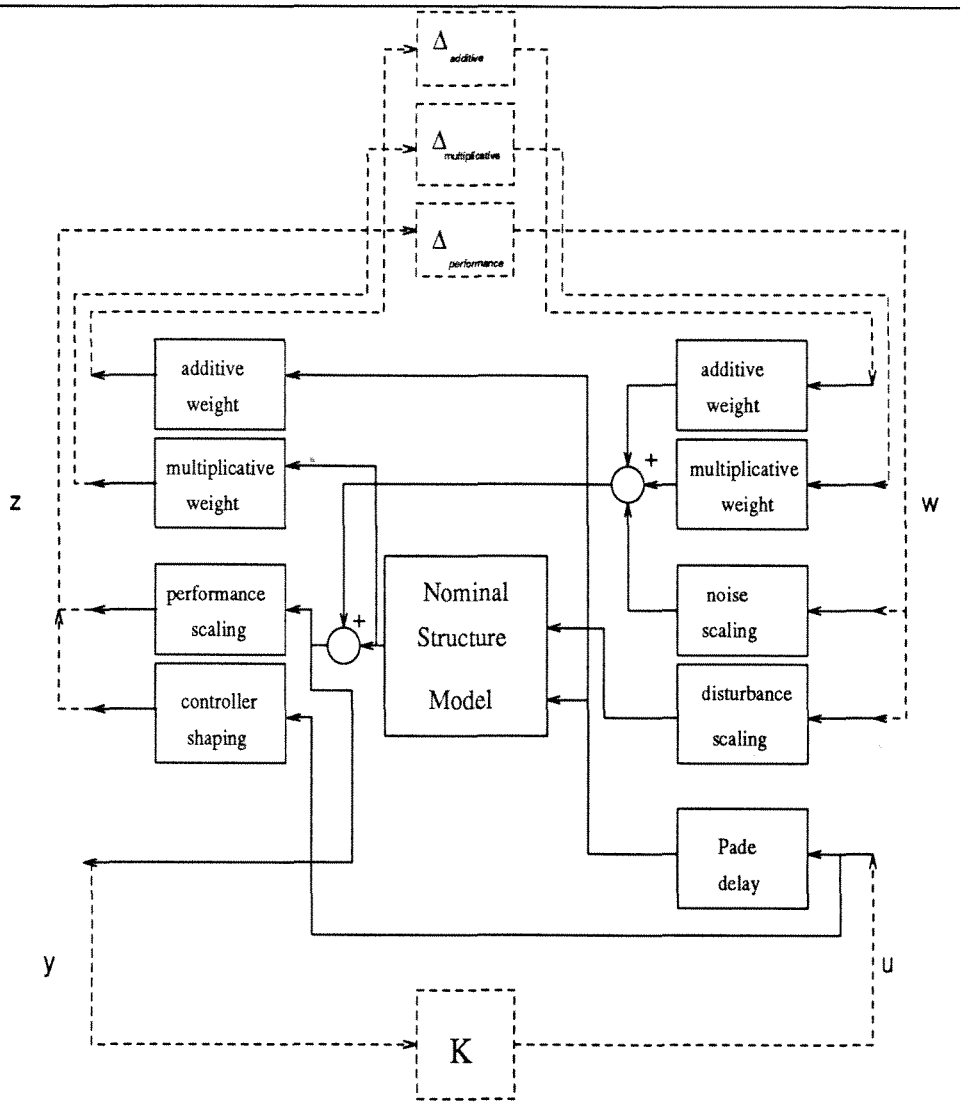

Figure 6.10. - Caltech Flexible Structure Synthesis Setup.
The solid lines show the setup which must be constructed at the beginning of the D-K iteration scheme. Closing the loop around the K gives the controlled synthesis setup which is then μ-analyzed for robustness and performance with respect to the Δ blocks.

controller effort. The performance specifications are fed through a Δ-block for performance. This loop is used so that μ can measure performance along with stability. D-scales are not fit for the performance block. Robust stability of the system is measured by calculating μ only with respect to the uncertainty Δ-blocks. (Please see [Pac] for a more thorough description.)

The main weight used to specify greater disturbance rejection is the disturbance scaling. This is increased for more overall performance of the system. A

scaling can also be placed on the performance outputs, but this changes the effects of the additive and multiplicative uncertainties in addition to increasing the scale on the disturbance. Specific paths in the synthesis setup may interact to create objectives other than those expected.

6.6 Conclusions

This chapter has detailed many of the implementational issues of H_∞/μ-synthesis, and has given details of the mathematical setup for synthesis of controllers. The procedure, while requiring significant user input, develops a very effective controller design procedure for complicated systems. In the following chapter, results of various experimental implementations of this type of controller are presented.

6.7 References for Chapter 6

Bmu: Balas, G., *et al.*, (1991),**μ-Analysis and Synthesis Toolbox,** MUSYN, Inc., and The Math Works, Inc., Natick, Massachusetts.

Ba2: Balas, G., (1990), **Robust Control of Flexible Structures: Theory and Experiments,** Ph.D. Thesis, Department of Aeronautical Engineering, California Institute of Technology, Pasadena, California.

Bla: Blackwood, G.H., (1988), "Experimental Component Mode Synthesis of Structures with Joint Freeplay," Report SSL#16-88, Space Systems Laboratory, Massachusetts Institute of Technology, Cambridge, Massachusetts.

CaO: Caughey, T.K., and O'Kelley, M.E.J., (1965), "Classical Normal Modes in Damped Linear Dynamic Systems," *Journal of Applied Mechanics,* Vol. 39, No. 3, pp. 583-588

Cau: Caughey, T.K., (1982), "Structural Dynamics Analysis, Testing, and Correlation," JPL Publication 81-72, Pasadena, CA.

CKR: Crowley, J.R., Klosterman, A.L., Rocklin, G.T., and Vold, H., (1984), "Direct Structural Modification Using Frequency Response Functions," *Proceedings of the 2^{nd} International Modal Analysis Conference,* Union College, Schenectady, NY, pp. 930-936.

Cra: Craig, R.R., Jr., (1985), "A Review of Time-Domain and Frequency-Domain Component Mode Synthesis Methods," **Combined Experimental/Analytical Modeling of Dynamic Structural Systems,** ASCE/ASME Mechanics Conference, AMD, Vol. 67, pp. 1-30.

DFT: Doyle, J., Francis, B., and Tannenbaum, A., (1992), **Feedback Control Theory,** Macmillan Publishing Co., New York.

DGK: Doyle, J., Glover, K., Khargonekar, P., and Francis, B., (1989), "State Space Solutions to standard H_2 and H_∞ Control Problems," *IEEE Transactions on Automatic Control* Vol. AC 34, pp. 831-847.

DGF: Doyle, J., Glover, K., Khargonekar, P., and Francis, B., (1988), "State Space Solutions to standard H_2 and H_∞ Control Problems," *Proceedings of the American Controls Conference,* Atlanta, GA.

Ewi: Ewins, D.J., (1985), "Modal Test Requirements for Coupled Structure Analysis Using Experimentally Derived Component Models," **Combined Experimental/Analytical Modeling of Dynamic Structural Systems,** ASCE/ASME Mechanics Conference, AMD, Vol. 67, pp. 1-30.

Fla: Flashner, H., (1986), "An Orthogonal Decomposition Approach to Modal Synthesis," *International Journal for Numerical Methods in Engineering* 23, p. 471-493.

HEN: Hedges, T., Elliot, S.J., and Nelson, P.A., (1988), "The Active Simulation of Structural Frequency Response Functions," *Proceedings of the* 6^{th} *International Modal Analysis Conference,* Kissimmee, FL, pp. 67-72

Hur: Hurty, W.C., (1965), "Dynamic Analysis of Structural Systems using Component Modes," *AIAA Journal,* Vol 3, No. 4, pp. 678-685.

Kai: Kailath, T., (1980), **Linear Systems**, Prentice-Hall, Englewood Cliffs, New Jersey.

KwS: Kwakernaak, H., and Sivan, R., (1972), **Linear Optimal Control Systems**, Wiley-Interscience, New York.

Mos: Moser, A.N., and Caughey, T.K., (1991) "Some Experience with Identification of the Caltech Experimental Space Structure." *Proceedings of the 1991 American Controls Conference,* Boston, Massachusetts.

Mo2: Moser, A.N., Doyle, J.C., and Caughey, T.K., (1992) "Component Mode Synthesis using Linear Fractional Transformations and Identified Models," *To be submitted.*

NeS: Newlin, M.P., and Smith, R.S., (1991), "Model Validation and a Generalization of μ," *Proceedings of the 30^{th} Conference on Decision and Control,* Brighton, England.

Pac: Packard, A., (1988), "What's New with μ," Ph.D. Thesis, Mechanical Engineering Department, University of California at Berkeley, Berkeley, California.

SpT: Spanos, J.T., and Tsuha, W.S., (1989), " Multibody Dynamics: Modeling Component Flexibility with Fixed, Free, Loaded, Constraint, and Residual Modes," *Proceedings of the 3^{rd} Annual Conference on Aerospace Computational Control,* JPL Publication 89-45, Pasadena, CA, pp. 761-777.

StF: Strang, G., and Fix, G.J., (1973), **An Analysis of the Finite Element Method** Prentice-Hall Inc., Englewood Cliffs, New Jersey.

WFC: Wada, B.K., Fanson, J.L., and Crawley, E.F., (1990), "Adaptive Structures," *Mechanical Engineering,* Vol. 112, No. 11, pp. 41-46.

Chapter 7. Experimental Control of the Caltech Flexible Structure - Without and With Str2 Attached

7.1 Introduction

This chapter presents results of experimental application of H_∞/μ-synthesis developed control algorithms on the Caltech flexible structure (CFS) and discusses some of the experimentally observed limitations of active structural control. The first group of experimental results are of control of the basic CFS using either the voice coil or the proof mass motors for actuation. The second group of results combines controller design with structural combination modeling. The setup for an uncertainty description based on a secondary structure attached to a primary system is given. Then, results of control of the CFS modified by Str2 are shown. The chapter finishes with a discussion of results.

7.2 Results of Control of the Caltech Flexible Structure

In this section, a presentation is made of the results of implementation of synthesized controllers on the experimental setup. The system to be controlled is the three bay configuration of the CFS. The main goal is vibration attenuation which is specified by trying to remove modal responses of the structure.

7.2.1. Measuring Performance

The system in question is a multiple input multiple output (MIMO), multiple degree-of-freedom (MDOF) structure with various additional dynamics such as those caused by the proof masses. Performance can therefore be measured in several ways including modal peak magnitude reductions, maximum transfer function gains (H_∞-norms), or energy under the transfer function curves (H_2-norms), just to name a few. Similarly, various combinations of actuator inputs and sensor outputs may be used to measure the performance of the compensator.

Unfortunately, when these metrics are used on digitally sampled systems, the values obtained depend on the resolution of the discrete fast Fourier transforms (FFTs) of the data. Also, values such as H_∞-norms are skewed by actuator or sensor dynamics. For example, the 2-zero rollup of the proof masses will place the peak transfer functions at high frequencies whereas the largest modal responses are really at lower frequencies. Similarly, H_2-norms are distorted because of the need to integrate over linearly spaced frequencies. Since the controller shifts energy from one region to another by adding energy to the system, the integration over frequency can give a larger H_2 norm for a controlled system than it gives for the open loop system.

The performance measures used here are comparisons in the frequency domain of the disturbance response of the open loop and the closed loop transfer functions. The transfer functions are obtained by doing a frequency by frequency divisions of the FFTs of the sensor outputs by the FFT of a chirp-type disturbance input. Since the performance objective for most of the controllers is to reduce modal (vibratory) responses at particular sensors to disturbances at certain actuators, the magnitude of these transfer functions are used. The magnitude plotted is the root mean square (RMS) sum of all the sensor signals generated as responses to excitations. Frequency point by frequency point summation is done across the relevant transfer channels.

The amount of peak reduction for each mode and the amount of increased response in the frequency regions between the peaks are discussed to rate the performance of the feedback algorithm. Good performance is indicated by reduction in modal peaks of the open loop response when the compensator is on. A few controllers are presented to demonstrate the limits of control that can be achieved on

the CFS. The experiments are quite repeatable. Systems with more powerful actuators and different kinds of sensors can probably produce more dramatic disturbance rejections than those obtained herein.

7.2.2. Control Experiments

There are two basic control arrangements that are discussed. In the first, the three voice coils are used to minimize motions at sensors 4, 5, and 6 with disturbances caused by proof mass 1. This is a good example of noncolocated multivariable control. The second configuration uses the three proof mass actuators to minimize motions at the bottom bay sensors (4, 5, and 6) when excitation is caused by voice coil 1. Since the proof masses are inertial actuators, and since they are smaller than the voice coils, they have significantly less control authority. Less performance is therefore expected from this colocated control experiment. This is not generally a feature of collocated systems, but because of the equipment used here, less performance is obtained.

The control algorithms are implemented on a Masscomp 5400 data acquisition computer which is set up for active control. While the system is configured to excite six actuators and to store data from ten sensors, it is only set up to actively control three actuators using three sensors with multivariable controllers. Additionally, it locally controls the three proof masses using their respective LVDTs. In the multivariable experiment which uses the proof masses for control, the central (MDOF) and the distributed (local) controllers work together.

As previously described, the controllers are synthesized in the continuous domain. Because of the uncertainty and performance specifications, they sometimes are on the order of 45 to 60 states. These are then model-reduced down to around 30 states using Hankel singular value methods. Only those states with Hankel singular values greater than 1×10^{-4} are kept. The controllers are then put in block diagonal real form, are transformed to the discrete domain (using a zero order hold), and are translated to a FORTRAN data set implementable on the MASSCOMP computer.

7.2.3. Performance Results - Voice Coil Control Actuation

Results of experimental control are presented first for the voice coil controller (noncolocated), followed by those for the proof mass control system (colocated). The

units on the magnitude plots are sampling bits of output divided by bits of input signal. The outputs are equivalent to 3.875×10^{-5} G/bit, the voice coils impart force at 6.5156×10^{-3} N/bit, and the proof masses give approximately 2.3×10^{-3} N/bit. The units are left as bit/bit since the real measure of performance is the comparison between the open loop and closed loop experiments, rather than the absolute quantities. The frequencies are all in rad/sec.

Figure 7.1 presents results of the most optimal voice coil controller experiment. Figure 7.1 has the RMS sums of the transfer functions from proof mass 1 to accelerometers 4, 5, and 6. The modal peak reduction is of at least 10:1 (open loop:closed loop) for the first few modes. Energy removed from these peaks is shifted to the regions between the open loop modes. The response of the system appears to be approaching that of a double differentiator. This corresponds to a two zero rollup of a rigid structural system excited by the proof mass actuator dynamics as previously discussed. The shift of energy to the zeroes is worth noting. In Figure 7.2 the transfer function (magnitude and phase) from proof mass 1 to accelerometer 6 seems to indicate that transmission zeroes are removed by the controller (particularly at around 18 rad/sec).

Many of the zeroes in the system are nonminimum phase (eigenvalues in the right half plane). For single input single output (SISO) systems, it is generally accepted that it will take infinite effort to cancel a nonminimum phase transmission zero. Here the results demonstrate that transmission zeroes can sometimes be bypassed by taking advantage of the MIMO and multivariable characteristics of the controller. The best explanation is that the transmission zeroes appear at particular frequencies only in certain input/output channels. In other channels the zeroes appear at other frequencies. Thus, the controller can take advantage of use of multiple channels to obtain responses at all sensors across the whole frequency range. Desire for robustness of controlled systems traditionally dictates that zero-removal should not be done. Here, however, it can be seen experimentally that robust controllers giving better servo-type control can be effectively implemented.

Figure 7.3 shows the RMS sum of responses at all six accelerometers to the excitation by proof mass 1. This plot points out that energy may be shifted to locations where there is no control sensing or where performance is not specified (sensors 1, 2, and 3). Even though the system model is quite good, the lack of sensing of modes 7, 8, and 9 by sensors 4, 5, and 6 reduces performance of these

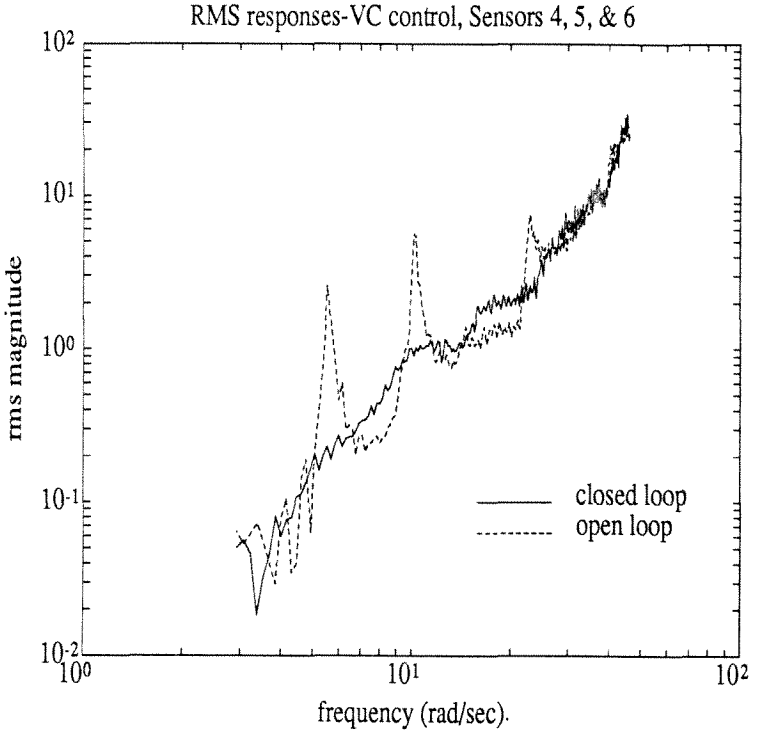

Figure 7.1 - Best Voice Coil Controller.
The RMS sum of the responses at sensors 4, 5, and 6 to proof mass #1 are presented. Good performance is obtained at all modes according to these plots. The modes appearing in the open loop response (dashed) are almost completely removed by the controller. The energy removed from the peaks appears as increased amplitudes of the closed loop (solid) response at the open loop valleys. The increase in amplitude with frequency is caused by the proof mass dynamics due to the displacement tracking controller.

modes at the second bay where their response is larger. Another explanation for these larger responses in closed loop is that the mode shapes are altered by the controller. The bottom bay begins to behave like a node for the various modes, and the energy of motion is shifted to the second bay.

With some of the controllers that are designed, the water bed effect increases the response of modes, particularly the last mode shown (mode 9 at 39 rad/sec). The best method to avoid this is to trade off performance with uncertainty. Similarly, the controllers can be designed with smaller effort and can be backed away from H_∞-optimality. Figure 7.4 presents behavior of the CFS with a controller where performance has been reduced and uncertainty has been increased. Performance at the lowest frequency modes is not as good as with the controller in Figure 7.3,

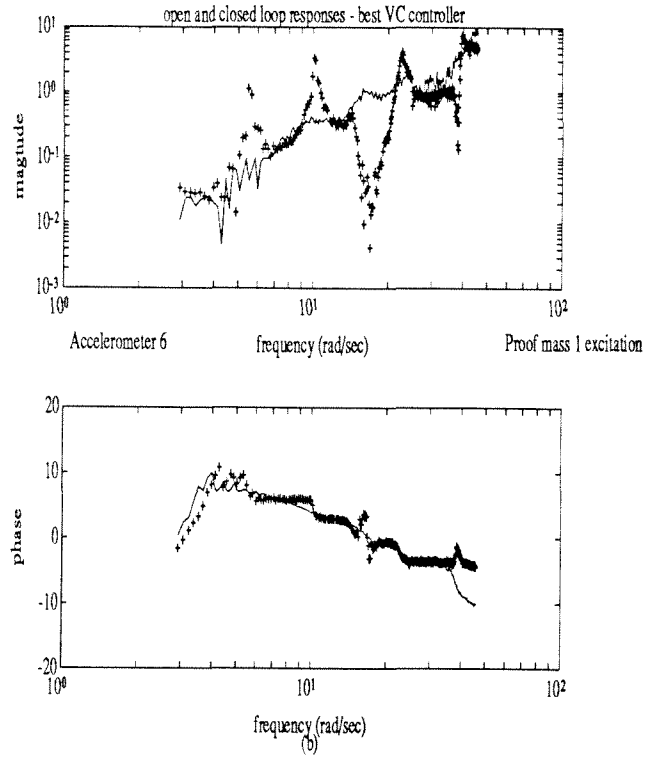

Figure 7.2 - Best Voice Coil Controller: PF 1 to Accel. 6.
The closed loop (solid) amplitude approaches the response of a rigid member: Peaks are reduced and valleys are filled in. Similarly, the phase of the response becomes smooth. Actuator dynamics are present

but excitation of the middle bay is smaller. Responses at all six accelerometers are presented.

7.2.4. Performance Results - Proof Mass Control Actuators

Figure 7.5 shows results of a proof mass controlled system for excitation by voice coil 1. Performance here is much less than that obtained by the voice coil controller for several reasons. First, the actuators are inertial, so they have less control authority than the voice coils which input force directly to the structure. Second, these actuators have significant stiction which is a nonlinear effect. Therefore, for different levels of motion, the linear controllers designed by H_∞methods may loose their validity. Most significantly, the force induced by these actuators is not in the structural load path directly, so it cannot exclusively counteract system motions. The plot in Figure 7.6 shows the response of the colocated sensor/actuator pair for the open loop system. It can be seen that structure dynamics are obscured by noise

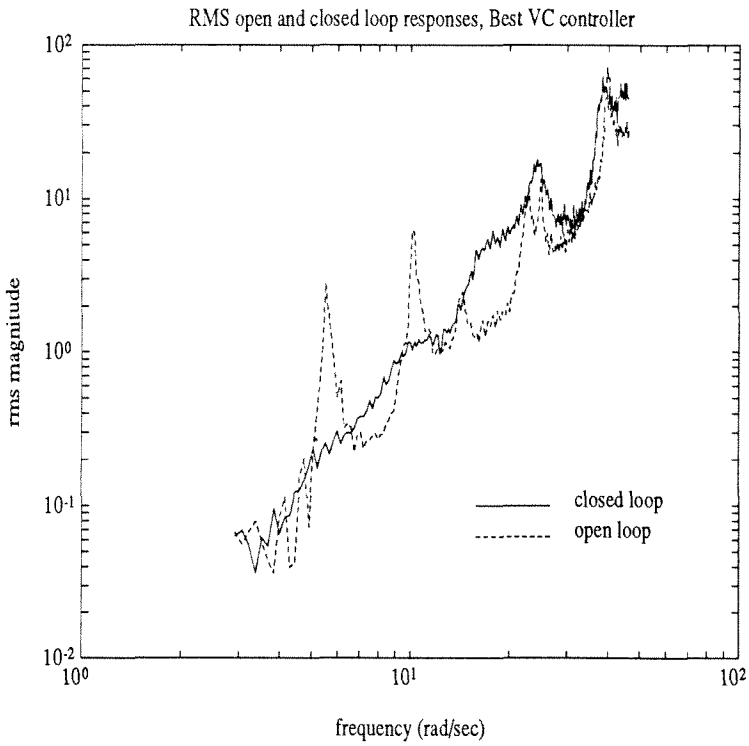

Figure 7.3 - Best Voice Coil Controller, Response at all Accelerometers. Redistribution of energy to sensors not used for control is quite evident here. The system remains stable, but the mid-bay responses of the structure are slightly increased. In this plot all the modes are evident, while in the plot for sensors 4, 5, and 6, some of the modes are almost not sensed. Respones could then be reduced by sensing in more locations. Performance is still quite good. (Proof mass dynamics are present.)

created by the actuator. The model is then inaccurate for this sensor/actuator pair. Thus, larger levels of uncertainty are needed.

When large disturbances are applied to the proof mass controller, it becomes unstable at higher frequencies. For small motions, performance can still be obtained. In Figure 7.4, the performance specification is reduction of the physical accelerations of the bottom bay. This heavily weights the first three modes.

The main conclusion from the proof mass and the voice coil control experiments is that H_∞/μ-synthesis methods are very effective for structural control. Particularly, the structure can be altered to behave like a rigid structure using active control methods. It does not seem likely that the behavior of the system

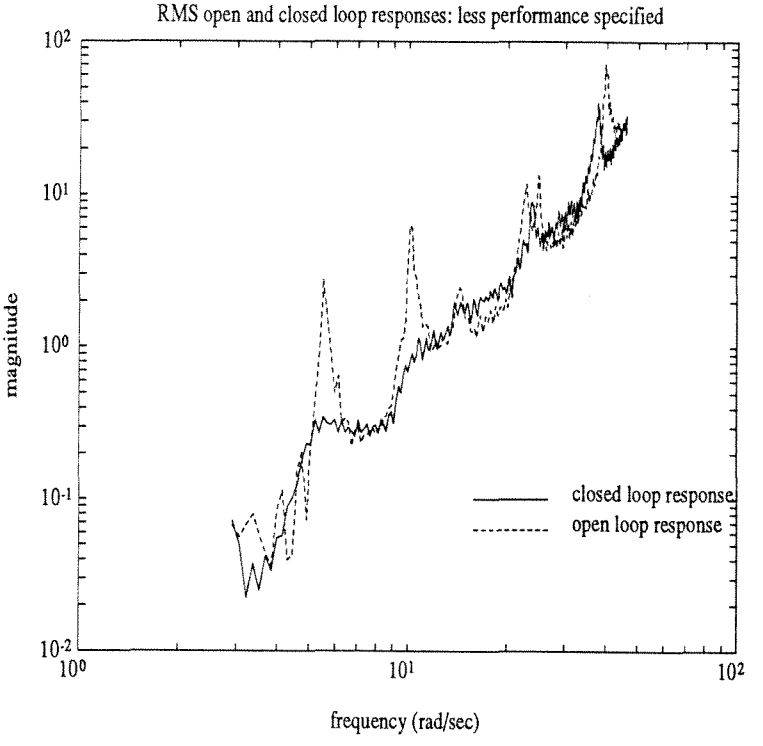

Figure 7.4 - Voice Coil Controller with Less Performance Specified, Response at all Accelerometers.
The lowest modes are removed less here than in the previous plot. The closed loop responses peak at the modal peaks, but with greater damping. Increased responses at frequencies between the modes and at unsensed modes is reduced significantly. Proof mass dynamics cause the roll up of amplitude with respect to frequency.

can be modified beyond this except in very small frequency ranges. For example, adding rollup or rolloff to the structure behavior does not seem possible over large frequency ranges. The energy shift necessary to accomplish this is too large.

Another strong conclusion is that actuators which work in the structural load paths are much more effective than inertial actuators for modal response attenuation. Use of inertial actuators also couples the flexible mode responses of the structure to its rigid body behavior. This can complicate position and orientation control for space systems.

7.3 Robust Control of Modified Structures

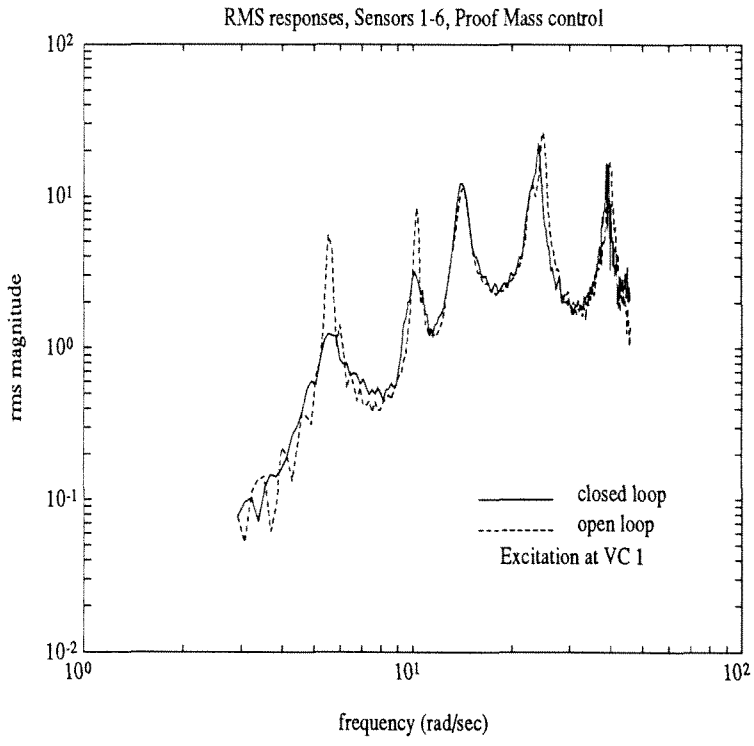

Figure 7.5 - Proof Mass Controller Response.
The excitation actuator here does not have any dynamics. The proof masses on the structure are less effective for control than the voice coils for several reasons: First, they must impart force inertially. Therefore, they are not in the structural load paths, as the voice coils are. Second, they are smaller in mass than the voice coils. And finally, they are somewhat nonlinear because of stiction. Here, some modal damping is still obtained at the lowest three modes. The plot shown here is the RMS sum of the responses at all accelerometers to excitation at voice coil 1.

In the above experimental implementations, the uncertainty descriptions are developed using purely *ad hoc* methods. Identification of uncertainties is still in formative stages [NeS], so trial and error methods are currently the primary tools for development of additive and multiplicative uncertainty descriptions. Demonstrations of controllers that are robust to uncertainty are difficult to carry out because models of the specific uncertainties are not available. Even parametric uncertainties are difficult to identify or implement on an experimental setup.

7.3.1. Setup for Structural Modification Uncertainty

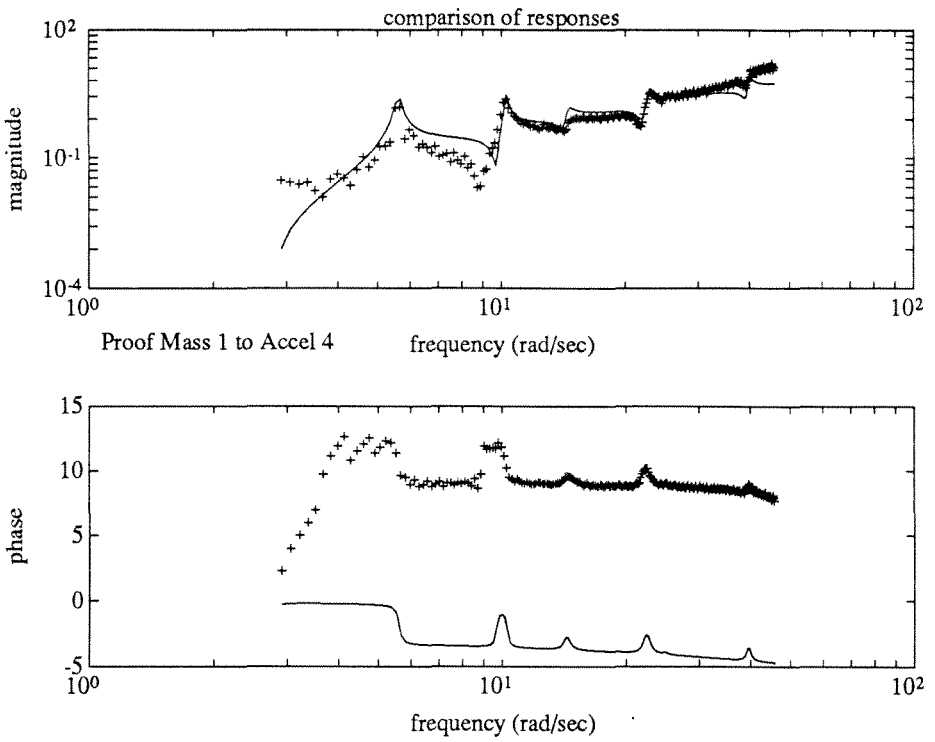

Figure 7.6 - Model and Experimental Response for Colocated Proof Mass/Accelerometer Pair.
This shows another cause for lower performance of the proof mass actuators: Signals at nearby accelerometers are corrupted by noise in the proof mass bearings. Good models, then are difficult to obtain.

When a specific uncertainty is known, controllers with stronger performance can be designed. In the case of structures, this motivates the use of linear fractional transformations (LFT) for modeling of structure modifications, and in particular for the design of controllers robust to the docking of structures.

With identified models of systems such as the CFS it is possible to model assembly of substructures using LFTs. That is, LFTs model the effect of one plant P on a controller K, and vice-versa. If the controller is replaced by an appropriate second plant model, and the plants are both structural, the interconnection of structures can be done with LFTs. The connection procedure works much like response mode synthesis [CKR], [Cra], [Ewi], [Hur]. For example, if the last set of inputs and outputs of P are the connection location for the secondary structure, and K is an input/output model of the secondary structure (model is of the same form as K), the connection of the two systems is calculated as $F_l(P, -K^{-1})$. The relations

that result from this can be determined without inverting K as presented in Chapters 4 and 5. The derivation of these relations can also be done by constraining the transfer function models P and K to be equal to each other at the connection locations.

The extension of the connection procedure to uncertainty descriptions is presented next. Supposing that there is a block $\hat{\Delta} = \hat{\delta}[I]$ where $\hat{\delta} \in [0,1] \in \Re$ is an uncertainty structure, the smallest family of plants generated by this $\hat{\Delta}$-block which includes the original plant P and the combined structure $F_l(P, -K^{-1})$ will be $F_l(P, -K^{-1}\hat{\Delta})$. When $\hat{\delta} = 0$, $F_l(P, -K^{-1}\hat{\Delta}) = P_{11}$, whereas when $\hat{\delta} = 1$,

$$\begin{aligned} &F_l(P, -K^{-1}\hat{\Delta}) = \\ &P_{11} - P_{12}K^{-1}[I + P_{22}K^{-1}]^{-1}P_{21} = \\ &P_{11} - P_{12}[K + P_{22}]^{-1}P_{21} \end{aligned} \tag{7.1}$$

The last equation is the model for the combined structural system. Since this framework is the same one used for μ-synthesis, it is possible to design compensators which are of high performance and are robust to the docking of K to P.

In the standard μ-synthesis problem, Δ can be modeled as $\Delta = \delta I$ where $\delta \in [-1,1]$. Thus the transformation $\hat{\delta} = (1-\delta)/2$ can be used to convert the connection problem to the standard μ-synthesis framework. Then, the model for the secondary plant needs to be collapsed into the model for the primary structure to create a nominal plant separate from the uncertainty block such that $F_l(P, -K^{-1}\hat{\Delta}) = F_l(\hat{P}, \Delta)$. The state space realization for $\hat{P}$ which generates a family of plants for the unconnected and the connected structures P and K is presented next. Figure 7.7 presents the schematic transformations from $\hat{\Delta}$ to Δ.

The steps in Figure 7.7 can be worked out by standard transfer function combinations that generate the matrix $\hat{P}$ in Figure 7.8. The only inversion necessary is $[K + \frac{1}{2}P_{22}]^{-1}$. The last outputs and inputs are fed through the Δ-block. In state space form, if

$$P = \begin{bmatrix} P_{11} & P_{12} \\ P_{21} & P_{22} \end{bmatrix} = \left(\begin{array}{c|cc} A & B_1 & B_2 \\ \hline C_1 & D_{11} & D_{12} \\ C_2 & D_{21} & D_{22} \end{array}\right)$$

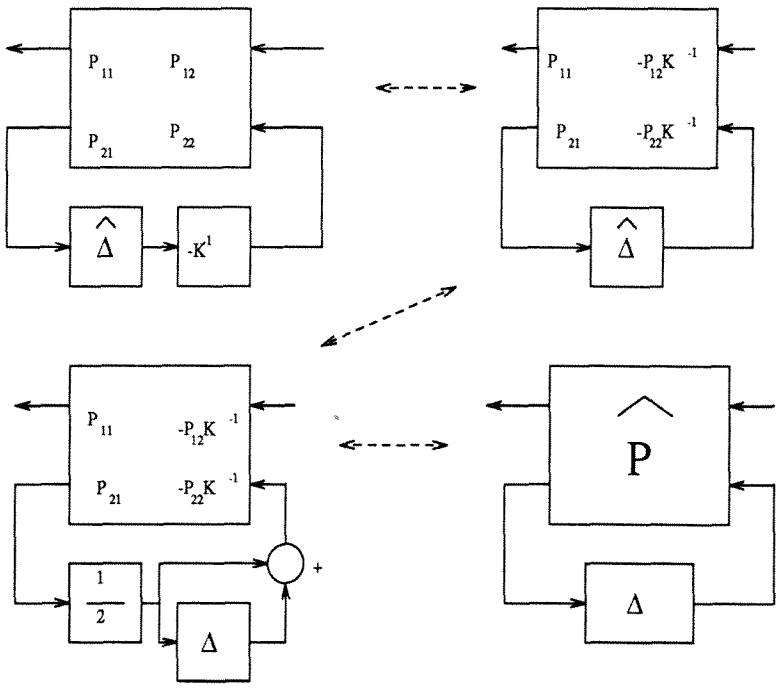

Figure 7.7. - Transformation from LFT in $\hat{\Delta}$ to one in Δ.
A schematic of the transformation from $\hat{\Delta} \in [0, 1]$ to $\Delta \in [-1, 1]$ is given. This allows use of standard μ-synthesis theory and software for controller synthesis.

$$\hat{P} = \begin{bmatrix} P_{11} - P_{12}[K + \frac{1}{2}P_{22}]^{-1}\frac{1}{2}P_{21} & -P_{12}[K + \frac{1}{2}P_{22}]^{-1} \\ K[K + \frac{1}{2}P_{22}]^{-1}\frac{1}{2}P_{21} & \frac{1}{2}P_{22}[K + \frac{1}{2}P_{22}]^{-1} \end{bmatrix}.$$

Figure 7.8. - Transfer Matrix for Structure Connection Uncertainty.

and

$$K = \begin{bmatrix} K_{11} & K_{12} \\ K_{21} & K_{22} \end{bmatrix} = \left(\begin{array}{c|c} E & F \\ \hline G & H \end{array}\right),$$

then the $\hat{P}$ system is given by Figure 7.9.

The extrema of this behavior may be verified by setting $\Delta = \delta I$, with $\delta = -1$ and $\delta = 1$. When $\delta = -1$, the resulting transfer function gives the original plant

$$\left(\begin{array}{cc|cc} A - B_2 Q \frac{1}{2} C_2 & -B_2 QG & B_1 - B_2 Q \frac{1}{2} D_{21} & -B_2 Q \\ -FQ \frac{1}{2} C_2 & E - FQG & -FQ \frac{1}{2} D_{21} & -FQ \\ \hline C_1 - D_{12} Q \frac{1}{2} C_2 & -D_{12} QG & D_{11} - D_{12} Q \frac{1}{2} D_{21} & -D_{12} Q \\ HQ \frac{1}{2} C_2 & -\frac{1}{2} D_{12} QG & HQ \frac{1}{2} D_{21} & -\frac{1}{2} D_{22} Q \end{array}\right)$$

$$\text{where } Q = [\frac{1}{2} D_{22} + H]^{-1}$$

Figure 7.9. - State Space Representation of Combined Structure Model for Structural Uncertainty Descriptions.
When the last inputs and outputs of this model are closed through a Δ block, a family of plants is generated which contains the original system and the docked systems.

P, while $\delta = -1$ generates the attached system $F_l(P, -K^{-1})$. The system $\hat{P}$ is the model for the original plant modified by 1/2 the attached plant. The identity matrix in $\Delta = \delta I$ is of size equal to the number of degrees of freedom for each connection point between the systems.

Controller synthesis via μ-synthesis is carried out by changing the nominal plant to $\hat{P}$, and by adding the Δ-block necessary for modification to the synthesis setup. The previously used additive and multiplicative uncertainties are still needed because of the errors in the models P and K. The number of states in $\hat{P}$ is the sum of the numbers of states in P and K.

7.3.2. Results of Modification Experiments

An idea of the effects of modification on controller effectiveness can be obtained by adding a mass to the actively controlled CFS. In Figure 7.10 the results of control of the mass-modified CFS are presented with the open loop response for the unmodified system. This plot presents two different modifications and the response of the original controlled system. The modifications involve addition of masses of size 430 grams and 953 grams to the bottom bay of the CFS. As can be seen, addition of these masses slightly reduces the higher frequency responses of the controlled system, thereby improving the controller performance. This controller had been designed with the 953 gram mass attached to the model of the CFS.

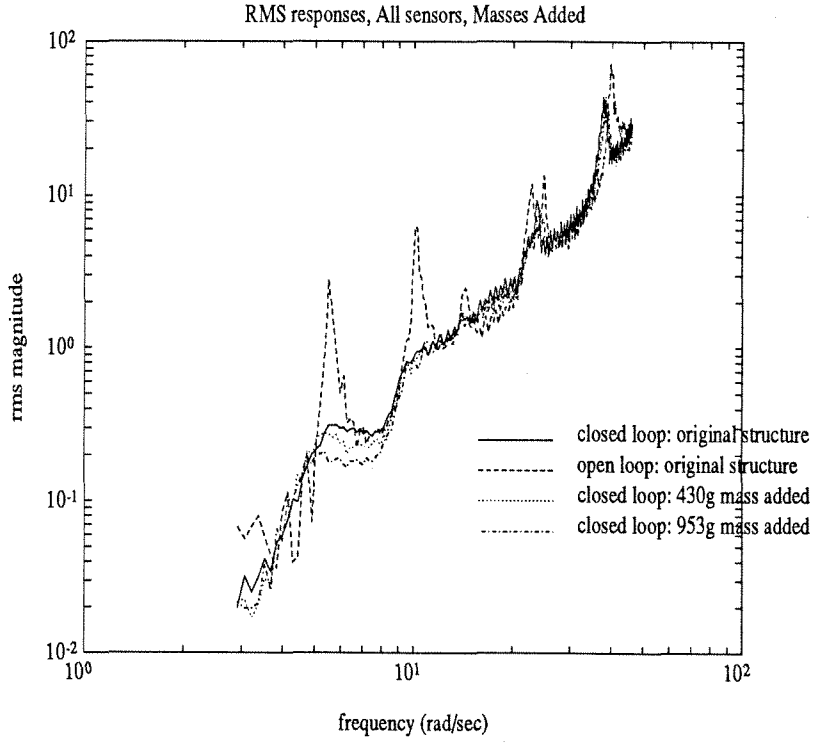

Figure 7.10 - Controller with Mass-Modified CFS.
Masses of different sizes were added to the bottom bay of the structure to test the robustness of a controller. This controller is not the best one as evidenced by the slightly modal responses of the lowest modes. Generally, additional mass seems to improve the controller response. Proof mass dynamics are present.

From these results, it appears that addition of mass improves the controlled system response when vibration minimization is the objective. Mass reduction therefore causes deterioration of performance. There is a likely explanation for this: Additional mass reduces the effect of disturbances on the system because the structure has a larger inertia. Unfortunately, in systems for which target tracking is the objective, additional mass will probably worsen performance because of the larger inertia of the system to be controlled.

The goals of the docked structure control experiments are to show that controllers can be designed to be robust to two structures, to show instability (or poor performance) of improperly designed compensators, and to measure the achievable performance of active control for a modified structure. Figure 7.11 presents the best

unmodified structure controller's effect on the CFS and the combined structural system. The RMS sums of the response at accelerometers 4, 5, and 6 to excitation from proof mass 1 are shown.

The properties of Figure 7.11(a) are discussed in a previous section. Control of the first five modes is excellent as demonstrated by the removal of the lightly damped modal peaks. There is a little shifting of energy to frequencies which had open loop transmission zeroes. Increases in responses with frequency in all the plots for voice coil controllers are caused by dynamics in the proof mass actuators.

In Figure 7.11(b), the best unmodified structure controller is applied to the CFS with Str2 connected to it. When the second structure is attached, the additional mode due to bending of Str2 in direction 1 at 11 rad/sec is excited by the compensator, so the performance and overall stability of the closed loop system is destroyed. The response is dominated by controller excitation of this mode. It is interesting to note that responses of the other structural modes are not seen. That is, it seems that although the controller destabilizes the Str2 mode, it still effectively controls the modes it was designed to attenuate. Visually, Str2's motion in its main direction 1 mode increased with time when the controller is on. Motions of the bottom bay of the CFS are kept very small until Str2's vibrations become large. Then, the forces due to these motions start exciting the CFS. A descriptive analogy is motions of the *tail wagging the dog.*

Using the same additive and multiplicative descriptions, but adding in the structural uncertainty, another controller is designed. The performance of this compensator on the original system is shown in Figure 7.12(a), and the response of the modified system is presented in Figure 7.12(b). When applied to the original system, this controller exhibits no loss of performance compared to the controller in Figure 7.11. In fact, there is less increase of responses at frequencies between the modes with this controller. When this compensator is applied to the combined system, there is a slight loss of performance, but the mode at 11 rad/sec is kept stable. In fact, it is even attenuated somewhat. The performance loss is evidenced by slight modal responses at 4.5 and 10 rad/sec. Thus, as intended this controller is robust to the structural docking.

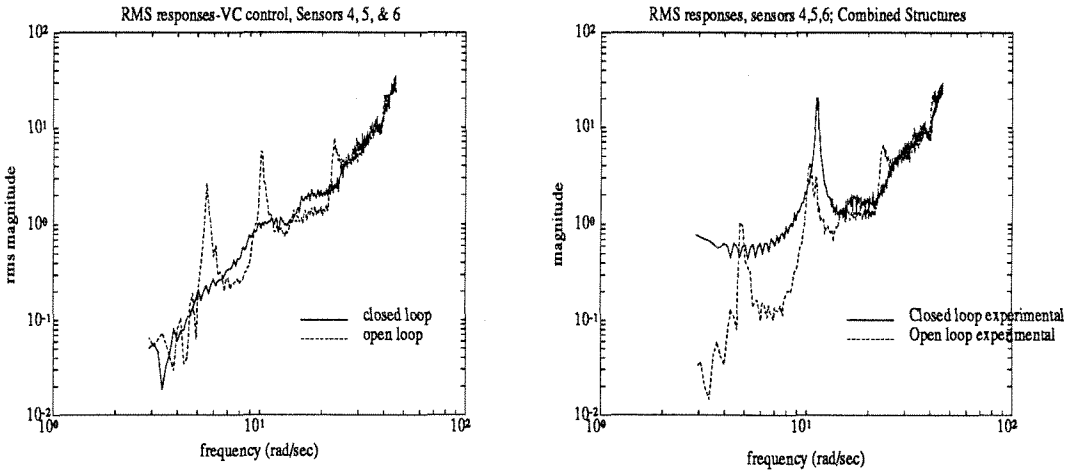

Figure 7.11. - Best Voice Coil Controller for Nominal System.
On the left, the controller is applied to the original system: good performance is obtained at the bottom bay sensors. On the right, the closed loop performance is unstable. This is shown by the large peak at 11 rad/sec, which resulted from increasing motions of the flexible mode of Str2. The bottom bay was quite still, but Str2 started moving quite significantly. Motions of Str2 then excited the rest of the structure. Proof mass dynamics create the rollup with frequency.

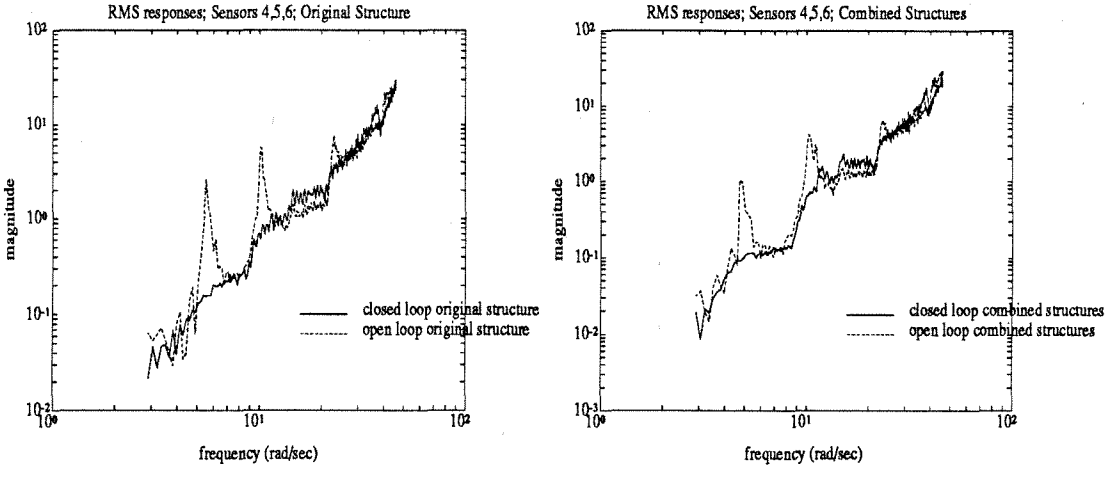

Figure 7.12. - Voice Coil Controller Robust to Structural Modification.
The structural modification uncertainty is used here to synthesize a controller which is robust to the docking, and which has good performance for the CFS (a) and for the CFS plus Str2 (b) configurations. Only slight modal responses can be seen in (b). (Proof mass dynamics are present.)

Controllers which are robust to the modification can also be designed using only additive and multiplicative uncertainties, but they have less performance. Fig-

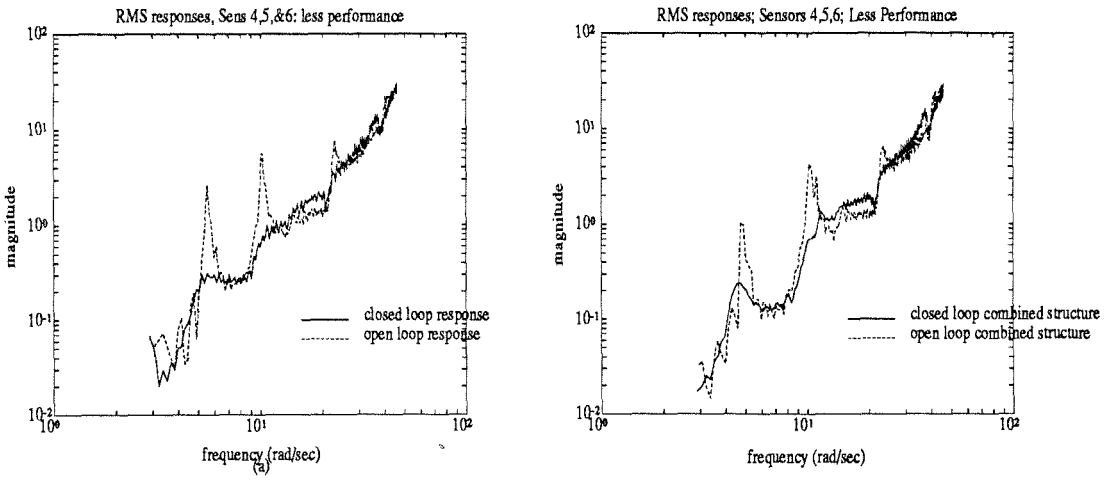

Figure 7.13. - Controller with Larger Uncertainty Acting on Both Plants. By just increasing the amount of additive and multiplicative uncertainties, controllers are developed which are stable for both configurations. Performance, however is reduced as evidenced by the modal responses of the closed loop systems (solid). Decent performance is still obtained. (Excitation dynamics are present.)

ure 7.13 shows the RMS sum of the measured transfer functions from proof mass 1 to sensors 4, 5, and 6 for the original CFS and combined CFS-Str2 structures. This compensator uses 10% additive and 10% multiplicative uncertainty without any structural uncertainty. Because of the larger specified uncertainties, desired performance is scaled back in the synthesis setup. Implemented performance, as can be seen, is is also less than that of the controller tailored to the specific uncertainty type, especially in the region of the added mode. The fundamental CFS modes have larger modal responses, especially in the combined configuration. So, although this controller is stable, its performance is not as good. These last experiments demonstrate that proper modeling of uncertainty allows for improvement in performance. Less conservative uncertainty descriptions result in more aggressive (and therefore higher performance) controllers.

Note on μ-synthesis for this case: The precise Δ-block structure for mass modification is a scalar times identity block. Thus, the Δ-block depends on just one real parameter $\delta \in [-1, 1]$. Unfortunately, computation of the D-scales is not yet available for real scalar times identity blocks. Instead, a full complex Δ-block is used here ($\overline{\sigma}(\Delta) \leq 1$), with a slight loss of performance and with an increase in robustness.

7.4 Conclusions

The strongest conclusion that can be drawn from this work is that MIMO multivariable controllers can be designed and implemented in experimental structural systems. By using multiple control channels, right half-plane transmission zeroes can be robustly controlled, leaving a system that acts like a rigid body. Similarly, it may be concluded that the limit of the vibration reduction problem, rigid system behavior, can be obtained experimentally over significant frequency bands.

Structural modification work is presented in this chapter to demonstrate that given a known uncertainty, high performance controllers can be designed and experimentally implemented. As shown experimentally poor uncertainty modeling leads to unstable controllers. In the case here, controllers which maintain good performance are designed for a system which has a secondary structure attached to it some of the time. The method for modeling the uncertain interactions between the structures based only on identified models of the system is also presented and shown to be effective. This provides an efficient method for design of controllers for use during docking of actively controlled structures.

7.5 References for Chapter 7

Bmu: Balas, G., *et al.*, (1991),**μ-Analysis and Synthesis Toolbox,** MUSYN, Inc., and The Math Works, Inc., Natick, Massachusetts.

Ba2: Balas, G., (1990), **Robust Control of Flexible Structures: Theory and Experiments,** Ph.D. Thesis, Department of Aeronautical Engineering, California Institute of Technology, Pasadena, California.

Bla: Blackwood, G.H., (1988), "Experimental Component Mode Synthesis of Structures with Joint Freeplay," Report SSL#16-88, Space Systems Laboratory, Massachusetts Institute of Technology, Cambridge, Massachusetts.

Cra: Craig Jr., R.R., Kurdila, A.J., and Kim, H.M., (1990), "State-Space Formulation of Multi-Shaker Modal Analysis," *International Journal of Analytical and Experimental Modal Analysis,* 5(3), pp. 169-183, July.

CKR: Crowley, J.R., Klosterman, A.L., Rocklin, G.T., and Vold, H., (1984), "Direct Structural Modification Using Frequency Response Functions," *Proceedings of the 2^{nd} International Modal Analysis Conference,* Union College, Schenectady, NY, pp. 930-936.

DFT: Doyle, J., Francis, B., and Tannenbaum, A., (1992), **Feedback Control Theory,** Macmillan Publishing Co., New York.

DGK: Doyle, J., Glover, K., Khargonekar, P., and Francis, B., (1989), "State Space Solutions to standard H_2 and H_∞ Control Problems," *IEEE Transactions on Automatic Control* Vol. AC 34, pp. 831-847.

DGF: Doyle, J., Glover, K., Khargonekar, P., and Francis, B., (1988), "State Space Solutions to standard H_2 and H_∞ Control Problems," *Proceedings of the American Controls Conference,* Atlanta, GA.

Ewi: Ewins, D.J., (1985), "Modal Test Requirements for Coupled Structure Analysis Using Experimentally Derived Component Models," **Combined Experimental/Analytical Modeling of Dynamic Structural Systems,** ASCE/ASME Mechanics Conference, AMD, Vol. 67, pp. 1-30.

Hur: Hurty, W.C., (1965), "Dynamic Analysis of Structural Systems using Component Modes," *AIAA Journal,* Vol 3, No. 4, pp. 678-685, April.

Kai: Kailath, T., (1980), **Linear Systems**, Prentice-Hall, Englewood Cliffs, New Jersey.

NeS: Newlin, M.P., and Smith, R.S., (1991), "Model Validation and a Generalization of μ," *Proceedings of the 30^{th} Conference on Decision and Control,* Brighton, England.

Pac: Packard, A., (1988), "What's New with μ," Ph.D. Thesis, Mechanical Engineering Department, University of California at Berkeley, Berkeley, California.

Chapter 8. Conclusions and Directions for Future Work

8.1 Main Results

In this thesis, three major portions of active control for structures have been addressed: identification, modeling of structural modifications, and design of active controllers. In Chapter 7, the topics were combined into active control of a modified structure quite effectively. The results of this work may be broken down into the particular fields of interest.

8.1.1. Identification

In structural identification, the development from this work is the demonstration that closely spaced modes can be separated without the previously specified resolution of frequency domain data. Similarly, more than one mode per sensor can be identified. This is done through use of multiple input and multiple output channels. The procedure is demonstrated on numerical and experimental setups. In particular, the experimental setup has three pairs of very closely spaced, lightly damped bending modes and three torsional ones spaced between the pairs. This greatly adds to the difficulty of identification, but excellent results are still obtained.

With the ability to develop models of this good quality from identification experiments alone, it may not be necessary to use results from estimation programs such as finite element codes for controller synthesis. The estimates should still be used for overall system physical design, but identified models should be used for compensator development. Use of the identification models also reduces problems

with assuring that amplifier gains are precisely known and with checking connections to make sure polarity of signals are not reversed. Implementation is thus easier.

8.1.2. Modification Modeling

The interesting component mode synthesis result is the extension of response mode synthesis to experimentally derived models of structures with noncolocated sensors and actuators. By doing two experiments on each structure, the behavior of the combined structures can be predicted in an input/output framework quite inexpensively computationally. This method also bypasses the need for measurement of the gains of amplifiers and actuators. (Their behavior can be changed by connections to different systems.) Finally, the method is general enough to be used with locally controlled actuators. Experimental results on a structure with closely spaced, lightly damped modes are given to show the connection of two structures identified independently. Several suggestions are made for improvement of experimental implementations of the proposed methods.

Here, once again, reliance on analytical estimates of system behavior is greatly reduced. Although more experimental procedures are necessary to obtain enough information for model connection, the results (if the experiments are properly carried out) are more accurate than prior estimates. The improved accuracy is mainly due to use of actual behaviors rather than estimated ones. Similarly, use of input/output behavior for connections removes the need for explicit amplifier and sensor modeling.

8.1.3. Active Control

The results of interest to active control are the demonstrations of robustness and performance for H_∞/μ-synthesis. Modal responses for several closely spaced modes are practically removed through use of multivariable optimal controller. Additionally, several transmission zeroes are shown to be bypassed by the active controllers, thereby opening up the possibility of greatly improved tracking by systems with nonminimum phase zeroes (when not controlled). Different actuation schemes are used to show that for structural vibration control, actuators that induce force through load paths are significantly more effective and simpler than inertial motors.

From an identification validation perspective, the excellent active control results indicate that the model developed through frequency domain modal curve fitting is effective. While some work still needs to be done on developing additive and multiplicative uncertainty description identification, the *ad hoc* procedures used here were adequate.

8.1.4. Active Control of a Modified Structure

Feedback compensation results are also presented to show the need for accurate uncertainty models. A system with a well modeled uncertainty - a structure to be attached to it - is shown to have unstable controlled behavior without proper modification modeling, but excellent controlled behavior when modeled correctly. Thus, more accurate descriptions of system uncertainties allow for more effective controllers. Similarly, poor uncertainty descriptions can easily lead to unstable or ineffective compensators, as demonstrated experimentally.

The work in this thesis combines structural dynamics and control theory to develop results which are useful in each field. The LFT control feedback framework is used to extend a structural dynamics procedure (response mode synthesis), and a structural control demonstration shows the possibilities of control implementation (removal of nonminimum phase structural transmission zeroes). The final experiment also gives a particular method for uncertainty modeling (structural modification).

8.2 Directions for Further Work

One of the questions that remains to be researched is how the MIMO multivariable control works for tracking problems with structural systems. The method seems to be able to modify the systems so they can achieve rigid body performance over a wide frequency range when the specified objective is vibration reduction. Since the tracking problem is not too different, it should be possible to obtain responses of these systems at frequencies higher than their first harmonic. This is the currently accepted performance limit for SISO controlled systems.

The structural modeling method presented also provides a possible tool for H_∞-optimal structural modification and for combined control-structure optimization.

One of the main restrictions of the assembly method was that sensors must be aligned so that radial torsional mode accelerations are not sensed. It will thus be worthwhile to extend the LFT framework to input-output nonlinear systems such as structures with sensing of radial accelerations due to torsion.

8.3 References for Chapter 8

Bal: Balas, G.J., (1990), "Robust Control of Flexible Structures: Theory and Experiments", Ph.D. Thesis, Aeronautical Engineering Department, California Institute of Technology, Pasadena, CA.

Fan: Fanson, J.L., (1987), "An Experimental Investigation of Vibration Suppression in Large Space Structures using Positive Position Feedback", Ph.D. Thesis, Applied Mechanics Department, California Institute of Technology, Pasadena, CA.

Smi: Smith, R.S., (1990), "Model Validation for Uncertain Systems," Ph.D. Thesis, Electrical Engineering Department, California Institute of Technology, Pasadena, California.

Appendix i. A Variational Incomplete Proof to the H_∞-optimal Controller Problem

i.1 Introduction

This is an incomplete proof for the H_∞-optimal controllers. It is not complete for two main reasons: First, the variational proof method provides only local optimality guarantees. For global optimality, an operator-theoretic approach such as that used in [DGK], [DGF], [GlD] should be used. Second, the proof for the observer is not complete because the setup for use of variational methods has not yet been determined. The full solutions are in [DGK] and [GlD], among other papers. The proof herein for the optimal Full Information (FI) problem is taken from [Hwa], although the problem setup has appeared in other works [Isi], [KwS].

In the following sections, lower case letters are used to denote vectors of appropriate sizes, and upper case letters represent matrices. Variables representing scalar quantities are so noted.

The basic problem may be separated into two parts based on the separation principle [DGK][KwS]. The first problem is: given that the system's state and the disturbance affecting it can be sensed fully, what is the best constant feedback matrix that minimizes the effects of the disturbance on the performance signal. Since in this system full information is rarely obtained, the second part of the problem arises: Given the measured output, what is the best estimate of the state and the disturbance affecting the system. Once the best output estimate (OE) is obtained, it can be used with the FI matrix to give the dynamic compensator.

The control problem to be solved is as follows. Given the system described by

$$\begin{aligned} \dot{x} &= Ax + B_1 w + B_2 u \\ z &= C_1 x + D_{11} w + D_{12} u \\ y &= C_2 x + D_{21} w + D_{22} u. \end{aligned} \tag{i.1}$$

where the states of the system are denoted as x, the control inputs to the system as u, the outputs to be minimized by the procedure as z, and the measured signal for control as y. In this case, D_{11} and D_{22} are taken as zero so that the algebra works more cleanly. The other assumption set used is $D_{12}^T D_{12} = I$ and $D_{21} D_{21}^T = I$. The goal is to minimize the $\mathcal{L}_2$-norm of z given exogenous disturbances w. Thus, it is desired to minimize the transfer function T_{zw} from w to z. When choosing to reduce $\|z\|_2 = (\int_0^\infty z^T z dt)^{\frac{1}{2}}$, the norm of T_{zw} to be minimized depends on the signal w. If $w = w_0 \delta(t)$ where w_0 is a constant and $\delta(t)$ is the Dirac function at zero, the induced norm by the transfer function is $\|T_{zw}\|_2$. This is the standard Linear Quadratic Regulator problem (LQR/H_2). If w is a persistent signal, the induced norm is $\|T_{zw}\|_\infty$; therefore, the H_∞ problem is obtained. Here, the H_∞ problem is discussed.

i.2 Full Information

The approach used here is variational calculus resulting in Lagrange's equations for minimization of a cost function. Basically, the goal is to find a control algorithm for u which minimizes $\|z\|_2^2 = \int_0^\infty z^T z dt$, subject to the state equation $\dot{x} = Ax + B_1 w + B_2 u$. To keep the algebra more straightforward, without loss of generality, the cost function may be taken as $.5\|z\|_2^2$, subject to constraints. Since w is unknown, the cost should also be minimized with respect to the worst case w. In this case, the worst case w is the one with the smallest $\|w\|_2$ which gives the largest $\|z\|_2$. This would be the one which maximizes $\|z\|_2^2 - \|w\|_2^2$. Since $\|z\|_2^2$ is constrained, the search is done for

$$\min_u \max_w \tfrac{1}{2}(\|z\|_2^2 - \|w\|_2^2) \tag{i.2}$$

subject to the constraint on evolution of the state.

Letting ϱ be a Lagrange constraint variable, the cost to be mini-maxed is

$$J_{FI} = \int_0^\infty \frac{1}{2}(z^T z - w^T w) + (-\dot{x}^T + x^T A^T + w^T B_1^T + u^T B_2^T)\varrho dt, \tag{i.3}$$

where all the vector quantities are functions of time, or by transformation to the frequency domain, functions of frequency. To mini-max this problem, a search is made for the stationary points of the cost, i.e., the points where $\delta J = 0$. Where δ represents a virtual variation. This gives rise to the Lagrange equations since

$$\delta J(q_1, q_2, \cdots, q_n) = (\frac{d}{dt}\frac{\partial J}{\partial \dot{q}_1} - \frac{\partial J}{\partial q_1})\delta q_1 + \cdots + (\frac{d}{dt}\frac{\partial J}{\partial \dot{q}_n} - \frac{\partial J}{\partial q_n})\delta q_n = 0. \tag{i.4}$$

Therefore, each term multiplying the variations δq_i, $i \in \{1, \cdots, n\}$ must equal zero.

Recalling that $z = C_1 x + D_{12} u$,

$$J_{FI} = \int_0^\infty \frac{1}{2}(x^T C_1^T C_1 x + 2x^T C_1^T D_{12} u + u^T D_{12}^T D_{12} u - w^T w) + (-\dot{x}^T + x^T A^T + w^T B_1^T + u^T B_2^T)\varrho dt. \tag{i.5}$$

The variation with respect to x and with respect to ϱ give

$$\dot{x} = Ax + B_1 w + B_2 u$$
$$\dot{\varrho} = -C_1^T C_1 x - C_1^T D_{12} u - A^T \varrho. \tag{i.6}$$

The first of these is just the state equation. Next taking the variations with respect to u and w and using that $D_{12}^T D_{12} = I$,

$$u = -[D_{12}^T C_1 x + B_2 \varrho]$$
$$w = B_1^T \varrho. \tag{i.7}$$

To determine if this is a maximum with respect to w, the second variation of J with respect to w is taken and found to be $= -1$. Therefore, this is a maximization with respect to w. Now, substituting the values for u and w into the equations 6, the following system is obtained.

$$\dot{\varrho} = -[C_1^T C_1 - C_1^T D_{12} D_{12}^T C_1]x - [A - B_2 D_{12}^T C_1]^T \varrho$$
$$\dot{x} = [A - B_2 D12^T C_1]x + [B_1 B_1^T - B_2 B_2^T]\varrho. \tag{i.8}$$

Noting that since $D_{12}^T D_{12} = I$, $[I - D_{12} D_{12}^T] = [I - D_{12} D_{12}^T]^T [I - D_{12} D_{12}^T]$. So equation i.8 becomes

$$\begin{aligned}\dot{\varrho} &= -C_1^T[I - D_{12}D_{12}^T]^T[I - D_{12}D_{12}^T]C_1 x - [A - B_2 D_{12}^T C_1]^T \varrho \\ \dot{x} &= [A - B_2 D12^T C_1]x + [B_1 B_1^T - B_2 B_2^T]\varrho.\end{aligned} \tag{i.9}$$

At this point, it is worth discussing the proof method a little more. When full information feedback is used, a constant gain matrix K_{FI} is needed such that $u = K_{FI}x$ minimizes the cost function. Using the result for u in equation i.7 and the FI gain matrix definition

$$u = -D_{12}^T C_1 x - B_2 \varrho = K_{FI} x. \tag{i.10}$$

For this to hold, ϱ must be a function of x, which shall be taken as linear, so $\varrho = X_\infty x$. Substituting into Equation i.10, and into Equation i.8, the system becomes the one shown in Figure i.1.

$$\begin{pmatrix} I \\ X_\infty \end{pmatrix} \dot{x} = \begin{bmatrix} A - B_2 D_{12}^T C_1 & B_1 B_1^T - B_2 B_2^T \\ -C_1^T (I - D_{12} D_{12}^T)^T (I - D_{12} D_{12}^T) C_1 & -[A - B_2 D_{12}^T C_1]^T \end{bmatrix} \begin{pmatrix} I \\ X_\infty \end{pmatrix} x$$

Figure i.1. - System of Differential Equations which Leads to an Algebraic Riccati Equation for X_∞.

Premultiplying both sides of the equation in Figure i.1 by $[X_\infty \quad -I]$, an algebraic Riccati equation results for X_∞.

$$\begin{aligned}0 =& X_\infty (A - B_2 D_{12}^T C_1) + (A - B_2 D_{12}^T C_1)^T X_\infty \\ &+ C_1^T (I - D_{12} D_{12}^T)^T (I - D_{12} D_{12}^T) C_1 \\ &+ X_\infty (B_1 B_1^T - B_2 B_2^T) X_\infty\end{aligned} \tag{i.11}$$

The solution X_∞ for this may be computed if the bracketed (Hamiltonian) matrix in Figure i.1 does not have any eigenvalues on the imaginary axis. There are two optimal solutions for X_∞: one of which is positive definite and the other which is negative definite. For stability, the positive definite solution is used. The solution is symmetric. Once X_∞ is obtained, the FI feedback and the worst case disturbance w_{wc} can be computed as

$$u = -[D_{12}^T C_1 + B_2^T X_\infty]x = K_{FI}x$$
$$w_{wc} = B_1^T \varrho = B_1^T X_\infty x. \tag{i.12}$$

i.3 The Output Estimation Problem

Now that the FI problem is solved, the best estimate of the state is needed. The state estimate $\hat{x}$ then replaces x in $u = K_{FI}x$. Similarly, the estimate $\hat{w}$ of the worst case disturbance w_{wc} becomes $\hat{w} = B_1^T X_\infty \hat{x}$. Since the system evolution equations are given, and y can be measured, the estimator equation can be set up. The estimate $\hat{y}$ of y may be obtained as $\hat{y} = C_2\hat{x} + D_{21}\hat{w}$. Then the equation for the estimator can be chosen as

$$\dot{\hat{x}} = A\hat{x} + B_1\hat{w} + B_2 u + H(\hat{y} - y). \tag{i.13}$$

The term $H(\hat{y} - y)$ is the *driving* term, and H is a constant gain matrix to be determined. If w and the initial state are known exactly, the driving term is not necessary. Subtracting the state estimate equation from the state equation, the state error (e) equation may be obtained. Letting $\overline{w} = w - \hat{w}$ and $\overline{y} = y - \hat{y}$,

$$\dot{e} = (A + HC_2)e + (B_1 + HD_{21})\overline{w}$$
$$\overline{y} = C_2 e + D_{21}\overline{w}. \tag{i.14}$$

A method is presented which gets very close to constructing the Riccati equation for the optimal output estimator. As previously stated, this proof is incomplete, but is presented here to aid in the understanding of H_∞control.

A possible objective is minimization of the difference between the actual sensed output and a predicted sensed output. It would also be useful to minimize the error between the control signal generated by the estimated state and that created using the actual state. The errors in the state and in the disturbance estimates are then minimized, thereby reducing the driving term in the observer equation. This can be done subject to the worst case disturbance and subject to the evolution equation for the state error. Mathematically, the goal is to minimize $.5(\|\overline{y}\|_2^2 + \|\overline{u}\|_2^2)$ where $\overline{w} = B_1^T X_\infty e$. Substituting $\overline{y} = C_2 e + D_{21}\overline{w}$ and $\overline{u} = -[D_{12}^T C_1 + B_2^T X_\infty]e \equiv F_\infty e$, the cost is

$$J_{OE} = \int_0^\infty \frac{1}{2}(e^T F_\infty F_\infty e + e^T C_2^T C_2 e + 2\overline{w} D_{21}^T C_2 e + \overline{w}^T D_{21}^T D_{21} \overline{w}) + [-\dot{e}^T + e^T(A + HC_2)^T + \overline{w}^T(B_1 + HD_{21})^T]\lambda dt. \quad \text{(i.15)}$$

where λ is a Lagrange undetermined coefficient. Variation with respect to λ, e, and $\overline{w}$ produces the following system.

$$\begin{aligned} \dot{e} &= (A + HC_2)e + (B_1 + HD_{21})\overline{w} \\ \dot{\lambda} &= -F_\infty^T F_\infty e + -C_2^T C_2 e - C_2^T D_{21}\overline{w} - (A + HC_2)^T\lambda \\ D_{21}^T D_{21}\overline{w} &= -D_{21}^T C_2 e - (B_1 + HD_{21})^T\lambda. \end{aligned} \quad \text{(i.16)}$$

Using $D_{21}D_{21}^T = I$, the last equation can be premultiplied by D_{21} to give

$$D_{21}\overline{w} = -D_{21}(D_{21}^T e + D_{21}B_1^T\lambda + D_{21}^T H^T\lambda). \quad \text{(i.17)}$$

The relation $\overline{w}_{wc} = B_1^T X_\infty e$ from the FI problem can be substituted into the equation resulting from variation of $\overline{w}$. For this expression to hold, λ is taken as a linear function of e, $\lambda = Y_{tmp}e$. From here, expressions for $H^T Y_{tmp}$ and for H are obtained.

$$\begin{aligned} H^T Y_{tmp} e &= -[C_2 + D_{21}B_1^T(Y_{tmp} + X_\infty)]e \\ H &= -Y_{tmp}^{-1}[C_2^T + (X_\infty + Y_{tmp})B_1 D_{21}^T] \end{aligned} \quad \text{(i.18)}$$

Y_{tmp} must therefore be sign definite so that the inverse exists. Substitution into the differential system leads to the system in Figure i.2 and to the Riccati equation:

$$\begin{pmatrix} Y_{tmp} \\ I \end{pmatrix} \dot{e} = \begin{bmatrix} -(A + HC_2)^T & -F_\infty^T F_\infty - c_2^T C_2 - C_2^T D_{21} B_1^T X_\infty \\ 0 & (A + HC_2) + B_1 B_1^T X_\infty + HD_{21} B_1^T X_\infty \end{bmatrix} \begin{pmatrix} Y_{tmp} \\ I \end{pmatrix} e$$

Figure i.2. - Initial System of Differential Equations for Y_{tmp}.

$$\begin{aligned} 0 &= -Y_{tmp}(A + HC_2) + (A + HC_2)^T Y_{tmp} \\ &\quad - Y_{tmp}B_1 B_1^T X_\infty - Y_{tmp} HD_{21} B_1^T X_\infty \\ &\quad - F_\infty^T F_\infty - C_2^T C_2. \end{aligned} \quad \text{(i.19)}$$

The FI Riccati equation gives the relation

$$F_\infty^T F_\infty = X_\infty A + A^T X_\infty + C_1^T C_1 + X_\infty B_1 B_1^T X_\infty, \qquad \text{(i.20)}$$

which is substituted into the system of equations. After some simplification, the following system is obtained.

$$\begin{aligned} 0 &= C_1^T C_1 - C_2^T C_2 \\ &(X_\infty + Y_{tmp})(A - B_1 D_{21}^T C_2) + (A - B_1 D_{21}^T C_2)^T (X_\infty + Y_{tmp}) \\ &+ (X_\infty + Y_{tmp}) B_1 (I - D_{21}^T D_{21}) B_1^T X_\infty \end{aligned} \qquad \text{(i.21)}$$

Note that if the X_∞ at the end of the last term is replaced by $X_\infty + Y_{tmp} \equiv Y_\infty$, a Riccati equation results with Hamiltonian given in Figure i.3. The solution of this system would be $Y_\infty = X_\infty + Y_{tmp}$, which can be used to generate the optimal state estimator.

$$\begin{bmatrix} (A - B_1 D_{21}^T C_2) & B_1 (I - D_{21}^T D_{21})(I - D_{21}^T D_{21}) B_1^T \\ C_1^T C_1 - C_2^T C_2 & -[A - B_1 D_{21}^T C_2]^T \end{bmatrix}$$

Figure i.3. - Hamiltonian for OE Riccati Equation.

The full compensator is assembled from the FI and the OE parts. Unfortunately, the term $(X_\infty + Y_{tmp}) B_1 (I - D_{21}^T D_{21}) B_1^T Y_{tmp}$ is missing in the setup, so this final Riccati equation is not obtained. This incomplete proof is presented here only to provide a motivation of the H_∞-optimal controller.

i.4 Complete OE Solution

The solution in [DGK] for the optimal observer is that Y_∞ is the solution to the same algebraic Riccati equation generated by the Hamiltonian in Figure i.3. In the correct solution, however, the relation for H is different from the one generated here algebraically.

i.5 References for Appendix i

DFT: Doyle, J., Francis, B., and Tannenbaum, A., (1992), **Feedback Control Theory,** Macmillan Publishing Co., New York.

DGK: Doyle, J., Glover, K., Khargonekar, P., and Francis, B., (1989), "State Space Solutions to standard H_2 and H_∞ Control Problems," *IEEE Transactions on Automatic Control* Vol. AC 34, pp. 831-847.

DGF: Doyle, J., Glover, K., Khargonekar, P., and Francis, B., (1988), "State Space Solutions to standard H_2 and H_∞ Control Problems," *Proceedings of the American Controls Conference,* Atlanta, GA.

GlD: Glover, K., and Doyle, J., (1988), "State Space Formulae for all Stabilizing Controllers that Satisfy an H_∞-norm Bound and relations to risk sensitivity," *Systems and Control Letters,* vol. 11, pp. 167-172.

Hwa: Hwang, C.N., et al., (1990), "Active Rejection of Persistent Disturbances in Flexible Space Structures," *Proceedings of the AIAA Guidance, Navigation, and Controls Conference,* Portland, Oregon, pp. 1032-1041.

Isi: Isidori, A., (1991), Notes from Presentations given at Caltech, November-December, 1991.

Kai: Kailath, T., (1980), **Linear Systems**, Prentice-Hall, Englewood Cliffs, New Jersey.

KwS: Kwakernaak, H., and Sivan, R., (1972), **Linear Optimal Control Systems**, Wiley-Interscience, New York.